

Copyright

by

Jeffrey Greer Baguley

2004

**The Dissertation Committee for Jeffrey Greer Baguley certifies that this is the  
approved version of the following dissertation:**

**MEIOFAUNA COMMUNITY STRUCTURE AND FUNCTION IN THE  
NORTHERN GULF OF MEXICO DEEP SEA**

**Committee:**

---

Paul A. Montagna, Supervisor

---

Gilbert T. Rowe

---

Kenneth H. Dunton

---

Jay A. Brandes

---

Edward J. Buskey

**MEIOFAUNA COMMUNITY STRUCTURE AND FUNCTION IN THE  
NORTHERN GULF OF MEXICO DEEP SEA**

**by**

**Jeffrey Greer Baguley, B.A.**

**Dissertation**

Presented to the Faculty of the Graduate School of

The University of Texas at Austin

in Partial Fulfillment

of the Requirements

for the Degree of

**Doctor of Philosophy**

**The University of Texas at Austin**

**December 2004**

## **DEDICATION**

For opening my eyes to an unknown world of microscopic life, this work is dedicated to Dr. Richard Farris; and for their love and support, this work is dedicated to my family: Thomas G. Baguley, Janis M. Baguley, Timothy A. Baguley, Rosa Lee Baguley, Irma Mayernick, and especially my fiancé Brittany M. Hartzell.

“...we must not recoil with childish aversion from the examination of the humbler animals. In every realm of nature there is something marvelous.”

-Aristotle

“...they will feast on the abundance of the seas, on the treasures hidden in the sand.”

-Deuteronomy 33:19

## ACKNOWLEDGMENTS

This manuscript would not have been possible without the effort of many mentors, colleagues, and friends. Paul Montagna, thank you for the opportunity to become part of a unique scientific community, for your guidance, and your unique ability to make sense all types of data. For there guidance and insight I thank my committee members: Ken Dunton, Jay Brandes, Ed Buskey, and especially Gil Rowe, director of the Deep Gulf of Mexico Benthos research project. A special thanks is extended to Dr. Wonchoel Lee (Hanyang University, S. Korea) for many months of harpacticoid species identification. Many people contributed time and energy to the processing of over 700 deep-sea box cores; from Texas A&M University I thank Lindsey Loughry, Karen Sell, Sophie DeBeukelaer, Melanie Beazley, and Andy Hebert; from The University of Washington I thank Shelly Carpenter; from Woods Hole Oceanographic Institution I thank Joan Bernhard, and from La Universidad Nacional Autónoma de México I thank Elva Escobar and her students. Bathymetry for all Gulf of Mexico maps was provided by Dr. William Bryant (Texas A&M University). Completion of this research would not have been possible without the countless hours of sample processing and by Larry Hyde, Kristi Jones, and Chris Kalke. For their insight and input, I thank Rick Kalke, Marc Russell, Sally Morehead, and Terry Palmer. Finally, for their love, support, and prayers I thank my parents Thomas and Janis Baguley, grandmothers Irma Mayernick and Rosa Lee Baguley, and fiancé Brittany Hartzell.

This research was funded in part by the U.S. Department of Interior, Minerals Management Service, contract No. 1435-01-99-CT-30991 via a subcontract from the Texas Engineering Experiment Station. The research is part of the Deepwater Program: Northern Gulf of Mexico Continental Slope Habitats and Benthic Ecology (DGoMB, Deep Gulf of Mexico Benthos, G.T. Rowe PI). Other partial support was provided by the University of Texas Marine Science Institute via a Lund Graduate Fellowship.

**MEIOFAUNA COMMUNITY STRUCTURE AND FUNCTION IN THE  
NORTHERN GULF OF MEXICO DEEP SEA**

Publication No. \_\_\_\_\_

Jeffrey Greer Baguley, Ph.D.

The University of Texas at Austin, 2004

Supervisor: Paul A. Montagna

Meiofauna, a highly diverse group of small metazoans, are ubiquitous in deep-sea soft sediments and exhibit high abundance and biomass compared to larger-sized invertebrates (e.g., macrofauna). The northern Gulf of Mexico deep sea is characterized by topographical contrasts, with the flat topography of the Florida slope followed by the precipitous depth increase of the Florida escarpment; the complex Texas/Louisiana slope with numerous basins and knolls; and numerous canyon features such as the Mississippi Trough and DeSoto Canyon. Meiofauna community structure (abundance, biomass, and diversity) and function (respiration and feeding rates) were analyzed along with environmental variables in a hypothesis-based univariate and multivariate design, to more fully understand the distribution meiofauna, regional species pools, processes

structuring communities, and how they respond to topographic, geochemical and physical forcing in the northern Gulf of Mexico.

Meiofauna abundance is significantly related to water depth, but also exhibits significant longitudinal differences resulting from proximity to Mississippi River outflow. Multivariate comparisons of meiofauna abundance and diversity with environmental variables reveals a strong Mississippi River influence. River outflow alters local sediment characteristics, and interacts with loop current eddies and dynamic slope topography to increase POM flux in the northeastern region, thus creating areas of enhanced meiofauna abundance, biomass, and respiration, but lower functional harpacticoid copepod diversity. However, most stations have unique harpacticoid species compositions, suggesting high regional (2700 species) and global ( $10^5$  -  $10^6$  species) diversity by extrapolation. Although highest harpacticoid diversity, in terms of expected number of species (rarefaction), is found at approximately 1200 meters, average taxonomic and average phylogenetic diversity continue to increase with depth, indicating greater morphological or functional diversity. High within versus between station variability suggests an interaction between small and region-scale processes maintaining high diversity. Allometric estimates indicate that meiofauna require 7% of their biomass per day to meet their metabolic energy budget, and account for 10-25% of whole sediment community respiration, indicating their importance in global biogeochemical cycles.



## TABLE OF CONTENTS

LIST OF TABLES .....	xi
LIST OF FIGURES .....	xv
Chapter 1: Meiofauna abundance in relation to environmental variables in the Northern Gulf of Mexico deep sea .....	1
Abstract .....	1
Introduction .....	2
Methods .....	6
Results .....	17
Discussion .....	24
Conclusion .....	33
Chapter 2: Spatial and Bathymetric Trends in Harpacticoida (Copepoda) Community Structure in the Northern Gulf Of Mexico Deep Sea .....	62
Abstract .....	62
Introduction .....	63
Methods .....	67
Results .....	75
Discussion .....	82
Conclusion .....	95
Chapter 3: Meiofauna biomass and weight-dependant respiration in the Northern Gulf of Mexico deep sea .....	117

Abstract .....	117
Introduction .....	118
Methods .....	120
Results .....	128
Discussion .....	131
Conclusion .....	138
Appendix .....	159
References .....	180
Vita .....	201

**LIST OF TABLES**

Table 1.1: Summary of meiofauna community structure experimental design: null hypotheses, design criteria, and stations included in analysis. . . . . 35

Table 1.2: Effect of core tubes size (inner diameter) on meiofauna counts and average density. Based on five replicates taken at station W-2. Abundance is detransformed from natural log (ln), so taxa averages do not sum to the total average. . . . . 36

Table 1.3: DGoMB station locations, depth, and average meiofaunal abundance (five replicate cores) for pooled taxonomic groups. . . . . 37

Table 1.4: Average abundance (AA), percent contribution (Contrib.%), and cumulative percent contribution (T%) of meiofauna major taxa per core (5.5 cm i.d.). Data summarized for all 51 stations (five replicates per station). . . . . 39

Table 1.5: ANOVA results, tests for differences in meiofauna abundance. Dependent variable =  $\log_{10}(N+1)$ . ANOVA abbreviations: DF = degrees of freedom, SS = sum of squares, MS = mean square, F = F-test value, P = Pr > F. Factor abbreviations: long. = longitude, basin = basin vs. non-basin stations, dfs = distance from shore, escarp. = escarpment vs. non-escarpment transects. . . 40

Table 1.6: Eigenvalues of the Correlation Matrix for the environmental PCA, proportion of variance explained by each principal component, and cumulative variance. . . . . 41

Table 1.7: Variable loads for the rotated (Varimax) factor pattern of the environmental PCA. ....	42
Table 2.1: Results of SIMPER analysis (Primer 5.0) indicating family percent contributions to total harpacticoid abundance. AA = Average abundance, Contrib.% = percent contribution of family, T% = cumulative percent contribution of families. ....	96
Table 2.2: Total species (S) and total individuals (N) per five pooled replicates cores (= 118.8 cm <sup>2</sup> ). Species diversity indices: expected species per 30 individuals [ES(30)], Shannon-Wiener diversity (H'), average taxonomic diversity ( $\Delta$ ), and average phylogenetic diversity ( $\Phi^+$ ) at each of the 43 stations where harpacticoid copepods were identified to species. ....	97
Table 2.3: ANOVA results of test for differences in Harpacticoida diversity. Dependent variable is average phylogenetic diversity ( $\Phi^+$ ). DFS = distance from shore; DFFS = distance from first station. ....	99
Table 3.1: Biomass contribution of the major taxonomic groups to total meiofaunal biomass (mg C m <sup>-2</sup> ) at each DGoMB station. NEMA = Nematoda, HARP = Harpacticoida, NAUP = Harpacticoida nauplii, POLY = Polychaeta, OSTR = Ostracoda, CYCL = Cyclopoida, TANA = Tanaidacea, ISOP = Isopoda, KINO = Kinorhyncha. ....	140
Table 3.2: Allometric estimations of the mass-dependent meiofauna respiration rate (R, in d <sup>-1</sup> units) and meiofauna community respiration (CO <sub>2</sub> , mg C m <sup>-2</sup> d <sup>-1</sup> ) and total	

organic carbon demand (OrgC, mg C m<sup>-2</sup> d<sup>-1</sup>). Mass-dependent respiration was calculated using an allometric rate law (*sensu* Mahaut et al. 1995) which is dependent upon the ratio (W) of biomass (B, mg C m<sup>-2</sup> d<sup>-1</sup>) to abundance (A, N m<sup>-2</sup>). Respiration (CO<sub>2</sub>, mg C m<sup>-2</sup> d<sup>-1</sup>) is the product of the mass-dependent rate (R) and the total biomass (B), and total carbon demand (OrgC) was calculated under the assumption that respiration equals 80% of the total metabolic budget (see discussion). . . . . 142

Table 3.3: Mean meiofaunal (MB) and bacterial (BB) biomass for pooled replicates and pooled taxonomic groups at the four experimental stations. Bacterial biomass courtesy of Jody Deming, University of Washington (unpublished DGoMB data). . . . . 144

Table 3.4: ANOVA results of the test for differences in grazing rate between treatments (experimental vs. control) and stations, separated by taxonomic group. Significant treatment by station interactions were observed for all taxa (a = 0.05). Polychaetes were the only taxa to show consistent grazing, and overall grazing rates for all taxa were low (refer to Table 3.5 & Fig. 3.9 below). . . . . 145

Table 3.5: Measured meiofaunal grazing on bacteria is only 9.8 to 0.0001% of their theoretical required consumption. Measured meiofauna grazing rate (GR, d<sup>-1</sup> units), bacterial biomass (BB, mg C m<sup>-2</sup> d<sup>-1</sup>), measured grazed bacterial carbon (GC = GRxBB, mg C m<sup>-2</sup> d<sup>-1</sup>), allometric carbon requirement (OrgC, mg C m<sup>-2</sup>

d<sup>-1</sup>), and the ratio of measured grazing to the allometric requirement (GC/OrgC), expressed as a percent. . . . . 146

Table 3.6: Comparison of whole community respiration (CR, mg C m<sup>-2</sup> d<sup>-1</sup>) to meiofauna allometric respiration estimates (MR, mg C m<sup>-2</sup> d<sup>-1</sup>). Meiofauna account for 10-25% of whole community respiration. Note: whole community respiration (mg C m<sup>-2</sup> d<sup>-1</sup>), converted from sediment community oxygen consumption (SCOC) as measured by the Benthic Lander (Gil Rowe, unpublished DGoMB data). SCOC (mmol O<sub>2</sub> m<sup>-2</sup> d<sup>-1</sup>) was converted to carbon using a respiratory quotient of 0.85 and stoichiometric conversion factor of 12 mg C/mmol O<sub>2</sub>. . . . . 147

## LIST OF FIGURES

- Figure 1.1: DGoMB station locations in the northern Gulf of Mexico deep sea. Note transect and topographic feature descriptions. . . . . 43
- Figure 1.2: Vertical distribution of meiofauna taxa from sediment cores collected at station W2 for Shakedown Cruise. Cores were sectioned in 1-cm increments, and fauna were enumerated from each 1-cm section. Plotted data is the average of five replicates (error bars = standard deviation) . . . . . 44
- Figure 1.3: Log (x+1) transformed meiofauna abundance ( $N\ m^{-2}$ ) versus water depth (m) for all stations sampled during DGoMB project. . . . . 45
- Figure 1.4: Spatial analysis of meiofauna abundance ( $N\ m^{-2}$ ) at all DGoMB stations. Buffer size equals relative meiofauna abundance. The highlighted contour equals 2000 meters. . . . . 46
- Figure 1.5: Number of major meiofauna taxa per core as a function of water depth. . . . . 47
- Figure 1.6: Expected number of taxa per 1000 individuals [ES(1000)] as a function of water depth, and quadratic regression. Dashed lines = 95% confidence intervals. . . . . 48
- Figure 1.7: Expected number of taxa per 20 individuals [ES(20)] for non-dominant meiofauna taxa (excluding nematodes, harpacticoid copepods, harpacticoid nauplii, and unknowns). A quadratic regression was fit to the data (dashed lines = 95% confidence intervals). . . . . 49

Figure 1.8: Meiofauna abundance ( $N\ m^{-2}$ ) as a function of depth for transects included in the test for differences over depth and longitude ( $H_{01}$  &  $H_{02}$ ). . . . . 50

Figure 1.9: Comparison of meiofauna abundance ( $N\ m^{-2}$ ) on two parallel transects to determine abundance differences related to canyon (MT transect) versus non-canyon (C transect) areas ( $H_{04}$ ) . . . . . 51

Figure 1.10: Comparison of meiofauna abundance and a function of water depth along two transects to determine abundance differences related to the Florida Escarpment (S39-S44) versus a reference transect (W1-W6). . . . . 52

Figure 1.11 SeaWiFS chl-a (mg/L) biweekly average (November 1999 through April 2000). Chl-a concentration was adjusted for remineralization with depth (see Berger *et al.* 1988). A) Log-Log relationship of adjusted chl-a with depth, and B) Meiofauna abundance versus adjusted chl-a. . . . . 53

Figure 1.12: Meiofauna abundance ( $N\ m^{-2}$ ) as a function of sediment particulate organic carbon (POC). . . . . 54

Figure 1.13: Principal components analysis of environmental variables, A) variable loading scores for PC1 versus PC2, B) variable loading scores for PC2 versus PC3. . . . . 55

Figure 1.14: Meiofauna abundance ( $N\ m^{-2}$ ) regressed against environmental PC1 (A), designated “sediment properties,” and environmental PC2 (B), “POM Flux.” . . . . 56



Figure 1.15: MDS ordination of DGoMB stations, based on Bray-Curtis similarity (4<sup>th</sup> root transformation) of major taxa abundance. . . . . 57

Figure 1.16: MDS ordination of DGoMB stations, based on Bray-Curtis similarity (4<sup>th</sup> root transformation) of major taxa abundance. Symbols indicate depth zones of 1000 meter increments: ▼ = 200-1000 meters, ■ = 1000-2000 meters, ▲ = 2000-3000 meters, and ◆ = >3000 meters. Circled areas approximate stations above and below 2000 m. . . . . 58

Figure 1.17: MDS ordination of DGoMB stations, based on Bray-Curtis similarity (4<sup>th</sup> root transformation) of major taxa abundance. Bubble size equals relative nematode abundance at each station. The MDS plot strongly represents decreasing abundance with depth. . . . . 59

Figure 1.18: MDS ordination of DGoMB stations, based on Bray-Curtis similarity (4<sup>th</sup> root transformation) of major taxa abundance. Bubble size equals relative abundance of Tardigrada at each station. Tardigrades were one of the major taxonomic groups that did not follow the general pattern of decreased abundance with depth. . . . . 60

Figure 1.19: MDS ordination of DGoMB stations, based on Bray-Curtis similarity (4<sup>th</sup> root transformation) of major taxa abundance. Bubble size equals relative particulate organic carbon (POC) concentration. . . . . 61

Figure 2.1: Harpacticoid copepods were identified to species at a total of 43 stations in the northern Gulf of Mexico deep sea. . . . . 100

Figure 2.2: Harpacticoid copepod abundance (N) and species richness (S), adjusted to the number per 10 cm <sup>2</sup> , as a function of depth. Abundance and richness are highly correlated (r = 0.91) .....	101
Figure 2.3: Shannon-Wiener diversity index (H') as a function of depth for pooled replicate core samples of harpacticoid copepods. ....	102
Figure 2.4: Expected number of harpacticoid species per 30 individuals [ES(30)], for pooled replicate core samples of harpacticoid copepods. ....	103
Figure 2.5: Average taxonomic diversity ( $\Delta$ ) for pooled replicate core samples of harpacticoid. ....	104
Figure 2.6: Average phylogenetic diversity ( $\Phi^+$ ) for pooled replicate core samples of harpacticoid copepods. ....	105
Figure 2.7: The ratio of harpacticoid copepod species (S), genera (G), and families (F) per total individuals (N) in each depth zone. Zones are significantly different (P<0.01), with pairwise comparisons indicating differences among shallowest and deepest zones only .....	106
Figure 2.8: Average phylogenetic diversity ( $F^+$ ) as a function of depth for transects included in the test for depth and longitude differences ( $H_{01}$ and $H_{02}$ ). ....	107
Figure 2.9: Average phylogenetic diversity ( $F^+$ ) as a function of depth for transects included in the test for diversity differences between canyon (MT) and non-canyon (C) areas ( $H_{04}$ ). ....	108

Figure 2.10: Average phylogenetic diversity ( $F^+$ ) as a function of depth for transects included in the test for escarpment (S transect) effects on diversity ( $H_{05}$ ). . 109

Figure 2.11: Regression of average phylogenetic diversity ( $F^+$ ) as a function of **A**) environmental PC1 and **B**) PC2.  $F^+$  is not significantly related to sediment properties (PC1), but is significantly related to POM flux (PC2). . . . . 110

Figure 2.12: MDS orientation of stations based on harpacticoid species abundance. Symbols indicate depth zone:  $\blacktriangledown$  = 200-1000 meters,  $\blacksquare$  = 1000-2000 meters,  $\blacktriangle$  = 2000-3000 meters,  $\blacklozenge$  > 3000 meters. One-way analysis of similarity (ANOSIM) indicates significant depth differences ( $P < 0.01$ ). . . . . 111

Figure 2.13: MDS orientation of stations based on harpacticoid species abundance. Symbols indicate longitudinal zone:  $\blacktriangle$  = 94-96° W,  $\blacktriangledown$  = 91-93° W,  $\blacksquare$  = 88-90° W,  $\blacklozenge$  = 85-87° W. One-way ANOSIM indicates significant longitudinal differences ( $P < 0.01$ ). . . . . 112

Figure 2.14: Cluster analysis of Harpacticoid community composition, created using Bray-Curtis similarity, and group average linking. Zonation determined on basis of >20% similarity. . . . . 113

Figure 2.15: Harpacticoid copepod species zonation in the northern Gulf of Mexico deep sea. Zones were chosen on the basis of >20% similarity using the Bray-Curtis similarity index. . . . . 114

Figure 2.16: Species accumulation curves used to estimate regional Harpacticoida species abundance in the Gulf of Mexico (extrapolation). . . . . 115

Figure 2.17: Cluster analysis illustrating within versus between station differences in harpacticoid community structure for all replicates at stations NB3 and NB4. .....	116
Figure 3.1: DGoMB station locations in the northern Gulf of Mexico deep-sea where meiofauna community biomass ( <i>sensu</i> Baguley et al. 2004) and allometric respiration ( <i>sensu</i> Mahaut et al. 1995) were estimated. ....	148
Figure 3.2: Process station locations for 2001 cruise. MT1 = 482 m; S42 = 763 m; S36 = 1826 m; MT6 = 2643 m .....	149
Figure 3.3: Meiofauna biomass (mg wet wt/m <sup>2</sup> ) versus water depth at all DGoMB station. ....	150
Figure 3.4: Average nematode wet weight (mg) per individual versus depth ....	151
Figure 3.5: Average harpacticoid wet weight (mg) per individual versus depth ..	152
Figure 3.6: Meiofauna grazing rates by taxonomic group for the four experimental stations. ....	153
Figure 3.7: A) Meiofauna mass-dependent respiration rate (d <sup>-1</sup> ) and B) meiofauna community respiration (mg C m <sup>-2</sup> d <sup>-1</sup> ) at each of the 51 DGoMB stations in the northern Gulf of Mexico deep-sea. ....	154
Figure 3.8: Spatial comparison of relative meiofauna biomass (mg wet wt. m <sup>-2</sup> ), where bubbles size is proportional to biomass. ....	155
Figure 3.9: Spatial interpolation of meiofauna biomass (mg wet mass m <sup>-2</sup> ) in the northern Gulf of Mexico deep sea. ....	156

Figure 3.10: Spatial interpolation of the meiofaunal organic carbon requirement ( $\text{mg C m}^{-2} \text{ d}^{-1}$ ), assuming respiration equals 80% of total metabolism. . . . . 157

Figure 3.11: Conceptual model of complex meiofaunal trophic interactions with microfauna (bacteria and protists) and two different detrital pools (phytodetritus, and recycled detritus). Not shown are predatory meiofauna (prey upon other meiofauna) or meiofaunal deposit feeders that ingest whole sediment particles and obtain carbon from one or more of the above standing stocks. Carbon is lost via respiration transfer to higher trophic levels via predation (cloud symbols).  
. . . . . 158

**CHAPTER 1: MEIOFAUNA ABUNDANCE IN RELATION TO ENVIRONMENTAL  
VARIABLES IN THE NORTHERN GULF OF MEXICO DEEP SEA**

**ABSTRACT**

Meiofauna are ubiquitous in deep-sea soft sediments and exhibit high abundance compared to larger-sized invertebrates (e.g., macrofauna). The northern Gulf of Mexico (NGOM) deep sea is characterized by topographical contrasts, with the flat topography of the Florida slope followed by the precipitous depth increase of the Florida escarpment; the complex Texas/Louisiana slope with numerous basins and knolls; and numerous canyon features such as the Mississippi Trough and DeSoto Canyon. In order to more fully understand the distribution of meiofauna and how they respond to topographic, geochemical and physical forcing in the northern Gulf of Mexico, meiofauna abundance and environmental variables were analyzed in a hypothesis-based univariate and multivariate design. Meiofauna abundance is significantly related to water depth, but also exhibits significant longitudinal differences resulting from proximity to Mississippi River outflow. Canyon features in proximity of Mississippi River outflow were found to greatly enhance meiofauna abundance. The Florida Escarpment interacts with Mississippi River inflow and the Loop Current to enhance meiofauna abundance at stations lying directly above and below the escarpment. Multivariate comparisons of meiofauna abundance with environmental variables reveals a strong Mississippi River influence. River outflow alters local sediment characteristics, and interacts with loop

current eddies and dynamic slope topography to increase POM flux in the northeastern region, thus creating areas of higher than normal meiofauna abundance.

## **INTRODUCTION**

The term “meiobenthos” was first used by Mare (1942) to describe benthic organisms of intermediate size, however studies of meiofauna-sized benthic invertebrates began with the discovery of the Kinorhyncha in 1851 (Dujardin 1851). Meiofauna are metazoan and protistan fauna that are smaller than macrofauna but generally larger than the microbenthos (e.g., bacteria, microalgae, and many protozoans). Since Mare’s seminal work, meiofauna research has become a specialized sub-discipline within the general field of benthic ecology. Several studies have inferred that marine meiobenthos are a biologically and ecologically separate group of animals (Schwinghamer 1981, Warwick 1984, Warwick *et al.* 1986, Giere 1993), a community concept that was described by Remane (1933) with respect to meiofaunal adaptations to the interstitial (between sand grains) environment. Meiofauna, although often overlooked in large-scale benthic studies, are ubiquitous in marine and freshwater sediments, an environment spanning approximately three quarters of the globe (Hick and Coull 1983, Giere 1993, Soltwedel 2000). Meiofauna also exhibit systematic diversity unparalleled by any other group of organisms, and have species diversity comparable to the Insecta (May 1980). Giere (1993) lists 24 of the 34 recognized phyla of the Kingdom Animalia as having meiofaunal representatives, and at least three taxa within the Kingdom Protista as having free-living meiofaunal representatives. Meiofauna are an important component of all

marine soft-sediment communities, play a key role in nutrient remineralization and transfer of carbon to higher trophic levels (Coull & Bell 1979 and references therein). Yet, despite the incredible abundance, biomass, and diversity of meiofauna, this group remains generally understudied, compared to their larger relatives.

The first quantitative study of deep-sea meiofauna ecology was by Wigley & McIntyre (1964). Subsequent studies have been conducted in all major ocean basins; including the Atlantic, Pacific, North Sea, Mediterranean, Red Sea, Gulf of Mexico, and Weddell Sea (see review by Soltwedel 2000). Recent deep-sea investigations have focused on bathymetric gradients of abundance (Tietjen 1971; Coull *et al.* 1977; Shirayama 1984a), relationships of community structure with food availability (Thiel 1978; Pfannkuche 1993; Danovaro *et al.* 1995; Gooday 1996; Relexans *et al.* 1996; Soltwedel 1997; Fabiano and Danovaro 1999) and relationships with environmental factors (Shirayama 1984a; Alongi and Pichon 1988; Vanhove *et al.* 1995; Soltwedel *et al.* 1996). Most meiofaunal studies have focused on limited geographic areas, not allowing region- or basin-scale patterns to emerge. Therefore, deep-sea investigations of meiofauna abundance in relation to environmental factors have been limited primarily to variation on the sample scale, i.e., correlations between abundance and physical or geochemical variables (Shirayama 1984a). Of studies in 48 regions, reviewed by Soltwedel (2000), between 2 and 21 stations were sampled, with 31 of 48 study locations having less than 10 stations sampled. Meiofauna abundance has been reported from only 15 deep-sea stations (350-2800 meters) in the Northern Gulf of Mexico (Pequegnat *et*



*al.* 1990), and from 16 stations (200-540 meters) in the Southern Gulf of Mexico (Escobar *et al.* 1997).

Understanding organism distributions and how they respond to topographic, geochemical and physical oceanographic features has not been fully elucidated for deep-sea communities (Etter and Mullineaux 2001). The northern Gulf of Mexico continental slope is physically and geologically complex, with numerous basins, knolls, and canyons. The anticyclonic loop current is a permanent feature in the Gulf of Mexico and produces anticyclonic/cyclonic gyre pairs that can be both short (days) or long-lived (weeks to months) mesoscale features (Biggs and Müller-Karger 1994). Meiofauna ecology in the Gulf of Mexico deep sea has only been sparsely investigated, and focused primarily on bathymetric abundance gradients (Pequegnat *et al.* 1990) or regional trends along the same isobath (Escobar *et al.* 1997).

In order to more fully understand meiofaunal community structure in relation to the complex physical setting of the Northern Gulf of Mexico continental slope, meiofauna abundance was compared from the Florida continental slope to the Texas continental slope. The study was hypothesis-based in order to select stations covering nearly the entire northern region, taking into account the diverse physical setting. The sampling design was formulated based on the following six null hypotheses:  $H_{01}$ ) there is no difference in meiofaunal abundance with **depth**,  $H_{02}$ ) there is no difference in meiofaunal abundance with **longitude**,  $H_{03}$ ) there is no difference in meiofaunal abundance in versus out of submarine **basins**,  $H_{04}$ ) there is no difference in meiofaunal

abundance in versus out of submarine **canyons**,  $H_{05}$ ) there is no difference in meiofaunal abundance with respect to **escarpments**, and  $H_{06}$ ) there is no difference in meiofaunal abundance with respect to overlying water column **primary production**.

The depth hypothesis ( $H_{01}$ ) follows one of the fundamental observations of deep-sea ecology, as depth increases abundance decreases (Soltwedel 2000) reflecting the decrease in particulate organic matter (POM) flux with depth (Turley et al. 1995). The longitude hypothesis ( $H_{02}$ ) was specifically designed to test for effects of the Mississippi River in shaping faunal compositions. Mississippi River discharge is a major source of new nutrients and organic matter into the northern Gulf of Mexico, with a mean daily discharge of nearly 1 billion  $m^3$  (<http://water.usgs.gov>). The *a priori* hypothesis was that a longitudinal gradient of abundance exists, which is maximized near Mississippi River inflow. The basin hypothesis ( $H_{03}$ ) was designed to test for faunal differences in basins and adjacent non-basin stations on the Texas/Louisiana slope. Basins, along with canyons ( $H_{04}$ ) may have a concentrating effect on the rain of POM and therefore enhance meiofauna abundance. Escarpments ( $H_{05}$ ) may interact with deep water currents and internal waves to create flows that influence food supply (Etter and Mullineaux 2001). The *a priori* hypothesis was increased abundance directly below the escarpment, as a result of increased sedimentation of particulate organic matter (POM) resulting from the interaction with physical oceanographic processes (Etter & Mullineaux 2001). The escarpment transect was compared to a reference transect in the Western Gulf (W) that experiences a gradual and relatively constant depth increase. Increased overlying

chlorophyll(a) biomass ( $H_{06}$ ) due to interactions among Mississippi River outflow, the Loop Current, and mesoscale anticyclonic/cyclonic gyre pairs likely affect meiofauna abundance. Univariate and multivariate statistical methods was used to integrate regional differences in relation to the physical environment with environmental variables in order to more fully understand the processes controlling meiofauna abundance in the Northern Gulf of Mexico deep sea.

## **METHODS**

### **Field Methods**

*Station Locations* – A total of 51 stations in the northern Gulf of Mexico were sampled for meiofauna community structure (Fig. 1.1) as part of the Deepwater Program: Northern Gulf of Mexico Continental Slope Habitats and Benthic Ecology program (henceforth referred to as DGoMB). A total of seven transects were investigated from 200 to 3000 meters. In the northwest (RW) region, seven stations were sampled, including one station in the Alaminos Canyon (AC1). An additional western (W) transect was included, which was a historical transect from a previous study (Pequegnat *et al.* 1990). In the west-central region (WC) two historical stations from Pequegnat *et al.* (1990) study were included, but stations in this region were mainly designed to test for faunal differences between basin (B) and non-basin (NB) locations. The central transect (C) was also sampled by Pequegnat *et al.* (1990), but included to test for differences from the adjacent Mississippi Trough (MT) transect. In the northeast region 10 stations, from two transects, were sampled perpendicular to the Florida slope and

escarpment (S). Additional stations not included in the original experimental design, but added to the sampling scheme, were a high productivity station (HIPRO) in the northeastern region, a station from the Green Knoll Furrow (GKF) region, a station on Bush Hill (BH), and five stations on the Sigsbee abyssal plain as part of the Joint Studies of the Sigsbee Deep (JSSD) collaboration with La Universidad Nacional Autónoma de México.

*Sample Collection* – Survey samples were collected on a 60-day cruise aboard the *R/V Gyre* (Texas A&M University) during the months of May and June 2000. One core sample was taken from each boxcore sample, and stored for meiofaunal community analysis. Five total replicate cores were taken at each community structure station. Meiofauna were collected by a 5.5 cm inner diameter (i.d.) core tube that was mounted inside the boxcorer. A mounted corer within a box will ensure that meiofauna are collected from an undisturbed surface. Insertion of a core tube after the sample has already been sloshed around the deck of the ship is known to create artifacts including loss of organisms. Surface disturbance can occur when the boxcore is placed on the ship's deck. Taking the sample from an inner subcore reduces edge effects (Eckman and Thistle 1988). The bow waves of sampling devices in deep water can have an impact on estimates of surface dwelling meiofauna (Hulings and Gray 1971). Bow wave effects were reduced by heavily weighting the boxcore and slowing penetrating sediments.

There are two critical issues for sampling deep sea meiofauna: core size and sampling depth. To resolve these two issues, a study was performed during a shakedown

cruise aboard the *R/V Gyre* (Texas A&M University), 16-18 February 2000, to determine the most appropriate core size and vertical sampling depth for meiofauna in the current study area. To compare sizes, four cores ranging from 2.2 cm to 6.7 cm inner diameter (i.d.) were used to collect the top 1 cm of sediment, and five replicates were taken. Differences in meiofauna abundance with core size was compared using one-way analysis of variance (ANOVA). To exam the vertical distribution of meiofauna, a 5.5 cm core tube was used. Samples were taken at 1 cm intervals down to 20 cm, and five replicates were taken. All samples were taken at station W2 in water depths of approximately 661 meters. A third, although less critical issue was sampling gear type. Two types of boxcores, the GOMEX (Gulf of Mexico) boxcore (Boland and Rowe 1991) and USNEL(US Naval Electronic Laboratory) boxcore (Hessler and Jumars 1974) are commonly used. To exam for differences between two different boxcores, a 2.2 cm core tube was mounted within each and samples were taken to a depth of 1 cm. The sampling characteristics of the GOMEX boxcore and USNEL boxcore were compared using a paired t-test.

*Preservation* – After core sections were collected, meiofauna were narcotized in 7% MgCl<sub>2</sub> (isotonic to seawater). Narcotizing meiofauna is necessary to minimize body shape distortion during the preservation process, allowing for more accurate biomass estimates by the semi-automated microphotographic approach (Baguley *et al.* 2004) (see chapter three of this dissertation). Samples were then preserved in an equal volume of 10% buffered formalin (yielding a final concentration of 5% formalin) (Hulings and

Gray 1971). The buffered formalin was made up with seawater that was filtered through a 0.042 mm mesh to exclude plankton. Rose bengal was added to the preservative to easily distinguish meiofauna during the sorting process. Samples were then stored and returned to The University of Texas Marine Science Institute (Port Aransas, TX) for analysis.

### **Laboratory Methods**

*Abundance* – By convention, the definition of meiofauna is those animals that pass through a 500 micron mesh sieve but are retained on a 63 micron mesh sieve (Hulings and Gray 1971; Coull and Bell 1979; Giere 1993). Because deep-sea organisms are small, most meiofaunal ecologists use 42 micron mesh sieves to retain meiofauna (eight of nine papers reviewed in Thistle *et al.* 1991). To conform with other studies of deep-sea meiofauna, a 45 micron mesh sieve was used to retain meiofauna.

Meiofauna were extracted from sediment using the Ludox centrifugation technique (deJonge and Bouwman 1977). Recent quality control studies have shown that the technique extracts 95-99% of organisms over all sediment grain sizes (Burgess 2001). Samples were then sorted and counted to a major metazoan taxonomic category. Meiofaunal communities are composed of two groups. Temporary meiofauna are those juveniles of the macrofauna that will eventually grow into larger organisms. Permanent meiofauna are those groups where adults are less than 300 micrometers in length, e.g., Nematoda, Copepoda, Gastrotricha, Turbellaria, Acari, Gnathostomulida, Kinoryncha, Tardigrada, Ostracoda, and some Nemertinea, Oligochaeta, and Polychaeta. The two

standard meiofauna texts (Higgins and Thiel 1988; Giere 1993) were used in the identification of major taxonomic groups.

*Environmental Variables* – A full suite of sedimentary environmental variables were analytically measured from 5 replicate cores (6.7 cm i.d.), from separate boxcores, at most DGoMB stations. All chemical, geochemical, and geological analyses were performed by collaborators at Texas A&M University including: Drs. Luis Cifuentes, Bobby J. Presley, William Bryant, Terry Wade, John Morse, Doug Biggs, and their respective associates. Sediment grain size was determined using the standard Folk settling method (Folk 1974). Total organic and inorganic carbon were determined by standard LECO combustion techniques or by Carlo Erba elemental analyzer. Hydrocarbon contaminants (mainly PAH's) were measured using NOAA status and trends methods (Denoux et al. 1998; Qian et al. 1998) using gas chromatography-mass spectrometry (GC-MS). Trace metal analyses included atomic absorption spectroscopy (AAS), instrumental neutron activation analysis (INAA), and/or inductively coupled plasma-mass spectroscopy (ICP-MS) (e.g., Taylor and Presley 1998). Geochemical variables were measured using a number of methods and/or instruments: O<sub>2</sub>, H<sub>2</sub>S, Fe, and Mn were measured with microelectrodes (Brendel and Luther 1995; Luther et al. 1998); total CO<sub>2</sub> (DIC) was measured via gas chromatography; sulfate was measured via ion chromatography; pH was measured with electrodes; nutrients (nitrate, nitrite, ammonia, urea, phosphate, and silicate) were measured using standard autoanalyzer techniques; dissolved organic carbon was measured using a high temperature combustion DOC

analyzer; organic carbon and nitrogen were measured using a Carlo Erba elemental analyzer. Surface seawater chlorophyll(a) (chl-a) was estimated from Sea viewing Wide-Field Sensor (SeaWiFS) satellite imagery. The complete environmental variable data set is not presented here, but will be publically accessible from the Geochemical & Environmental Research Group (<http://www.gerg.tamu.edu/>) upon completion of the DGoMB final report (Rowe *et al.*, in prep).

### Statistical Analysis

*Hypothesis Testing* – Six main hypotheses were investigated for differences in meiofauna abundance. For statistical power, five replicate samples were taken per station, from five separate box cores.

Five transects, RW, W, C, MT and S, were included in the **depth/longitude** ( $H_{01}/H_{02}$ ) analysis ranging from the Texas slope in the West to the Florida Escarpment in the east (Fig. 1.1, Table 1.1). Five stations were included per transect, over five depth zones, consistent between transects. Differences in meiofaunal abundance at different depths and longitudes were tested using a two-way completely random analysis of variance (ANOVA) that is described by the following model:

$$Y_{ijk} = \mu + \alpha_j + \beta_k + \alpha\beta_{jk} + \varepsilon_{i(jk)}$$

where  $Y_{ijk}$  is the measurement for each individual replicate,  $\mu$  is the overall sample mean,  $\alpha_j$  is the main effect for transects and  $j = 1-5$ ,  $\beta_k$  is the main effect for depths and  $k = 1-5$ ,  $\alpha\beta_{jk}$  is the interaction term, and  $\varepsilon_{i(jk)}$  is the random error for each replicate measurement and  $i = 1-5$ . The test for differences between **basin and non-basin** ( $H_{03}$ ) locations



included three basin (B) and three non-basin (NB) stations (Fig. 1.1, Table 1.1). The sampling design blocked basin and non-basin stations (B1 with NB2, B2 with NB3, and B3 with NB4), to control for differing distances from shore. The experiment is a two-way completely random analysis of variance (ANOVA) that is described by the following model:

$$Y_{ijk} = \mu + \alpha_j + \beta_k + \alpha\beta_{jk} + \varepsilon_{i(jk)}$$

where  $Y_{ijk}$  is the measurement for each individual replicate,  $\mu$  is the overall sample mean,  $\alpha_j$  is the main effect for treatments and  $j = 1-3$ ,  $\beta_k$  is the main effect for distance from shore and  $k = 1-3$ ,  $\alpha\beta_{jk}$  is the interaction term, and  $\varepsilon_{i(jk)}$  is the random error for each replicate measurement and  $i = 1-5$ . The test for differences in meiofauna abundance between **canyon and non-canyon** ( $H_{04}$ ) locations included stations from the Mississippi Trough (MT) and adjacent central (C) transect (Fig. 1.1, Table 1.1). Five MT stations were paired with five C stations at five common depth zones, thus removing the effect of depth. Canyon differences were tested using a two-way completely random analysis of variance (ANOVA) that is described by the following model:

$$Y_{ijk} = \mu + \alpha_j + \beta_k + \alpha\beta_{jk} + \varepsilon_{i(jk)}$$

where  $Y_{ijk}$  is the measurement for each individual replicate,  $\mu$  is the overall sample mean,  $\alpha_j$  is the main effect for canyon and  $j = 1-2$ ,  $\beta_k$  is the main effect for depths and  $k = 1-5$ ,  $\alpha\beta_{jk}$  is the interaction term, and  $\varepsilon_{i(jk)}$  is the random error for each replicate measurement and  $i = 1-5$ . The effect of **escarpments** ( $H_{05}$ ) on meiofaunal abundance was tested by

comparing an escarpment transect to a non-escarpment transect (Fig. 1.1, Table 1.1). Six stations per transect were paired at approximately equal distance from shore and distances between stations. The experiment was tested using a two-way completely random analysis of variance (ANOVA) that is described by the following model:

$$Y_{ijk} = \mu + \alpha_j + \beta_k + \alpha\beta_{jk} + \varepsilon_{i(jk)}$$

where  $Y_{ijk}$  is the measurement for each individual replicate,  $\mu$  is the overall sample mean,  $\alpha_j$  is the main effect for transects and  $j = 1-2$ ,  $\beta_k$  is the main effect for distance from first station,  $k = 1-6$ ,  $\alpha\beta_{jk}$  is the interaction term, and  $\varepsilon_{i(jk)}$  is the random error for each replicate measurement and  $i = 1-5$ . Differences in meiofaunal abundance due to overlying **water column primary production** ( $H_{06}$ ) was tested by comparing surface water primary production estimates to meiofauna abundance at 43 stations. Mean biweekly chlorophyll(a) (chl-a) data (SeaWiFS satellite imagery), for the two months prior to community structure sampling (March-April 2000), was plotted against meiofauna abundance, and included in a nonlinear regression and multivariate comparison (see below) of biotic and abiotic variables. Averaging for two months prior to sampling was done to remove small-scale temporal variation

*Multivariate Analysis* – Abiotic variables are often correlated, so it is necessary to create reduced data sets that remove this autocorrelation. Then, these reduced data sets can be correlated with patterns of biotic responses (e.g., abundance). Principal components analysis was used to reduce the environmental variables. Principal components analysis is a procedure to reduce a large set of intercorrelated variables into

a smaller set of orthogonal (completely uncorrelated) variables. Each new variable (principal component) accounts for a percentage of the total variance in the original data set. The new variables are extracted in decreasing order of variance, such that the first few principal components (PC) explain most of the variation in the data set. The contribution of each environmental variable to the new PC is called a load. Typically, the new PC loads can be interpreted to indicate structure in the data set. Each observation contributing to the PC is called a score. Thus, the main advantage of PCA is the generation of station scores, which are interpretable, and can subsequently be used in other analyses (i.e. correlation or regression with abundance).

Environmental variables included in the environmental PCA included chl-a in the overlying water column as measured from SeaWiFS satellite images. Chl-a was adjusted for remineralization with increasing water depth by application of the exponential model proposed by Betzer *et al.* (1984), and updated by Berger *et al.* (1988). The amount of surface chl-a reaching the sea floor is described by the equation:

$$J_{(z)} = 0.409PP^{1.41}/Z^{0.628}$$

where  $J_{(z)}$  is the flux of chl-a transported downwards through some depth  $Z$ , and  $PP$  is the overlying water column chl-a concentration. The remaining variables were all from sediments and included grain size (sand, silt, and clay content), total polycyclic aromatic hydrocarbons (PAH) excluding perylene, the trace metals calcium (Ca), chromium (Cr), tin (Sn), and strontium (Sr), total organic nitrogen (OrgN), particulate organic carbon (POC), dissolved organic carbon (DOC), ammonium (NH<sub>4</sub>), urea, and nitrate (NO<sub>3</sub>).

Prior to analysis all data were transformed to validate assumptions of parametric tests, and to weight then contribution of high or low measurements. The angular transformation ( $x = \arcsin \sqrt{y}$ ) was used for the sediment grain size data, and a natural logarithm transformation ( $x = \log_e[y+1]$ ) was used on all other data.

One common problem with environmental data is that many variables measuring the same effects can skew the result. Thus, pre-analysis was performed to determine if certain classes of variables could be dropped from the analysis. Only the total PAHs was used because it served as a proxy for all organic contaminants. A total of 29 metals were measured and had to be reduced for the final analysis using an initial PCA of metals only. The first metals principal component (PC1) accounted for 70.1% of the total variance in the metals data set, and was the only PC with an eigenvalue greater than one. Thus, four metals, the two with highest positive and negative loadings, were chosen for the final PCA analysis. These four metals (listed above) served as a proxy for the general trace metal pattern seen at all stations.

Non-parametric procedures included multidimensional scaling (MDS) and analysis of similarity (ANOSIM) of meiofauna abundance data, and application of the BIOENV procedure (an analysis that gives maximum Spearman rank correlations between the major taxa abundance matrix and a subset of the most important environmental variables). MDS is often used in lieu of PCA to analyze multivariate abundance data, because this data may not conform to the assumptions of the general linear model (Clarke and Warwick 2001). MDS is a non-parametric method that is

based on similarities or dissimilarities between each observation (sample). The most commonly used similarity index is Bray-Curtis (Clarke and Warwick 2001), which serves to maximize the distances between observations in multidimensional space. Thus, the distances between stations in the MDS plot is proportional their similarities. Analysis of similarity (ANOSIM) is conceptually similar to multivariate analysis of variance (MANOVA), but ANOSIM is not based on the general linear model. ANOSIM can be performed to test for a statistical difference between stations, based on different factors, and was used to test for depth differences in meiofauna major taxa abundance on a Gulf-wide scale. The BIOENV procedure calculates Spearman rank correlations between meiofauna abundance and environmental variables. Thus, it is possible to determine the subset of environmental variables with the highest correlations with meiofauna major taxa abundance.

*Statistical Software* – ANOVA and PCA procedures were accomplished using SAS statistical software (SAS Institute Inc. 1991). Non-parametric MDS and BIOENV procedures, as well as rarefaction indices (ES) were conducted with Primer 5.0 (Primer-E, 2000).

*GIS Spatial Analysis* – Geographic information systems (GIS)-based analyses were performed (ArcView 9.0, ESRI) to further examine spatial trends in the data set. The relative abundance at each station was compared by generating bubble values, where bubble size (the size of circle at each station location) is relative to total meiofauna abundance at each station. Observing spatial trends in meiofauna abundance on a Gulf-

wide scale allows for comparison with physical oceanographic processes (Loop Current, Loop Current eddies, the effect of River inflow, etc.), or other mechanisms that may be interacting to influence the benthic community.

## **RESULTS**

### **Sampling Issues**

*Core size comparison* – More organisms were found in progressively larger cores (Table 1.2). But, there were no statistically significant differences for abundances of total meiofauna ( $P = 0.6324$ ), nematodes ( $P = 0.7800$ ), harpacticoids ( $P = 0.3385$ ) and other taxa ( $P = 0.8238$ ) among different core sizes. Thus, even though total abundance (adjusted for unit area) in the smallest core was about half that found in the three larger cores, it was not statistically different. Because each core yielded the same abundance estimate, total counts per core were used to choose the appropriate core size. For statistical purposes, it is imperative to obtain  $> 30$  organisms per taxa per sample. Therefore, the 5.5 cm core was chosen for the benthic survey.

*Sediment sampling depth* – Nearly all meiofauna were found in surface sediments and no meiofauna were found below 13 cm sediment depth, so just the top 13 cm are plotted (Fig. 1.2). Most organisms were found in the top 3 cm. A total of 87% of total meiofauna were in the top 3 cm, and 97% of the harpacticoid copepods. In addition, 77% of the harpacticoid copepods were found in the top 1 cm. Because the distribution is so skewed to the surface, it was decided to sample the top 3 cm only during the benthic

community survey cruise. Because harpacticoid copepods were so restricted to the top 1 cm, the core was split into 2 sections: 0 - 1 cm and 1- 3 cm.

*Box core comparison* – There were no statistically significant differences for abundances of total meiofauna ( $P = 0.2281$ ), nematodes ( $P = 0.0632$ ), harpacticoids ( $P = 0.9999$ ) and other taxa ( $P = 0.1988$ ) among different box core types. Because of convenience, the GOMEX boxcore (Boland and Rowe 1991) was used throughout the study.

### **General Results**

A total of 586 samples from 51 stations in the study yielded  $1.71 \times 10^5$  individuals from 21 meiofauna taxa. Samples were collected from a depth range of 200-3700 meters in the northern Gulf of Mexico. Mean abundance (extrapolated to number of individuals per  $m^2$ ,  $Nm^{-2}$ ) per station was  $2.63 \times 10^5 Nm^{-2}$ , with standard deviation of  $2.01 \times 10^5$  (calculated from Table 1.3). Maximum and minimum meiofauna abundances were found at stations MT1 and JSSD3 with values of  $9.46 \times 10^5$  and  $0.60 \times 10^5 Nm^{-2}$ , respectively (Table 1.3). A strong linear relationship exists between log abundance ( $R^2 = 0.658$ ,  $P < 0.0001$ ) water depth (Fig. 1.3). Spatial variability in meiofauna abundance (bubble size representing relative abundance) indicates highest values in the shallow northeastern stations (Figs. 1.4). Relatively lower abundance was observed in the western transects, but the general trend of decreasing abundance was consistent along western transects (RW & W), and in the west-central area (WC5, WC12, B1-B3, NB2-NB5). Exceptionally high abundance was found at stations MT1, MT3, S35, S36, S42 and C7,

all located in the northeast region at depths ranging from approximately 450 - 1900 m. Variation from the general pattern of decreasing abundance with depth was observed at these northeastern stations.

The meiofauna community was composed of individuals from 21 taxonomic groups (Table 1.4). Nematoda and Harpacticoida (including nauplii) were the two dominant groups accounting for 65.3 and 25.4% of individuals, respectively. Unknown fauna were the next most abundant, comprising 6.6% of individuals. The unknown group likely included representatives from various soft-bodied taxa including (but not limited to) various taxa within the Turbellaria and representatives of the Protista (e.g., Ciliophora). Soft-bodied taxa, such as these, often become unrecognizable during bulk fixation with buffered formaldehyde. The remaining 3.7% of the meiofauna community was composed of representatives from various taxa, including: Polychaeta, Kinorhyncha, Ostracoda, Cyclopoida, Tardigrada, Tanaidacea, Nemertinea, Acari, Isopoda, Bivalvia, Gastrotricha, Anthozoa, Priapulida, Gastropoda, Aplousobranchia, Rotifera, Sipuncula, and Loricifera (Table 1.4). The complete major taxa data set is not presented here, but will be publically accessible from the Geochemical & Environmental Research Group (<http://www.gerg.tamu.edu/>) upon completion of the DGoMB final report (Rowe *et al.*, in prep).

The number of major taxa decreased with increasing water depth (Fig. 1.5). The expected number of major taxa per 1000 individuals [ES(1000)], follows a quadratic pattern, where major taxa diversity is maximized at stations just over 1000 meters, and



then decreases with increasing depth (Fig. 1.6). This pattern is also observed when only non-dominant taxa are considered (Fig. 1.7). The ES(20) for non-dominant taxa (excluding nematodes, harpacticoids, nauplii, and polychaetes) follows a similar quadratic pattern, but major taxa diversity is maximized at stations around 1800 meters, decreasing thereafter.

### **Univariate Analysis**

*Hypothesis Testing* – In the test for differences over depth and longitude ( $H_{01}$  &  $H_{02}$ ), significant main effects for longitude and depth were observed ( $P < 0.0001$ , Table 1.5), as well as a significant longitude by depth interaction term ( $P < 0.0001$ , Table 1.5). The two western transects (RW and W) had a gradual (very linear) decrease in abundance with depth (Fig. 1.8). With increasing proximity to the Mississippi River, (transects C and MT) abundance increases greatly at stations between 300 and 1000 meters (Fig 1.8). The Florida slope transect (S) has highest abundance at station S36 (ca. 2000 meters), which is located in the DeSoto Canyon. Transects become more similar with increasing depth, with abundance being very similar at all stations  $> 2500$  meters water depth (Fig. 1.8).

In the test for differences between basin and adjacent non-basin stations ( $H_{03}$ ), no significant difference was observed between main effects ( $P = 0.5421$ , and  $P = 0.7773$ , Table 1.5), and no significant interaction was observed ( $P = 0.6980$ , Table 1.5).

In the test for differences between canyon and adjacent non-canyon stations ( $H_{04}$ ), significant treatment ( $P = 0.0059$ ) and depth zone ( $P < 0.0001$ ) effects were observed (Table 1.5), but a significant interaction term was also observed ( $P = 0.0058$ , Table 1.5). Abundance is elevated at the head of the canyon (MT1 & MT3) compared to stations of similar depth in the adjacent transect (C1 & C7) (Fig. 1.9). However, the two transects become increasingly similar with depth, and show no differences at stations greater than 1500 meters (Fig. 1.9).

In the test for differences in meiofauna abundance due to the presence of an escarpment ( $H_{05}$ ), no significant escarpment effect was observed in comparison to the reference transect ( $P = 0.791$ ). However, a significant main effect was observed for distance from shore ( $P < 0.0001$ , Table 1.5), and a significant interaction term was observed ( $P = 0.002$ , Table 1.5). Abundance was dramatically lower below the Florida Escarpment than above (Fig. 1.10). Station S41 had nearly twice the abundance of stations S40 and S39, which are of similar depth, but further offshore. Comparison to the reference transect in the western gulf (stations W1-W6) illustrates deviation of the escarpment transect from an expected decrease in abundance along a relatively constant slope, with elevated abundance just above and below the escarpment (Fig. 1.10).

The amount of overlying water column chl-a biomass that reaches the sea floor decreases in a log-log relationship with depth (Fig. 1.11A). Meiofauna abundance increases with increasing overlying water column chl-a biomass (Fig. 1.11B). Although considerable variability exists in the linear regression ( $R^2 = 0.413$ ), the relationship is

significant ( $P < 0.0001$ ). Accordingly, meiofauna had a moderate, and significant relationship with sediment POC concentration (Fig. 1.12,  $R^2 = 0.331$ ). Although null hypothesis six ( $H_{06}$ ) was not tested with ANOVA as above, detailed analysis of the meiofauna community with respect to food availability and sediment environmental variables was accomplished with multivariate procedures (see below).

### **Multivariate Analysis**

*Principal Components Analysis* – In the PCA, the first three principal components accounted for 61.5 percent of the total variance in the data set (Table 1.6). However, four PCs out of 15 had eigenvalues greater than one, which means the first four were significant. The sign of variable loads (negative or positive) indicates gradients in concentrations. Variables that load negatively will have highest concentrations for negative PC loads with decreasing concentrations moving in the positive direction, and vice versa. PC1 accounted for 33.5% of the total variance, had high positive loadings by clay, total PAH's, tin, chromium, and high negative loadings by sand, strontium and calcium (Table 1.7, Fig. 1.13A). PC1 is interpreted as the **sediment properties**, with high silt, clay, organic (PAH) and metal (Cr and Sn) contaminants near the Mississippi River, and higher sand and natural background metals (Ca and Sr) with increasing distance from the Mississippi River.

PC2 accounted for 16.7% of the total variance and highly positive loadings by chl-a and POC, weak positive loadings by OrgN and  $\text{NH}_4^+$ , and weak negative loadings by  $\text{NO}_3^-$  and urea (Table 1.7, Fig 1.13A). PC2 is interpreted as **particulate organic**

**matter (POM) flux.** PC3 accounted for 11.3% of the total variance and had highly positive loadings by DOC, and highly negative loadings by urea (Table 1.7, Fig. 1.13B). PC4 accounted for 10.2 % of the total variance and had moderate positive loadings by silt,  $\text{NH}_4^+$ ,  $\text{NO}_3^-$ , and PAH (Table 1.7). However, PC3 and PC4 did not have obvious interpretations. PCs 1-4 were regressed against abundance to determine if they were significantly related to the biotic community. PC1 had a weak, but significant, positive relationship with meiofauna abundance, but accounted for only 22% of the variance in the biotic data set (Fig. 1.14A,  $R^2 = 0.215$ ). PC2 had a moderate, and significant, relationship with meiofauna abundance (Fig. 1.14B,  $R^2 = 0.303$ ). PC3 and PC4 did not have significant relationships with abundance.

*Multidimensional Scaling* – MDS ordination of meiofauna major taxa abundance (Fig. 1.15) condenses multivariate station similarities into a two-dimensional plot, where distances between stations are proportional to their similarities (Bray-Curtis similarity). MDS analysis of major taxa abundance data shows a strong trend with depth (Fig. 1.16). Depth zones of 1000-meter depth increments group together with only moderate overlap. Two groups can be defined, one representing stations less than 2000 m, a second group greater than 2000 meters (Fig. 1.16). These two groups are statistically different by ANOSIM ( $P < 0.01$ ). The depth trend is a reflection of decreasing abundance of the dominant taxonomic groups, for example Nematoda (Fig. 1.17), where the bubble value is proportional to nematode abundance. Variation in the MDS vertical dimension (i.e. not reflecting depth) is due to minor taxonomic groups that do not follow the general

pattern of decreasing abundance with increasing depth, for example the Tardigrada (Fig. 1.18). POC also influences the MDS pattern, which can be observed by overlaying bubble values proportionate to variable concentration (Fig. 1.19). POC concentration also follows the MDS depth trend, and reflects decreasing food supply, and therefore abundance, with increasing water depth.

*BIOENV Procedure* – The final abiotic-biotic matching analysis was performed using the BIOENV procedure (Primer-E Ltd). This process is conceptually similar to regressing environmental PC's against meiofauna abundance, but is more informative in that Spearman rank correlation values are generated for multiple pairs of abiotic variables. The BIOENV procedure was performed on the major taxa similarity matrix (Bray-Curtis, with 4<sup>th</sup> root transformation), allowing up to 5 variables in the output. Highest Spearman rank correlation (0.474) was found with 5 variables: chl-a, POC, OrgN, Cu and P. Second highest correlation (0.467) was found with 4 variables: chl-a, POC, OrgN, and Cu.

## **DISCUSSION**

Meiofauna are ubiquitous in all marine ecosystems and especially prominent in soft-sediment communities (Coull and Bell 1979; Hicks and Coull 1983; Giere 1993), including the deep sea (Soltwedel 2000). However, most ecological studies of deep sea community structure have been focused on macro- or megafaunal-sized organisms (Etter and Mullineaux 2001). But, ecological literature since 1971 has shown that meiofauna are different from macrofauna and have different roles in marine ecosystems (for reviews

see: Coull and Bell 1979, Coull and Palmer 1984, Giere 1993). Even where meiofauna share ecological properties with macrofauna the processes operate on much smaller spatial and shorter temporal scales for the meiofauna (Bell 1980). Regardless of size, the distributions of organisms and how they respond to topographic, geochemical, any physical forcing features is largely unknown for deep-sea environments (Etter and Mullineaux 2001). Therefore, the purpose of the current study was to integrate the physical complexity of the northern Gulf of Mexico continental slope with environmental variables, in a hypothesis-based study, in order to more fully understand the processes controlling meiofauna abundance.

Meiofauna abundance is significantly correlated with water depth (Figs. 1.3, Table 1.5), a trend that has been observed worldwide (Soltwedel 2000, and references therein). Depth related trends are attributed to a decreasing supply of organic matter with increasing depth and distance from land (Thiel 1978; Pfannkuche 1993; Danovaro *et al.* 1995; Gooday 1996; Relexans *et al.* 1996; Soltwedel 1997; Fabiano and Danovaro 1999; Shimanaga and Shirayama 2000; Gooday 2002). This general pattern is observed in the Northern Gulf of Mexico (Figs. 1.3 & 1.4), but some variability exists that may be attributed to physical and geological complexity of the continental slope and interactions with overlying water column processes.

A significant longitude by depth interaction ( $P < 0.0001$ , Table 1.5), indicates that meiofauna abundance changes differently with depth depending on proximity to Mississippi River outflow (Fig. 1.8). Maximum abundance values were observed in the

Mississippi Trough (Fig. 1.4). Mississippi River outflow brings nutrients that drive overlying primary production, but also carries terrigenous organic matter, further fueling benthic secondary production (Meybeck 1993). Highest meiofauna abundance values within the Mississippi Trough also correspond with a significant canyon effect ( $P = 0.006$ ), compared to the adjacent C transect (Fig. 1.9). Although not included in the statistical analysis for canyon effects, station S36, which lies in the DeSoto Canyon, also has unusually high abundance; further evidence that canyon features support higher meiofaunal standing stocks (Figs. 1.4). On the contrary, basin features do not support higher meiofauna abundance compared with adjacent non-basin areas ( $P = 0.542$ ). This is not surprising because the basin/non-basin regions of the Texas/Louisiana slope lie west of Mississippi River influence, which is deflected to the east by the Loop Current and Coriolis forces.

The effect of the Florida Escarpment on meiofauna abundance, in comparison to a reference transect, had a highly significant interaction with distance from shore. The significant interaction indicates that meiofauna abundance responds differently to precipitous depth increases, compared to gradual depth increases. Spatial analysis using GIS (Fig. 1.4), and comparison to the reference transect in the Western Gulf (Fig. 1.10), both indicate abundance “hot spots” directly above (S42) and below (S41) the escarpment, confirming the *a priori* hypothesis. Deflection of the Loop Current to the East by Coriolis forces results in current impingement on the escarpment, which likely results in advection of nutrients and organic material from Mississippi River inflow and

additionally could create upwelling or downwelling zones along the escarpment, depending on the depth of the current. Upwelling would bring new nutrients to the surface and enhance surface primary production; conversely, downwelling could facilitate advected surface primary and secondary production to the benthos. Meiofauna abundance at station S42 is two fold greater than stations S43 and S44 (Fig. 1.10). Meiofauna abundance is greatly enhanced in the vicinity of the escarpment compared to the relatively constant Texas/Louisiana slope (Fig. 1.10).

Although a direct comparison of photosynthetic pigments within the benthic boundary layer water column was not possible due to a lack of CTD data, meiofauna abundance was compared to surface water chl-a biomass estimates by SeaWiFS satellite imagery, adjusted for remineralization with depth (Berger *et al.* 1988) (Fig. 1.11B). Meiofauna abundance had a significant relationship with adjusted chl-a biomass (Fig. 1.11B). It is not surprising that highest chl-a biomass is observed in the vicinity of the Mississippi Trough, corresponding to highest meiofauna abundance. Estimates of chl-a biomass by satellite imagery should be interpreted with caution. SeaWiFS accuracy is quite high and acceptable for blue water environments with little or no river plume influence (Hu *et al.* 2003). On the contrary, stations with high river plume influence tend to be overestimated due to the presence particulate inorganic and organic matter in terrestrial runoff. All DGoMB stations were in blue water, but occasional interactions with Loop Current eddies in the Mississippi Trough region, which results in offshore



advection of turbid shelf water (Hu *et al.* 2003), could have resulted in slight overestimation of chl-a biomass in this region.

Benthic-pelagic coupling has been well studied in recent investigations (reviewed by Gooday 2002). Abundance and body size of benthic metazoan and protistan fauna have both been correlated with overlying chloroplastic pigment equivalents. However, seasonal responses to food pulses have not been well demonstrated for metazoan meiofauna in deep-sea environments (Pfannkuche 1992, 1993). Soltwedel *et al.* (1996) observed seasonal changes in nematode body length and volume. Shimanaga and Shirayama (2000) found that meiofauna abundance fluctuated seasonally, but they were not able to confirm statistical differences between seasons. Bacteria and Foraminifera show much more pronounced responses to pulses of phytodetritus. Lochte (1992) found that bacteria standing stocks were capable of doubling from spring to summer months following the spring bloom. Likewise, benthic Foraminifera production is highly responsive to food pulses (Gooday *et al.* 1992). Slower responses by metazoan meiofauna suggest slower population turnover times and life cycles on the order of one year (Soltwedel *et al.* 1996).

Previous deep-sea investigation has found that abundance is regulated by numerous spatial and temporal factors, including: depth (Soltwedel 2000), current regimes (Thiel 1975; Eckman and Thistle 1991), seasonal variations in primary production (Thiel *et al.* 1987), and bottom-up (regulated by primary production) (Rieper 1978) or top-down (regulated by predation) (Marinelli and Coull 1987) trophic

interactions. Several previous studies have compared biological communities with environmental variables in a multivariate design (Shirayama 1984a; Gray *et al.* 1990; Warwick and Clarke 1991; Montagna and Harper 1996; de Skowronski and Corbisier 2002; and others). Multivariate analysis generally involves a parametric procedure to analyze continuous data (i.e., environmental variables), *sensu* Montagna and Harper (1996), and non-parametric procedures to detect differences in community structure (*sensu* Warwick and Clarke 1991).

PCA of environmental variables indicates that stations differ with respect to geochemistry, trace metal concentration, grain size, and organic contaminants (Figs. 1.14A & B), depending on their proximity to Mississippi River outflow. Regression of environmental PC1 (sediment properties) against meiofauna abundance (Fig. 1.14A) indicated that this component accounted for 22% of the variance in the meiofauna standing stock. Differences in sediment grain size and heterogeneity have been previously shown to influence meiofauna abundance (Gerlach 1977; Coull *et al.* 1982); with a trend toward increasing meiofauna abundance in silt dominated sediments, as observed here for stations with positive PC1 scores (Fig. 1.14A). Sediment porosity greatly affects vertical meiofauna distribution, with deeper dwelling organisms in sandy or calcareous ooze environments compared to clay-dominated sediments (Shirayama 1984b). Although a few northern Gulf of Mexico stations highly sandy sediments (S43, S44, W2, W3, and MT5), most stations had moderate sand and clay, and low silt, except stations near Mississippi River outflow, which had high silt (Bryant, DGoMB data) and

highest meiofauna abundance. Given the nature of NGOM sediments, it is not surprising that most metazoan meiofauna reside in above the 3-cm sediment depth horizon (Fig. 1.2). Meiofauna and other benthic organisms are concentrated into surface sediments (Thiel 1972; Coull *et al.* 1977; Dinet & Vivier 1977; Vivier 1978; Shirayama 1984b), which has been attributed to food and oxygen availabilities (Ansari *et al.* 1980; Shirayama 1984b) resulting from differing sediment regimes.

Meiofauna abundance was more strongly related to environmental PC2 (POM flux), which accounted for 30% of the variance in meiofaunal abundance (Fig. 1.14B). Meiofauna respond to organic matter input (Thiel 1978; Pfannkuche 1993; Danovaro *et al.* 1995; Gooday 1996; Relexans *et al.* 1996; Soltwedel 1997; Fabiano and Danovaro 1999; Vanaverbeke *et al.* 2004). Recent investigations over the North Sea continental shelf have observed significant temporal changes in nematode abundance and diversity (both species and functional diversity) with spring bloom phytodetrital deposition (Vanaverbeke *et al.* 2004).

Although the current study did not have a temporal component, non-parametric MDS analysis (Figs. 1.15-1.19) revealed differences in major taxa community composition. The MDS station ordination (Fig. 1.16) reflects decreasing abundance of dominant taxa, e.g., Nematoda (Fig. 1.17) and Harpacticoida (not shown) with depth. However, minor taxonomic groups are less affected by the depth gradient with greatest numbers of individuals at mid-bathyal to lower bathyal, e.g., Tardigrada (Fig. 1.18). The expected number of major taxa per 1000 individuals (ES[1000]) for all taxa (Fig. 1.6),

and expected number of major taxa per 20 individuals (ES[20]) for non-dominant taxa (Fig. 1.7), follow the previously observed parabolic relationship with maximum diversity in the mid-bathyal and decreasing diversity moving into abyssal environments (Paterson and Lambshead 1995; Etter and Mullineaux 2001, and references therein; Lambshead *et al.* 2002; and others). Maximum diversity of non-dominant taxa is found nearly 1000 meters deeper (Fig. 1.7), compared to all taxonomic groups combined (Fig. 1.6), suggesting a reduction in dominance by nematodes and harpacticoids with depth.

Comparison of major meiofaunal abundance with environmental variables via the BIOENV procedure closely matched the results generated from regressing abundance versus environmental principal components. The greatest Spearman rank correlation (0.474) corresponded with five variables chl-a, POC, OrgN, Cu, and P. Overlaying POC concentration on the MDS abundance ordination reveals a similar pattern of decreasing POC with increasing depth. Shirayama (1984a) used stepwise regression analysis to discriminate important from unimportant environmental factors, and found that two variables, organic carbon and calcium carbonate, were able to account for 64% of the variance in the dataset (i.e.,  $r = 0.80$ ). Alongi and Pichon (1988) used simple correlation analysis and found significant relationships between metazoan meiobenthos and bacterial abundance, ciliate abundance, chlorophyll, and phaeopigments.

Spatial analysis of meiofaunal abundance (Fig. 1.4) across the entire NGOM reveals strong differences between northwestern and northeastern stations, which was confirmed by a significant depth by longitude interaction (Table 1.5, Fig. 1.8). The

northwestern GOM is also characterized by very regular patterns of seasonal primary production, with winter chl-a maxima (December - February), and summer chl-a minima (Müller-Karger *et al.* 1991). In comparison, the northeastern GOM has high biweekly variations in surface chl-a biomass, even throughout summer months (Hu *et al.* 2003; Belabbassi *et al.*, in revision). Differences in surface water chl-a biomass between northwestern and northeastern regions of the GOM are attributed an interaction between two factors; 1) the presence of the Loop Current, which enters the GOM through the Yucatan Straights and turns anticyclonically exiting the GOM through the Florida Straights (Schmitz 2004), and 2) Mississippi River outflow in the northeastern GOM, which averages 1 billion m<sup>3</sup> d<sup>-1</sup> (<http://water.usgs.gov>).

Loop Current eddies impinge onto the continental slope and shelf in the northeastern GOM resulting in lateral transport of low salinity/high chl-a waters from the shelf over the slope (Qian *et al.* 2003; Belabbassi *et al.*, in revision). Offshore transport of shelf waters over the slope can influence underlying benthic communities by stimulating greater overlying water column primary production, by lateral input terrigenous organic matter, or lateral input of organic matter produced over the shelf. Loop current eddies were regularly observed in the northeastern GOM in the months prior to and during community structure sampling (Rowe *et al.*, in prep).

Canyon and escarpment features in the northeastern GOM also interact to enhance meiofaunal abundance (Table 1.5, Figs. 1.9 and 1.10, respectively). Large topographical features likely interact to create flows that alter food supply (Gage and

Tyler 1991; Etter and Mullineaux 2001), and therefore increases abundance (Thistle *et al.* 1985, 1991). High shallow and mid-depth abundance in the Mississippi Trough and DeSoto Canyon, respectively, suggest canyon features have a concentrating effect on POM flux. Loop Current, or Loop Current eddy impingement on the Florida Escarpment (Schmitz 2004) creates a high energy hydrodynamic environment as observed by shipboard ADCP (Acoustic Doppler Current Profiler) current profiles during sampling cruises (Rowe *et al.*, in prep). Therefore, it is not surprising that meiofauna abundance was greatly enhanced directly above and below the Florida Escarpment (Figs. 1.4 & 1.10).

## **CONCLUSION**

Meiofauna abundance in the northern Gulf of Mexico deep sea is regulated by interactions between sediment characteristics and POM flux, which are related to Mississippi River outflow, physical oceanographic circulation processes, and the complex topographic nature of the continental slope. Meiofauna abundance is significantly related to water depth, but also exhibits significant longitudinal differences resulting from proximity to Mississippi River outflow. Canyon features in proximity of Mississippi River outflow were found to greatly enhance meiofauna abundance. The Florida Escarpment interacts with Mississippi River outflow and the Loop Current to enhance meiofauna abundance at stations lying directly above and below the escarpment. Multivariate comparisons of meiofauna abundance with environmental variables reveals a strong Mississippi River influence. River outflow alters local sediment characteristics,

and interacts with loop current eddies and dynamic slope topography to increase POM flux in the northeastern region, thus creating meiofauna abundance hot spots. In contrast, northwestern Gulf of Mexico stations exhibited a typical bathymetric pattern of decreasing abundance with depth, and basin features west of Mississippi River influence did not support enhanced abundance. Therefore, the meiofauna community in the northern Gulf of Mexico deep sea is regulated by complex spatial interactions between Mississippi River outflow, physical oceanographic processes, and the physical complexity of the continental slope, which regulate the supply of particulate organic matter to the sea floor.

Table 1.1: Summary of meiofauna community structure experimental design: null hypotheses, design criteria, and stations included in analysis.

Null Hypotheses	Design Criteria	Stations Included	No. Stations
$H_{01}$ & $H_{02}$ : Depth & longitude	Five replicate transects spanning the entire northern GOM continental slope, over five depths	MT1, 3-6 RW1-2, 4-6, AC1 C1, 4, 7, 12, 14 W1, 3-6 S35-37, 39, 44	25
$H_{03}$ : Basin/non-basin	Three basin stations, three non-basin stations, over three distances from shore	B1-3 NB2-4	6
$H_{04}$ : Canyon/non-canyon	Two replicate transects over five depths	MT1, 3-6 C1, 4, 7, 12, 14	10
$H_{05}$ : Escarpment/non-escarpment	Two replicate transects over six distances from shore	S39-44 W1-6	12



Table 1.2: Effect of core tubes size (inner diameter) on meiofauna counts and average density. Based on five replicates taken at station W-2. Abundance is detransformed from natural log (ln), so taxa averages do not sum to the total average.

	<b>Counts (<i>n</i>/core)</b>				<b>Abundance (<i>n</i>/10 cm<sup>2</sup>)</b>			
<u>Core Size (cm i.d.)</u>	2.2	3.1	5.5	6.7	2.2	3.1	5.5	6.7
<u>Taxa</u>								
Nematodes	20.2	64.8	161.0	219.0	31.3	59.4	50.5	54.3
Harpacticoids	5.4	30.8	74.2	99.4	2.3	26.1	20.8	24.4
Nauplii	7.2	38.6	72.2	85.6	0.2	29.2	22.9	19.0
Others	12.2	14.0	27.8	45.8	3.6	14.5	8.5	10.6
Total	45.0	148.2	335.2	449.8	54.0	135.7	111.3	112.2

Table 1.3: DGoMB station locations, depth, and average meiofaunal abundance (five replicate cores) for pooled taxonomic groups.

<b>Station</b>	<b>Latitude</b>	<b>Longitude</b>	<b>Depth (m)</b>	<b>Abundance (N m<sup>-2</sup>)</b>
AC1	26.393567	-94.573082	2440	129974
B1	27.202542	-91.405218	2253	157417
B2	26.550012	-92.215082	2635	139907
B3	26.164445	-91.735100	2600	155817
BH	27.780000	-91.500000	545	407852
C1	28.059838	-90.249917	336	369129
C12	26.379730	-89.240298	2924	138792
C14	26.938238	-89.572505	2495	146578
C4	27.453150	-89.763083	1463	273585
C7	27.730437	-89.982033	1066	542119
GKF	27.000000	-90.250000	2460	84348
HIPRO	28.550000	-88.580000	1565	343118
JSSD1	25.000000	-92.000000	3545	87547
JSSD2	23.500000	-92.000000	3725	87295
JSSD3	24.750000	-90.750000	3635	60441
JSSD4	24.250000	-85.500000	3400	63451
JSSD5	25.500000	-88.250000	3350	135698
MT1	28.541110	-89.825018	482	945657
MT2	28.447925	-89.671945	677	535216
MT3	28.221510	-89.494045	990	885995
MT4	27.827605	-89.166145	1401	246058
MT5	27.332838	-88.656065	2267	128964
MT6	27.001648	-87.999130	2743	155312
NB2	27.134833	-92.000068	1530	168276
NB3	26.558033	-91.822550	1875	165245
NB4	26.246750	-92.392287	2020	148409
NB5	26.245400	-91.209908	2065	117263
RW1	27.500142	-96.002847	212	411809
RW2	27.254027	-95.746807	950	219457
RW3	27.008356	-95.492362	1340	248752
RW4	26.751420	-95.250175	1575	232842
RW5	26.507527	-94.996722	1620	170633
RW6	25.997303	-94.495578	3000	144453
S35	29.335152	-87.046363	668	501629
S36	28.918513	-87.672150	1826	799963

<b>Station</b>	<b>Latitude</b>	<b>Longitude</b>	<b>Depth (m)</b>	<b>Abundance (N m<sup>-2</sup>)</b>
S37	28.553627	-87.766848	2387	291179
S38	28.279947	-87.327592	2627	157164
S39	27.483675	-86.999815	3000	83170
S40	27.839477	-86.751415	2972	99501
S41	28.013642	-86.573348	2974	181408
S42	28.251003	-86.419270	763	492537
S43	28.502943	-86.076790	362	276279
S44	28.749993	-85.747703	212	318516
W1	27.577165	-93.551005	420	387228
W2	27.413927	-93.340328	625	263315
W3	27.172397	-93.323293	875	262642
W4	26.730823	-93.319727	1460	187806
W5	26.267772	-93.332723	2750	104552
W6	26.002845	-93.320277	3150	124166
WC12	27.323242	-91.555810	1175	218447
WC5	27.775912	-91.765678	348	412061

Table 1.4: Average abundance (AA), percent contribution (Contrib.%), and cumulative percent contribution (T%) of meiofauna major taxa per core (5.5 cm i.d.). Data summarized for all 51 stations (five replicates per station).

<b>Taxa</b>	<b>AA</b>	<b>Contrib.%</b>	<b>T%</b>
Nematoda	415.0	65.3	65.3
Nauplii	74.8	13.1	78.4
Harpacticoida	74.0	12.3	90.7
Unknown	37.3	6.6	97.3
Polychaeta	12.5	1.5	98.8
Kinorhyncha	2.7	0.3	99.1
Ostracoda	2.7	0.3	99.5
Cyclopoida	2.1	0.2	99.6
Tardigrada	1.0	0.1	99.8
Tanaidacea	0.8	0.1	99.9
Nemertinea	0.6	0.1	99.9
Acari	0.3	0.0	100.0
Isopoda	0.3	0.0	100.0
Bivalvia	0.2	0.0	100.0
Gastrotricha	0.1	0.0	100.0
Anthozoa	0.1	0.0	100.0
Priapulida	0.1	0.0	100.0
Gastropoda	0.0	0.0	100.0
Aplacophora	0.0	0.0	100.0
Rotifera	0.0	0.0	100.0
Sipuncula	0.1	0.0	100.0
Loricifera	0.0	0.0	100.0

Table 1.5: ANOVA results, tests for differences in meiofauna abundance. Dependent variable =  $\log_{10}(N+1)$ . ANOVA abbreviations: DF = degrees of freedom, SS = sum of squares, MS = mean square, F = F-test value, P = Pr > F. Factor abbreviations: long. = longitude, basin = basin vs. non-basin stations, dfs = distance from shore, escarp. = escarpment vs. non-escarpment transects.

Source	DF	SS	MS	F	P
<b>H<sub>01</sub> &amp; H<sub>02</sub> – Depth/Longitude</b>					
Long.	4	1.222	0.305	12.07	<.0001
Depth	4	5.867	1.467	57.94	<.0001
Long.*Depth	16	3.104	0.194	7.67	<b>&lt;.0001</b>
Error	100	2.531	0.025		
<b>H<sub>03</sub> – Basins</b>					
Basin	1	0.012	0.012	0.38	0.5421
DFS	2	0.016	0.008	0.25	0.7773
Basin*DFS	2	0.023	0.011	0.37	0.6980
Error	56	1.708	0.031		
<b>H<sub>04</sub> – Canyons</b>					
Canyon	1	0.167	0.167	8.58	0.0059
Depth	4	3.931	0.982	50.41	<.0001
Canyon*Depth	4	0.338	0.085	4.34	<b>0.0058</b>
Error	36	0.702	0.019		
<b>H<sub>05</sub> – Escarpment</b>					
Escarp.	1	0.001	0.001	0.07	0.7906
DFS	5	2.998	0.600	50.51	<.0001
Escarp.*DFS	5	0.279	0.056	4.70	<b>0.0015</b>
Error	46	0.546	0.012		

Table 1.6: Eigenvalues of the Correlation Matrix for the environmental PCA, proportion of variance explained by each principal component, and cumulative variance.

	<b>Eigenvalue</b>	<b>Difference</b>	<b>Proportion</b>	<b>Cumulative</b>
1	5.019	2.504	0.335	0.335
2	2.515	0.818	0.168	0.502
3	1.697	0.162	0.113	0.615
4	1.535	0.606	0.102	0.718
5	0.929	0.077	0.062	0.780
6	0.851	0.217	0.057	0.837
7	0.635	0.044	0.042	0.879
8	0.591	0.060	0.039	0.918
9	0.530	0.218	0.035	0.954
10	0.312	0.111	0.021	0.974
11	0.201	0.066	0.013	0.988
12	0.135	0.105	0.009	0.997
13	0.030	0.017	0.002	0.999
14	0.014	0.008	0.001	1.000
15	0.005	0.000	1.000	1.000

Table 1.7: Variable loads for the rotated (Varimax) factor pattern of the environmental PCA.

	<b>Factor1</b>	<b>Factor2</b>	<b>Factor3</b>	<b>Factor4</b>	<b>Factor5</b>
Chla	0.11096	0.90356	-0.00047	0.08619	0.03993
Sand	-0.76437	0.21025	0.20489	-0.19623	-0.48221
Silt	0.43118	-0.03573	0.05246	0.65701	0.25268
Clay	0.65541	-0.28278	-0.27347	-0.09372	0.52084
NH4	-0.26511	0.35890	0.18627	0.66324	0.12841
POC	-0.04478	0.81893	0.06908	0.05581	0.08796
UREA	0.01605	-0.14464	-0.80871	-0.09793	0.09566
NO3	-0.19939	-0.49356	-0.21657	0.53803	-0.07637
DOC	-0.09904	-0.03622	0.87375	-0.00081	-0.06273
OrgN	-0.00531	0.27374	-0.10288	0.11126	0.88406
TPAHWP	0.55797	0.14311	0.14306	0.55440	-0.19339
Ca	-0.87212	-0.30214	0.09420	-0.23840	0.02223
Sr	-0.85733	-0.25022	0.14018	-0.20549	0.05741
Cr	0.86572	-0.12582	-0.06502	-0.16531	0.09411
Sn	0.83863	-0.00196	0.14965	-0.17825	-0.01304

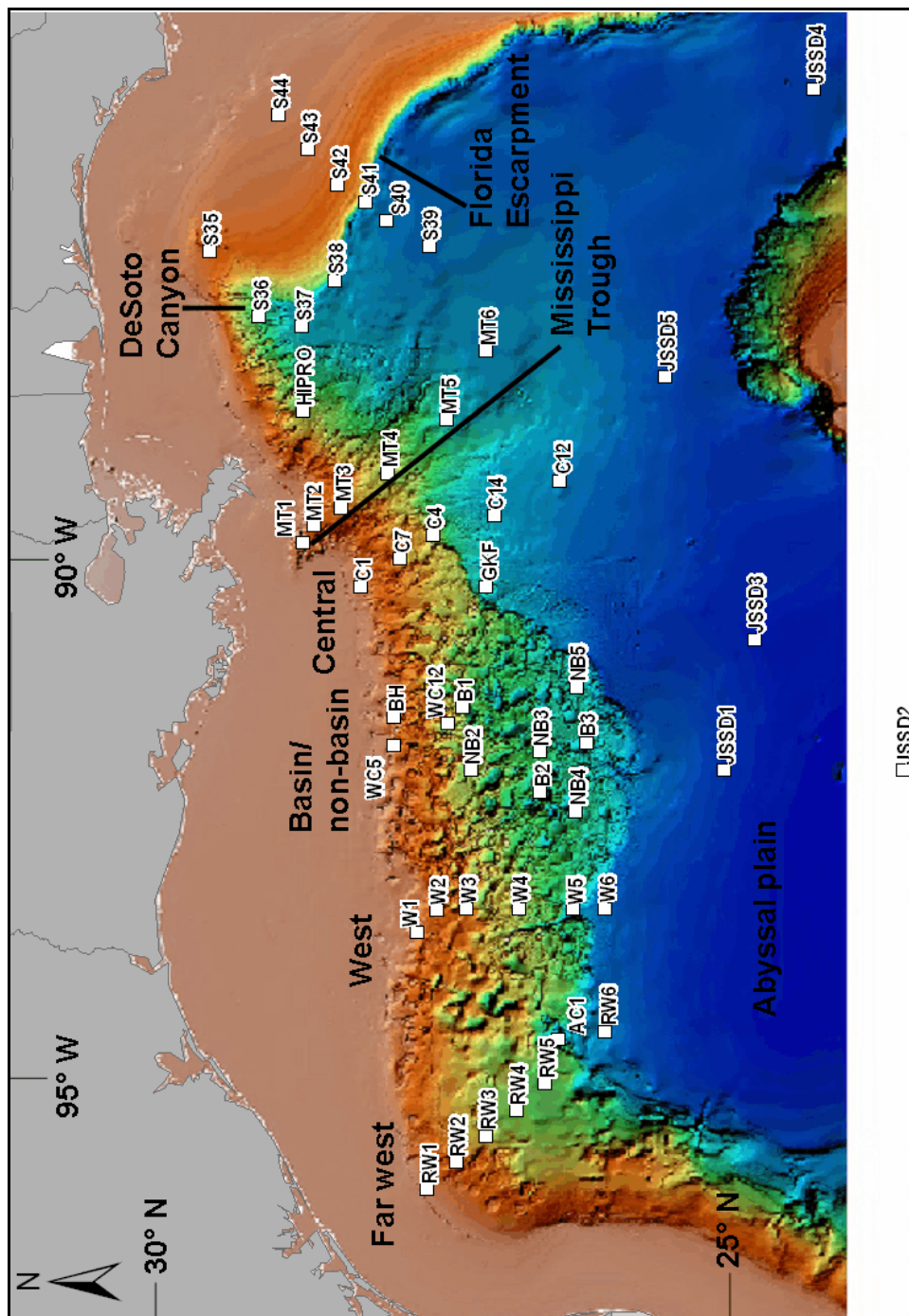


Figure 1.1: DGoMB station locations in the northern Gulf of Mexico deep sea. Note transect and topographic feature descriptions.



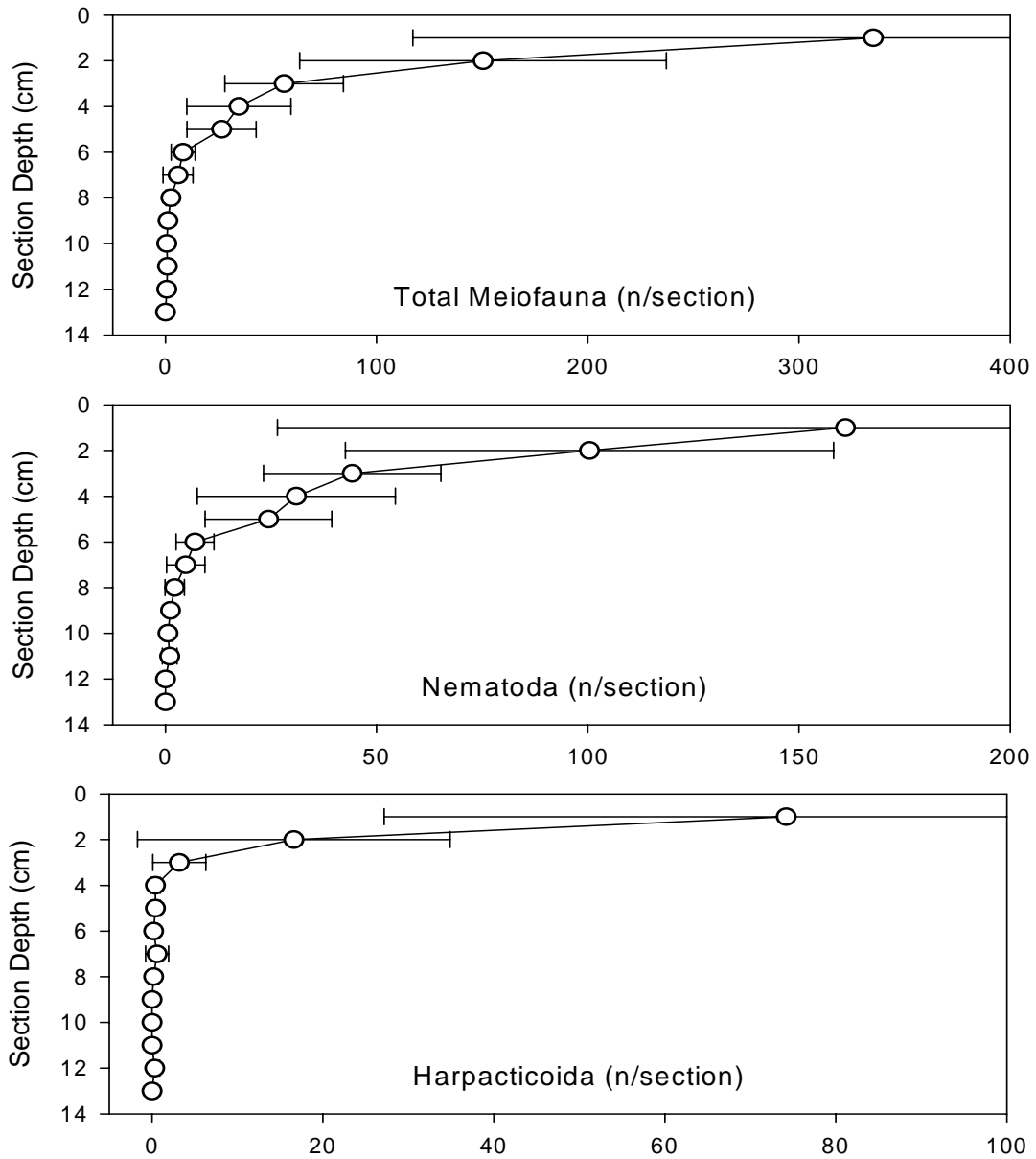


Figure 1.2: Vertical distribution of meiofauna taxa from sediment cores collected at station W2 for Shakedown Cruise. Cores were sectioned in 1-cm increments, and fauna were enumerated from each 1-cm section. Plotted data is the average of five replicates (error bars = standard deviation).

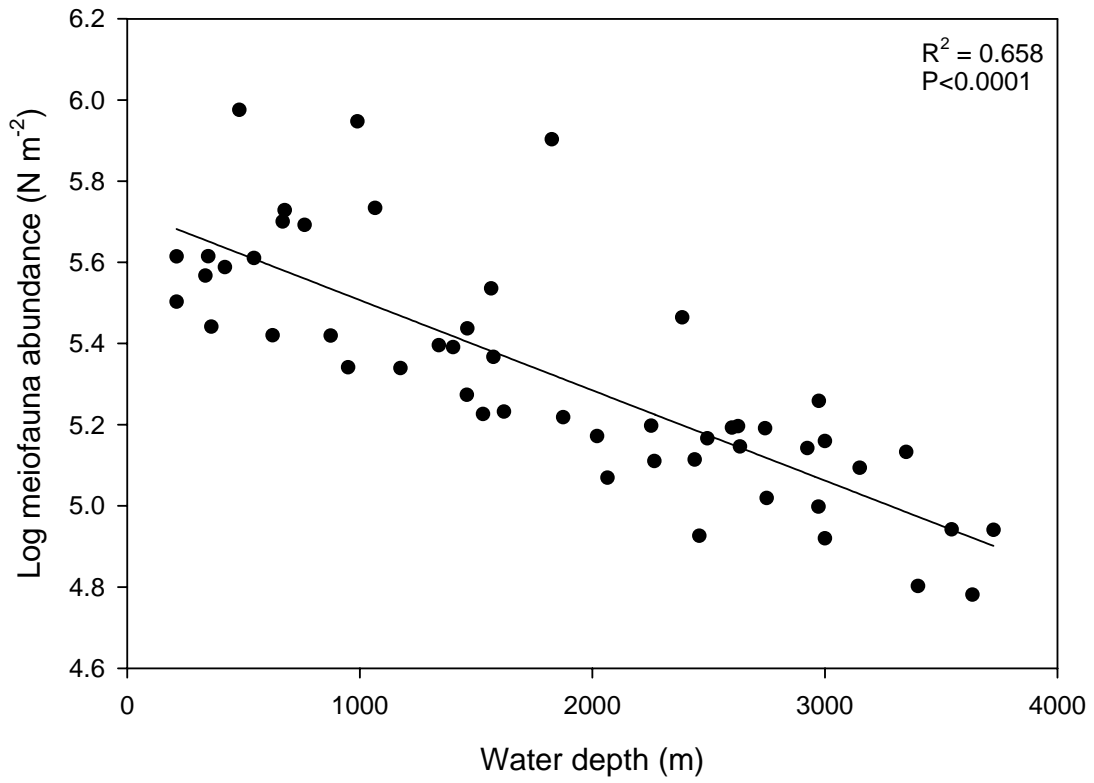


Figure 1.3: Log (x+1) transformed meiofauna abundance (N m<sup>-2</sup>) versus water depth (m) for all stations sampled during DGoMB project.

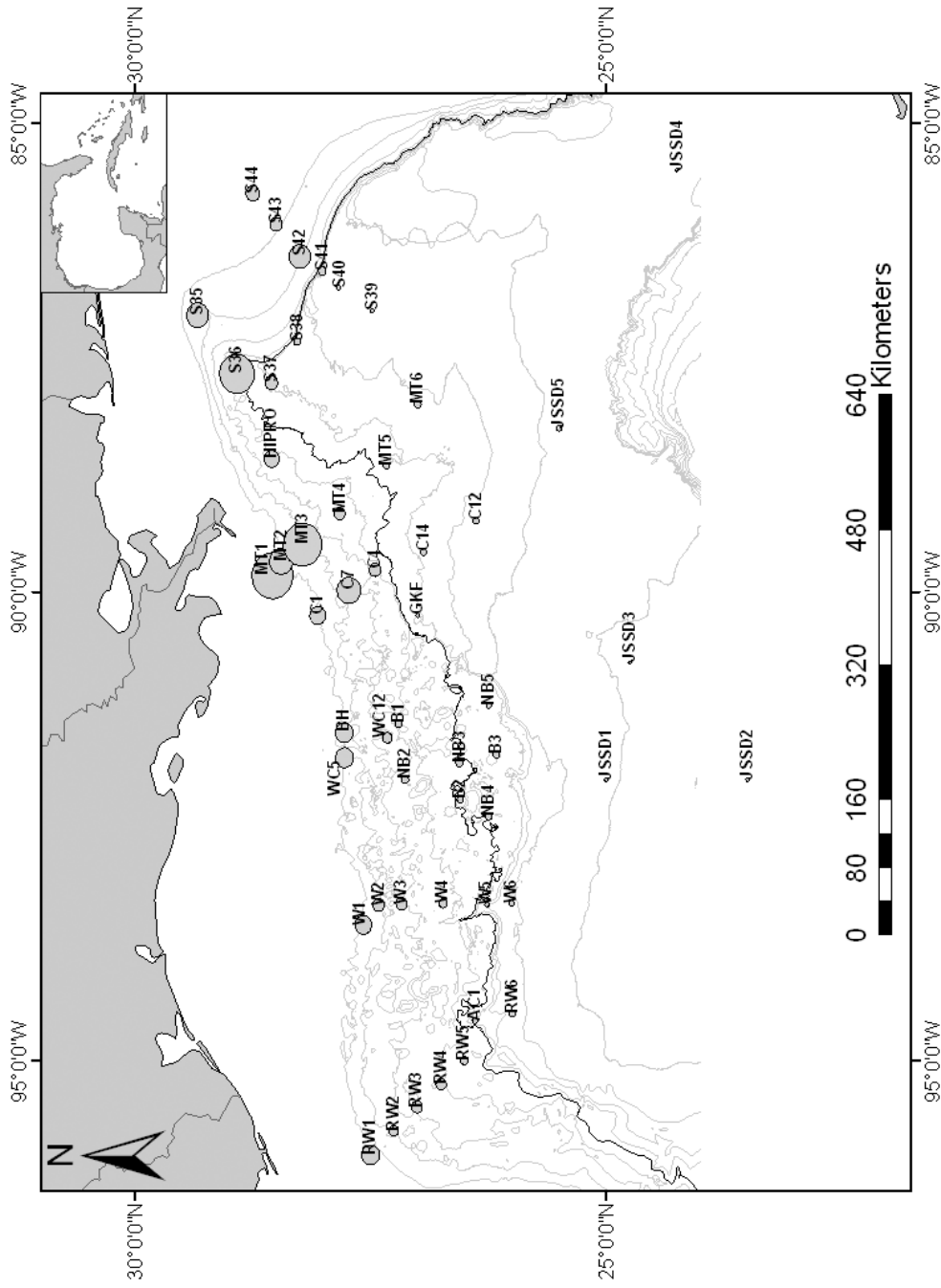


Figure 1.4: Spatial analysis of meiofauna abundance ( $N\ m^{-2}$ ) at all DGoMB stations. Buffer size equals relative meiofauna abundance. The highlighted contour equals 2000 meters.

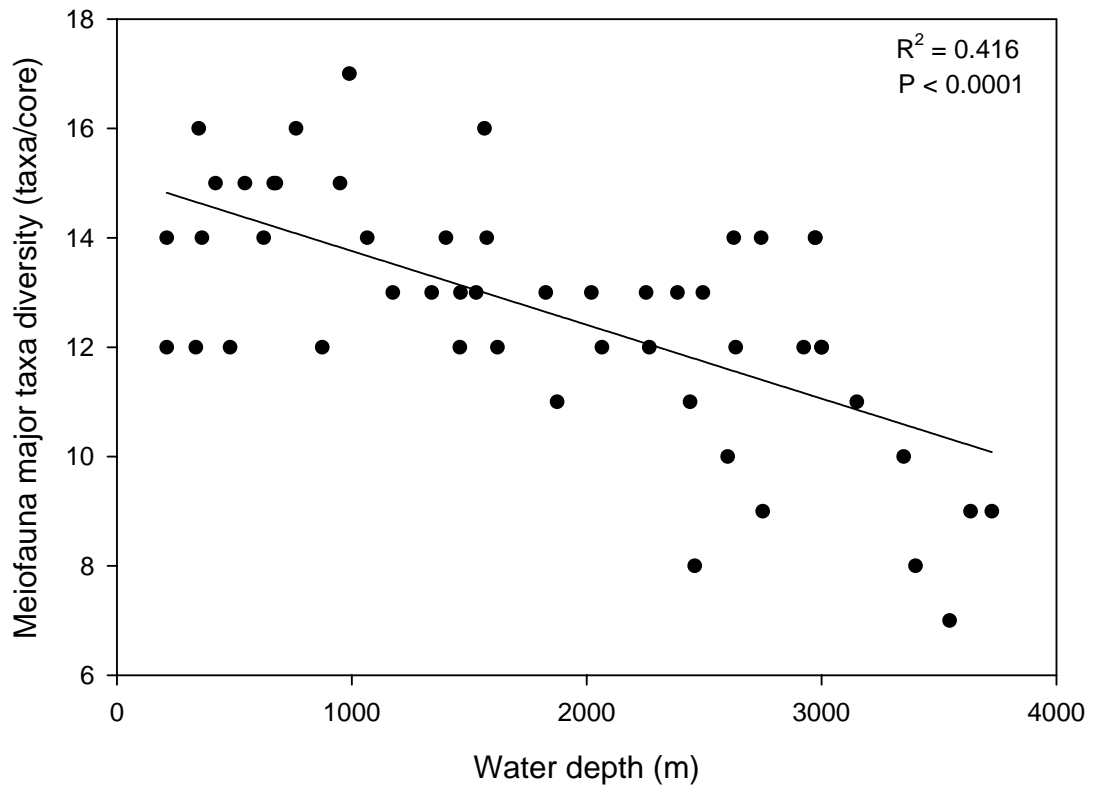


Figure 1.5: Number of major meiofauna taxa per core as a function of water depth.

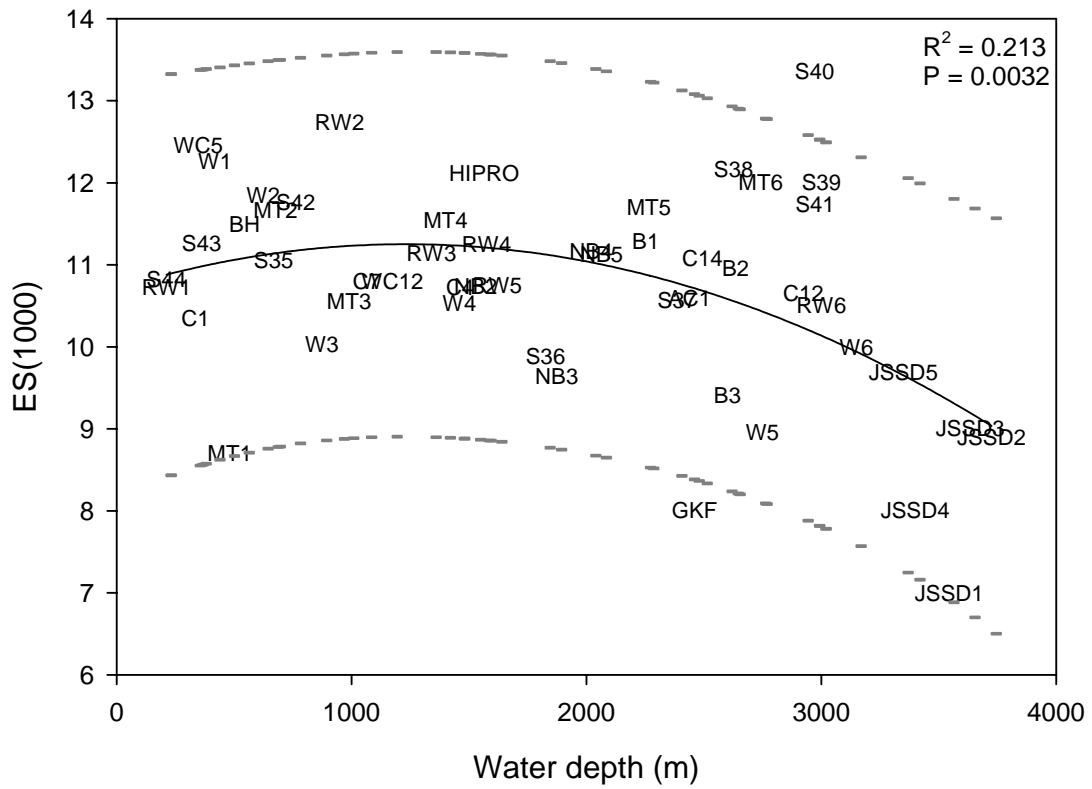


Figure 1.6: Expected number of taxa per 1000 individuals [ES(1000)] as a function of water depth, and quadratic regression. Dashed lines = 95% confidence intervals.

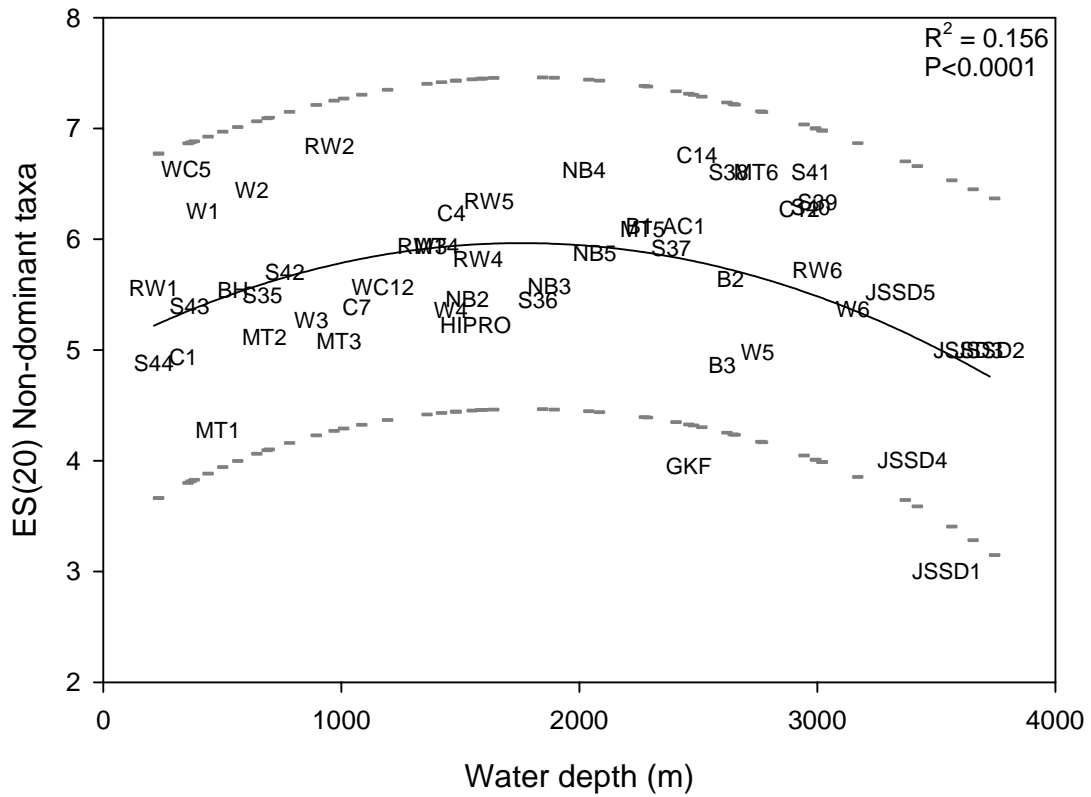


Figure 1.7: Expected number of taxa per 20 individuals [ES(20)] for non-dominant meiofauna taxa (excluding nematodes, harpacticoid copepods, harpacticoid nauplii, and unknowns). A quadratic regression was fit to the data (dashed lines = 95% confidence intervals).

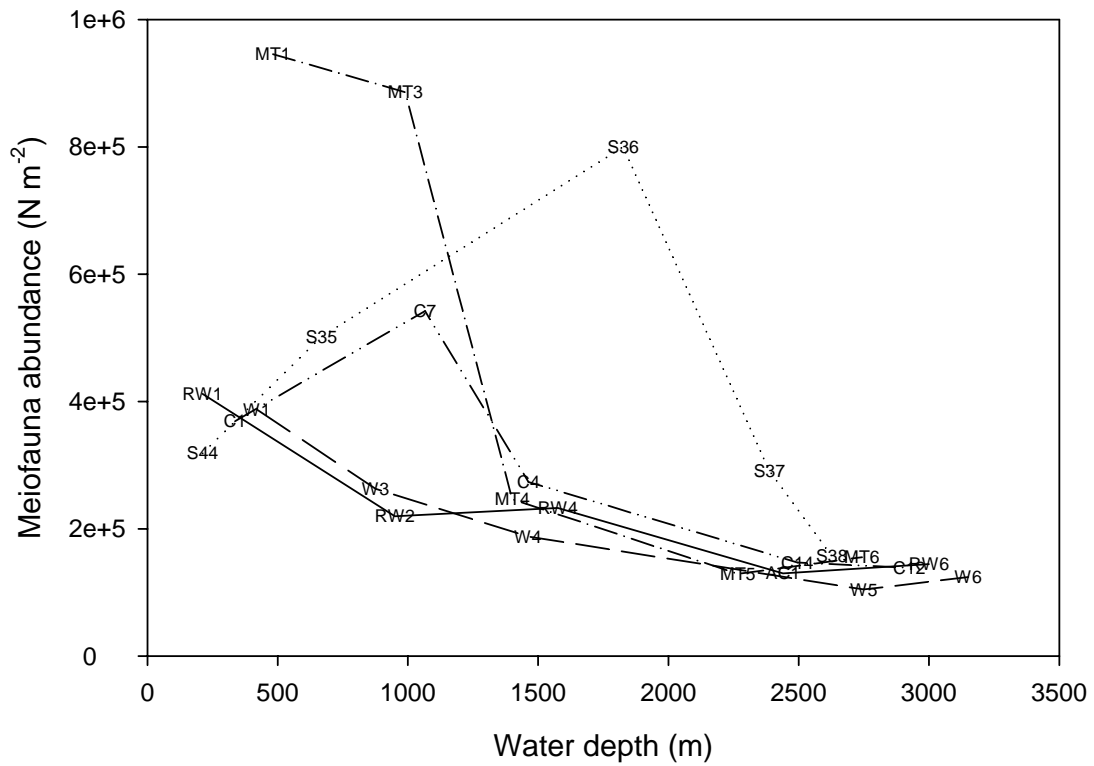


Figure 1.8: Meiofauna abundance ( $N m^{-2}$ ) as a function of depth for transects included in the test for differences over depth and longitude ( $H_{01}$  &  $H_{02}$ ).

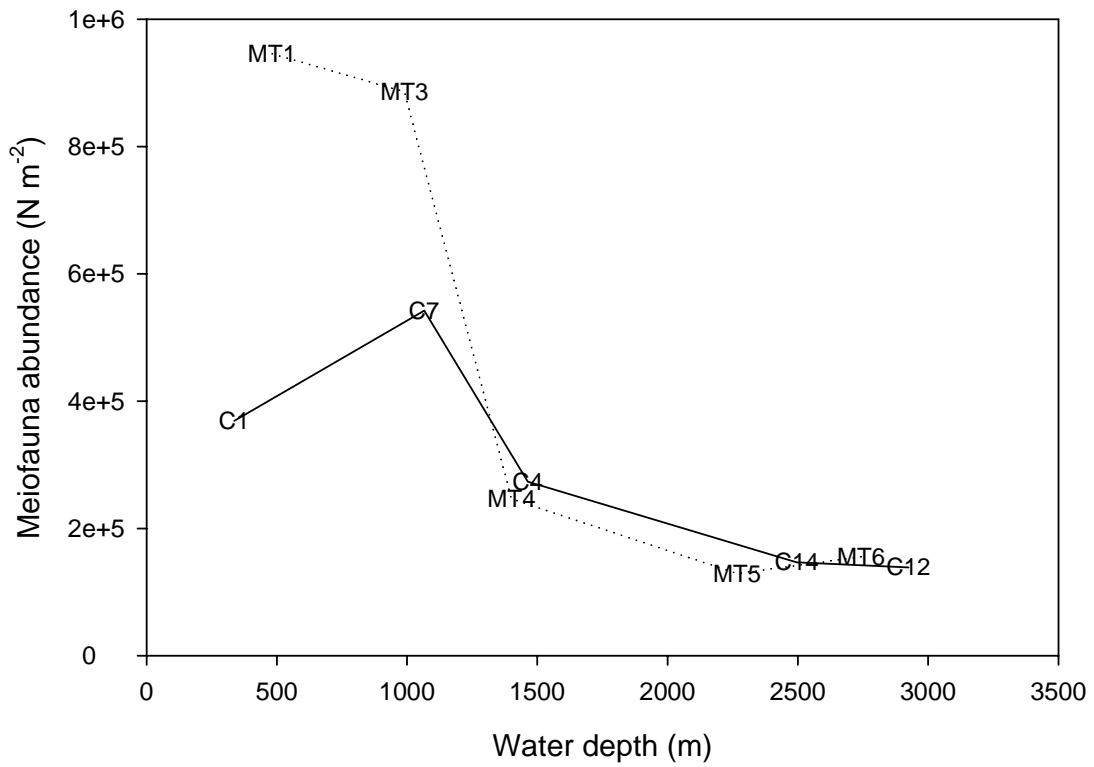


Figure 1.9: Comparison of meiofauna abundance ( $N m^{-2}$ ) on two parallel transects to determine abundance differences related to canyon (MT transect) versus non-canyon (C transect) areas ( $H_{04}$ ).



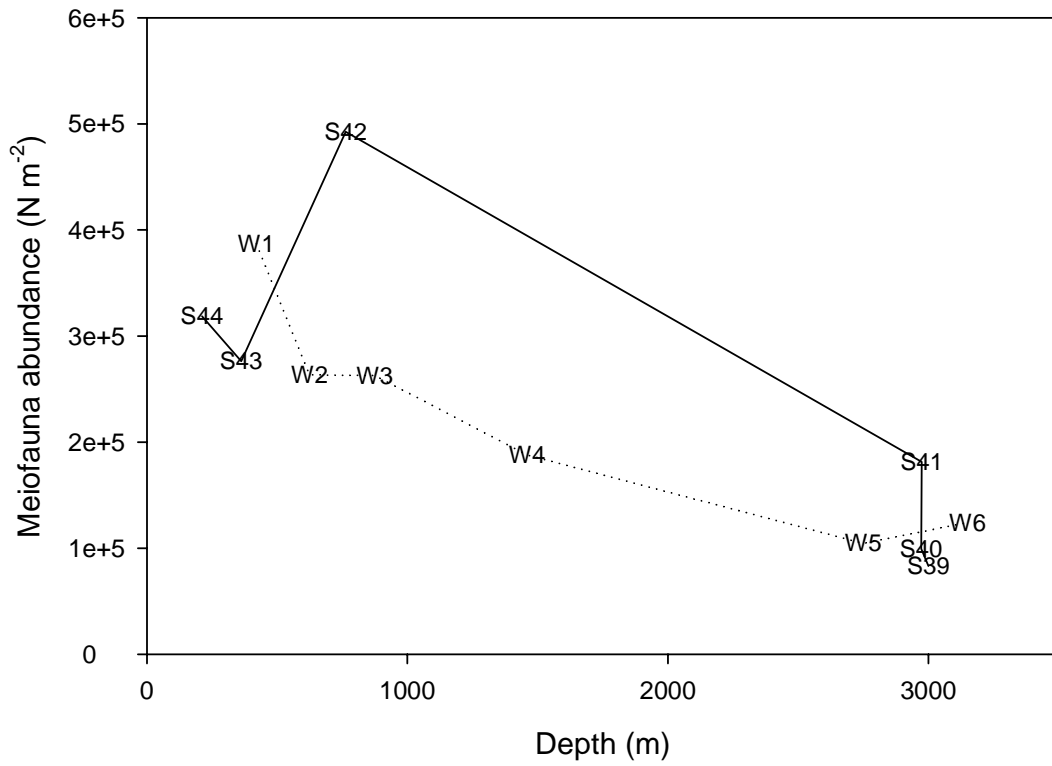


Figure 1.10: Comparison of meiofauna abundance and a function of water depth along two transects to determine abundance differences related to the Florida Escarpment (S39-S44) versus a reference transect (W1-W6).

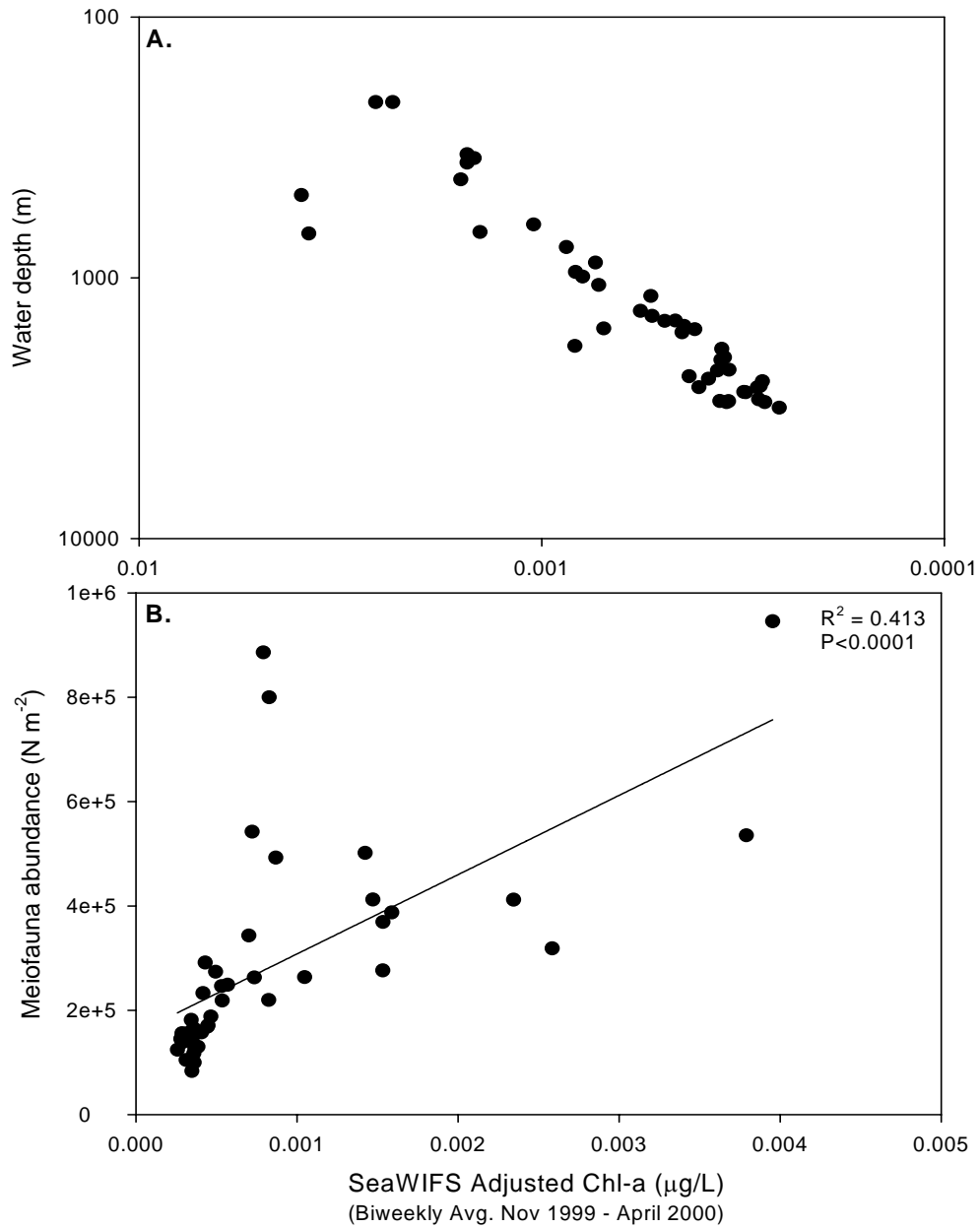


Figure 1.11 SeaWIFS chl-a ( $\mu\text{g/L}$ ) biweekly average (November 1999 through April 2000). Chl-a concentration was adjusted for remineralization with depth (see Berger *et al.* 1988). A) Log-Log relationship of adjusted chl-a with depth, and B) Meiofauna abundance versus adjusted chl-a.

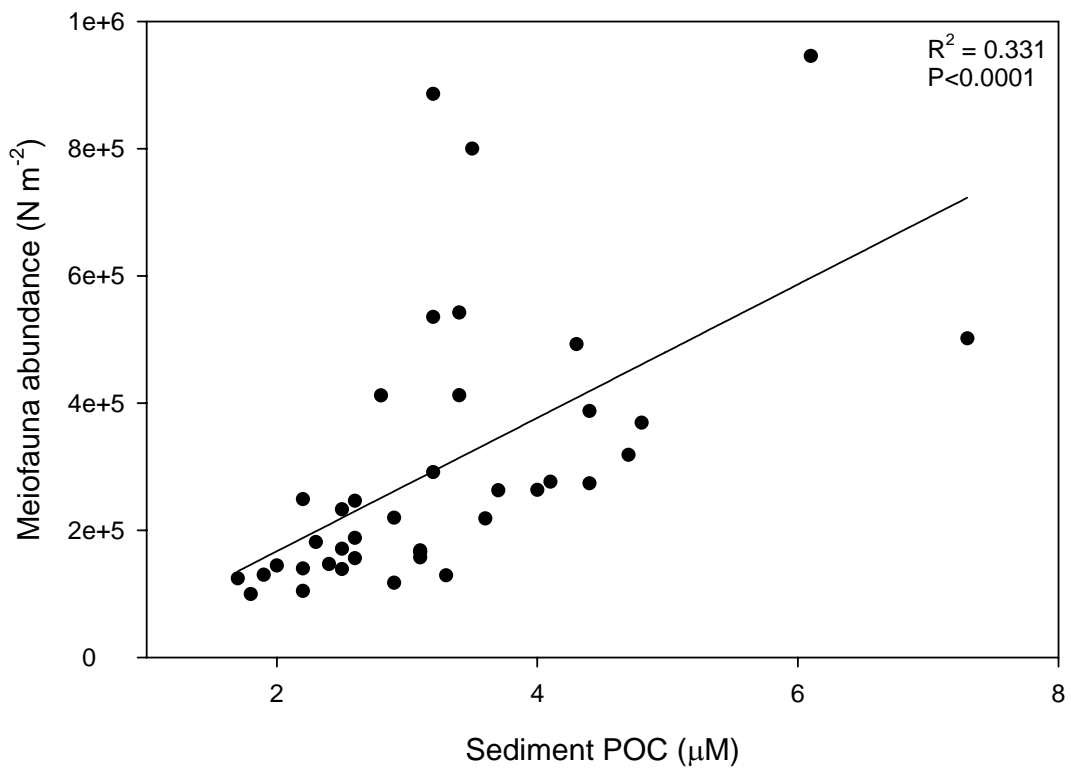


Figure 1.12: Meiofauna abundance ( $N m^{-2}$ ) as a function of sediment particulate organic carbon (POC).

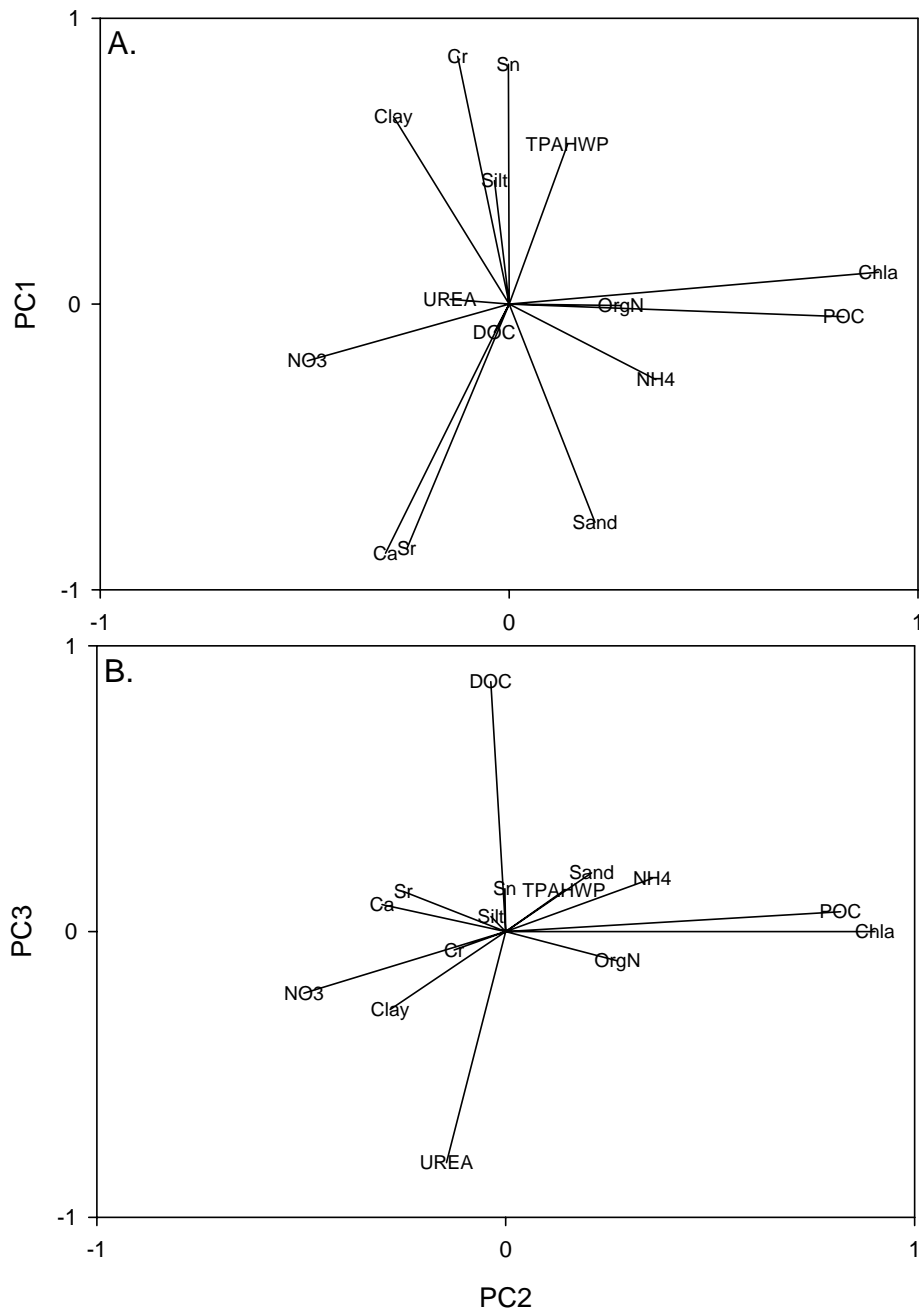


Figure 1.13: Principal components analysis of environmental variables, A) variable loading scores for PC1 versus PC2, B) variable loading scores for PC2 versus PC3.

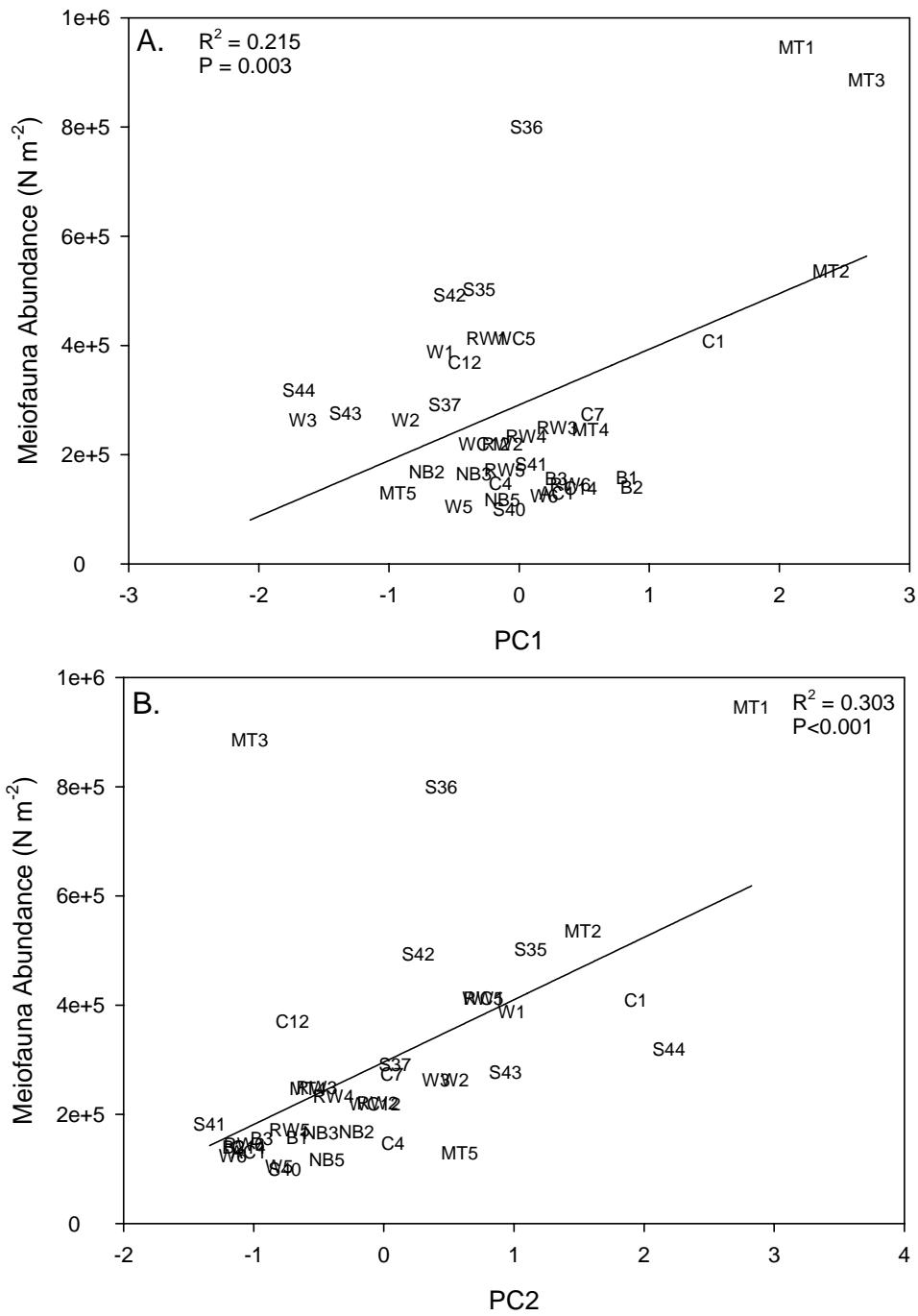


Figure 1.14: Meiofauna abundance ( $N m^{-2}$ ) regressed against environmental PC1 (A), designated “sediment properties,” and environmental PC2 (B), “POM Flux.”

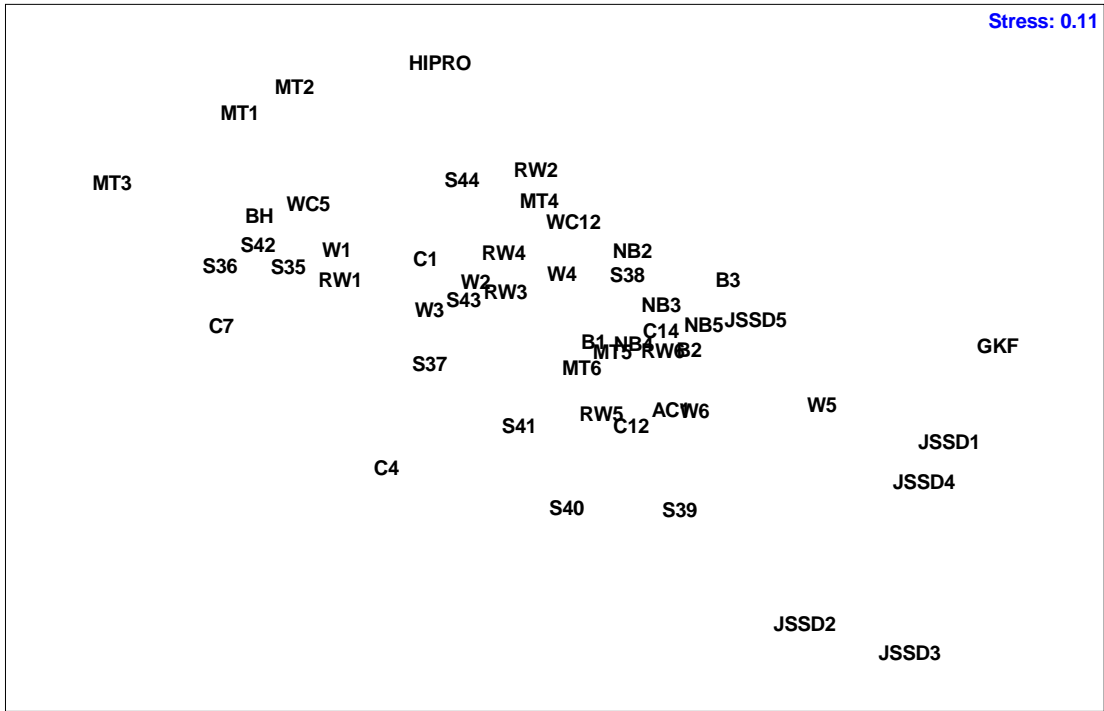


Figure 1.15: MDS ordination of DGoMB stations, based on Bray-Curtis similarity (4<sup>th</sup> root transformation) of major taxa abundance.



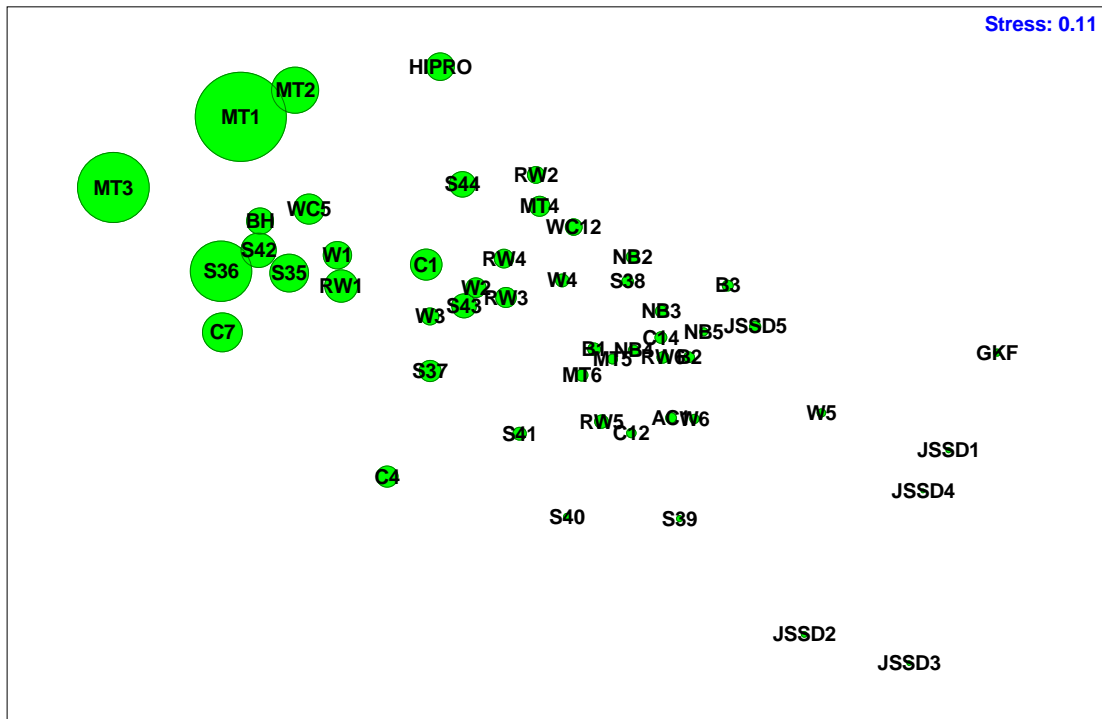


Figure 1.17: MDS ordination of DGoMB stations, based on Bray-Curtis similarity (4<sup>th</sup> root transformation) of major taxa abundance. Bubble size equals relative nematode abundance at each station. The MDS plot strongly represents decreasing abundance with depth.



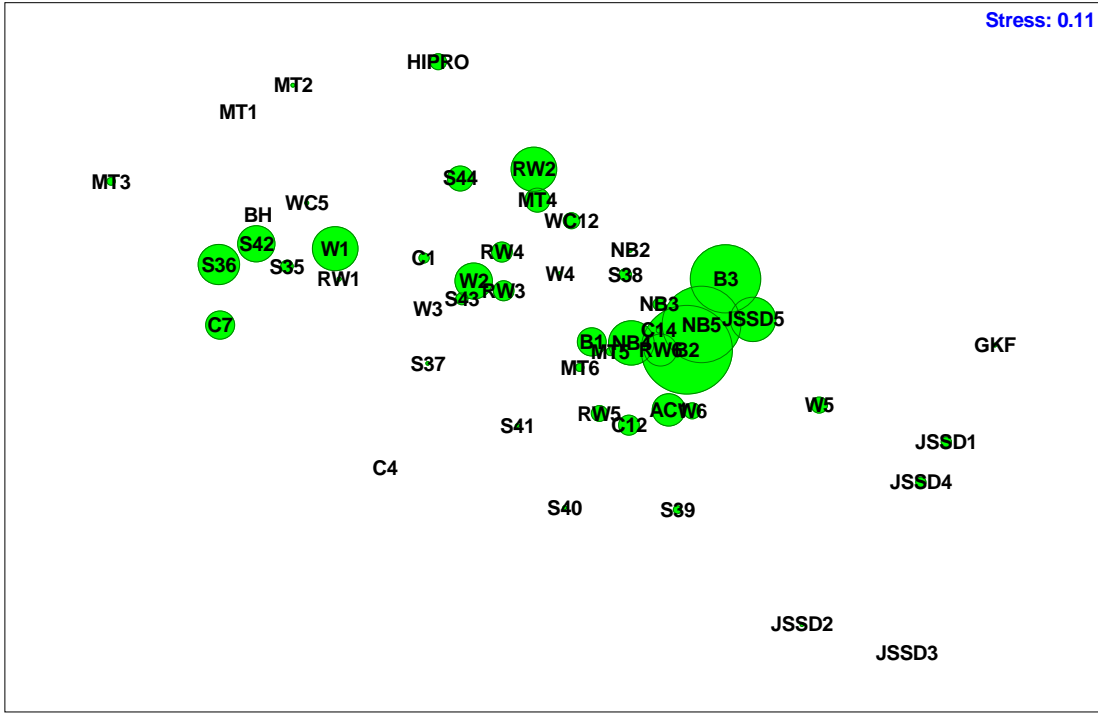


Figure 1.18: MDS ordination of DGoMB stations, based on Bray-Curtis similarity (4<sup>th</sup> root transformation) of major taxa abundance. Bubble size equals relative abundance of Tardigrada at each station. Tardigrades were one of the major taxonomic groups that did not follow the general pattern of decreased abundance with depth.

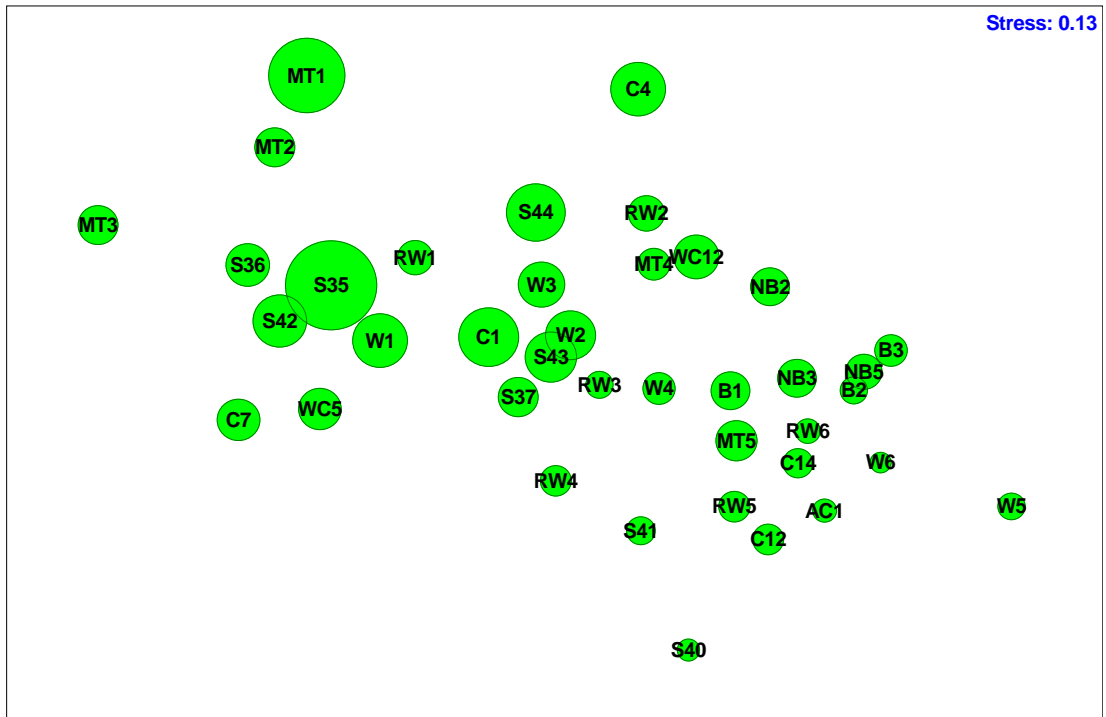


Figure 1.19: MDS ordination of DGoMB stations, based on Bray-Curtis similarity (4<sup>th</sup> root transformation) of major taxa abundance. Bubble size equals relative particulate organic carbon (POC) concentration.

**CHAPTER 2: SPATIAL AND BATHYMETRIC TRENDS IN HARPACTICOIDA  
(COPEPODA) COMMUNITY STRUCTURE IN THE NORTHERN GULF OF MEXICO  
DEEP SEA**

**ABSTRACT**

The deep sea has been a focus of intense research because of its vast size and importance in global biogeochemical cycles, and because it has been shown to have a highly diverse fauna. Meiofauna are ubiquitous in marine soft-sediment communities, are often dominant in deep-sea sediments, and have incredible phylogenetic diversity. Harpacticoida (Copepoda) are the second most abundant taxon within the meiofauna and an important component of deep-sea meiofaunal communities. The northern Gulf of Mexico is a dynamic environment with complex continental shelf topography and longitudinal gradients of water column primary production due to Mississippi River outflow. Harpacticoid copepod community structure was analyzed at 43 stations in the northern Gulf of Mexico deep sea to test regional and bathymetric patterns of diversity. Harpacticoid copepod diversity is significantly related to depth and longitude. Most stations have unique species compositions, suggesting high regional (2700 species) and global ( $10^5$  -  $10^6$  species) diversity by extrapolation. Although highest diversity, in terms of expected number of species (rarefaction), is found at approximately 1200 meters, average taxonomic and average phylogenetic diversity continue to increase with depth, indicating greater morphological or functional diversity. Multivariate analysis reveals

significant inverse relationships between diversity and POM flux, which are confirmed by a significant region-scale depth and longitude differences. However, within versus between station variability suggests an interaction between small and region-scale processes maintaining high diversity.

## **INTRODUCTION**

Harpacticoida, an order within the subclass Copepoda, is comprised of individuals ranging in size from 0.2 to 0.5 mm (Hicks and Coull 1983). This primarily meiobenthic order contains 54 families (Integrated Taxonomic Information System, <http://www.itis.usda.gov>), approximately 600 genera, and more than 4500 described species (Giere 1993). Harpacticoid copepods inhabit multiple habitat types, including: all marine environments, most freshwater environments, and some terrestrial habitats where sufficient availability of water allows for existence (Hicks and Coull 1983, Dahms and Qian 2004). Harpacticoid copepods are ubiquitous in marine soft-sediment habitats, and generally the second most abundant meiobenthic taxon after the numerically dominant Nematoda (Coull and Bell 1979; Hick and Coull 1983; Higgins and Thiel 1988; Giere 1993). Harpacticoid copepod ubiquity extends into deep-sea environments where they have been shown to have morphological adaptations (Montagna 1982), have proportionally increasing abundance compared to macrobenthos (Thistle 2001), and exhibit high diversity (Coull 1972; Thistle 1978).

Deep-sea species diversity has been a topic of much interest and debate since Hessler and Sanders (1967) presented evidence that these communities are often more

diverse than those in similar shallow water environments. Several hypotheses have been presented during the past 35 years of research attempting to explain why an oligotrophic environment, in which virtually all the fauna rely on precious few labile components of surface derived detritus for nutrition (Sanders and Hessler 1969; Hessler and Jumars 1974; Gage and Tyler 1991), and that is apparently less structurally complex than a typical “high diversity” environment, can support such a rich fauna. Etter and Mullineaux (2001) summarized some recent hypotheses attempting to answer this question: 1) local spatial heterogeneity (MacArthur 1972; Tilman 1982), 2) nonequilibrium dynamics (Caswell 1978; Armstrong and McGehee 1980), 3) interactions among three or more trophic levels (Janzen 1970), and 4) recruitment limitation (Tilman 1994; Hurtt and Pacala 1995). However, all of these hypotheses seem to be explainable by the balance between competitive exclusion and frequency of disturbance, which results in patchiness on biologically influential scales, i.e. millimeter-to-meter (Grassle and Sanders 1973; Grassle 1989; Lamshead 1993) leading to microhabitat specialization (Jumars 1975, 1976; Thistle 1983; 1998; Thistle and Eckman 1990). Meiobenthic community structure is regulated on small spatial scales (mm to cm) where patch dynamics are a function of biogenic structures (Thistle 1983; Thistle and Eckman 1990), and conversely on larger scales (m to km) where benthic currents (Hicks 1988; Thistle 1998) and shifts in sediment grain size (Gray 1968, 1974) regulate community structure. Although much work has been accomplished describing meiofauna community structure on small spatial scales, few studies have addressed large

region-scale patterns. More specifically, the knowledge of regional species pools, processes structuring communities on various scales, and the distributions of organisms and how they respond to topographic, geochemical, and physical oceanographic forcing is largely unknown for deep-sea environments (Etter and Mullineaux 2001). The present study focuses on harpacticoid copepod community structure in the northern Gulf of Mexico (NGOM) deep sea. The sampling design was formulated based on the following six null hypotheses:  $H_{01}$ ) there is no difference in harpacticoid diversity with **depth**,  $H_{02}$ ) there is no difference in harpacticoid diversity with **longitude**,  $H_{03}$ ) there is no difference in harpacticoid diversity in versus out of submarine **basins**,  $H_{04}$ ) there is no difference in harpacticoid diversity in versus out of submarine **canyons**,  $H_{05}$ ) there is no difference in harpacticoid diversity with respect to **escarpments**, and  $H_{06}$ ) there is no difference in harpacticoid diversity with respect to overlying water column **primary production**.

The depth hypothesis ( $H_{01}$ ) follows one of the most dramatic paradigm shifts in marine ecology, that the deep sea is actually more diverse than shallow water environments (Hessler and Sanders 1967). However, the majority of deep-sea diversity studies, and hypotheses of mechanisms maintaining deep-sea diversity, have come from studies of macro- or megafaunal-sized organisms (Etter and Mullineaux 2001). However, meiofauna live on much smaller spatial and temporal scales (Bell 1980; Schwinghamer 1981), and mechanisms maintaining meiofauna diversity may be different than those for the larger-sized fauna.

As discussed thoroughly in chapter one of this dissertation, interactions between

Mississippi River outflow, physical oceanographic processes, and sea floor topography create areas of enhanced meiofauna abundance in the northeastern Gulf of Mexico due to increased POM flux. The effect of these interactions on diversity must be explored. The longitude hypothesis ( $H_{02}$ ) was specifically designed to test for effects of the Mississippi River in shaping harpacticoid diversity. Mississippi River discharge is a major source of new nutrients and organic matter into the northern Gulf of Mexico (Meybeck 1993), with a mean daily discharge of nearly 1 billion  $m^3$  (<http://water.usgs.gov>). The *a priori* hypothesis was that a longitudinal gradient of diversity exists due to organic enrichment from Mississippi River outflow. Bathymetric and latitudinal patterns in deep-sea diversity have been attributed in part to gradients in POM flux (Rex 1981, Rex et al. 1993). Increased productivity is thought to increase the number of species that can coexist (Wright 1983), but very high levels of POM flux to the deep-sea floor may lower diversity due to increased dominance by opportunistic species (Levin and Gage 1988). The basin hypothesis ( $H_{03}$ ) was designed to test for diversity differences in basins and adjacent non-basin stations on the Texas/Louisiana slope. Although basins were shown not to enhance meiofauna abundance (chapter one), they may isolate populations, therefore creating zones of distinct harpacticoid communities. Canyons ( $H_{04}$ ) do have a concentrating effect on POM flux (chapter one), and may enhance or depress diversity as discussed above. Increased abundance directly above and below the Florida Escarpment ( $H_{05}$ ) (chapter one), as well as the precipitous depth change, may significantly alter harpacticoid bathymetric diversity patterns.

Therefore processes affecting overlying primary production ( $H_{06}$ ) and interactions among physical oceanographic process, sediment geologic and geochemical properties, and sea floor topography, likely affect harpacticoid species diversity in the northern Gulf of Mexico. Univariate and multivariate statistical methods were used to integrate these regional differences in relation to the physical environment with environmental variables in order to more fully understand the processes controlling harpacticoid copepod diversity.

## **METHODS**

### **Field & Laboratory Methods**

Field and laboratory methods for the collection and enumeration of harpacticoid copepods are described in chapter one of this dissertation. The reader is also referred to chapter one for descriptions of laboratory methods associated with environmental geochemical and geological variables. Briefly, survey samples were collected on a 60-day cruise aboard the *R/V Gyre* (Texas A&M University) during the months of May and June 2000. Meiofauna were collected by a 5.5 cm inner diameter (i.d.) core tube that was mounted inside the GOMEX boxcorer (Boland and Rowe 1991). One core sample was taken from each boxcore sample, and stored for meiofaunal community analysis. Five total replicate cores were taken at each station. In the laboratory, meiofauna were extracted from sediment using the Ludox centrifugation technique (deJonge and Bouwman 1977), and harpacticoid copepods were separated from the bulk meiofauna sample by manual picking. Animals were identified to species by Dr. Wonchoel Lee



(Hanyang University, Korea). Species were differentiated according to the two standard taxonomic dichotomous keys for marine Harpacticoida (Wells 1976; Huys *et al.* 1996), selected reference texts (Huys and Boxshall 1991, among others), and numerous recent descriptions of new species from peer reviewed journals. Lucid descriptions of harpacticoid species differentiation can be found in Huys and Boxshall (1991) and Huys *et al.* (1996).

### **Experimental Design, and Statistical Analyses**

The experimental design included a total of 43 stations, from seven transects, along the northern continental slope and abyssal plain of the northern Gulf of Mexico deep sea (Fig. 2.1). Although a total of 51 stations were sampled for bulk meiofauna abundance and major taxonomic community structure, only 43 were selected for harpacticoid copepod identification, due to funding limitations. In the northwest (RW) region, seven stations were sampled, including one station in the Alaminos canyon (AC1). An additional western (W) transect was included, which was a historical transect from a previous study (Pequegnat *et al.* 1990). In the west-central region (WC) two historical stations a previous study were included (Pequegnat *et al.* 1990), but stations in this region were mainly designed to test for faunal differences between basin (B) and non-basin (NB) locations. The central transect (C) was also sampled by Pequegnat *et al.* (1990), and was included here to test for differences from the adjacent Mississippi Trough (MT) transect. In the northeast region 10 stations, from two transects, were sampled perpendicular to the Florida slope and escarpment (S).

*Hypothesis Testing* – Six main hypotheses were investigated for differences in harpacticoid copepod diversity. Five transects, RW, W, C, MT and S, were included in the test for depth longitude differences ( $H_{01}$  &  $H_{02}$ ), ranging from the Texas slope in the West to the Florida Escarpment in the east (Fig. 2.1, Table 1.1). Five stations were included per transect, over five depth zones, consistent between transects. Diversity differences at different depths and longitudes were tested using a two-way completely random analysis of variance (ANOVA) that is described by the following model:

$$Y_{ijk} = \mu + \alpha_j + \beta_k + \alpha\beta_{jk} + \varepsilon_{i(jk)}$$

where  $Y_{ijk}$  is the measurement for each individual replicate,  $\mu$  is the overall sample mean,  $\alpha_j$  is the main effect for transects and  $j = 1-5$ ,  $\beta_k$  is the main effect for depths and  $k = 1-5$ ,  $\alpha\beta_{jk}$  is the interaction term, and  $\varepsilon_{i(jk)}$  is the random error for each replicate measurement and  $i = 1-5$ .

The basin hypothesis ( $H_{03}$ ) three basins and three adjacent non-basin stations on the Texas/Louisiana slope (Fig. 2.1, Table 1.1). The experimental design blocked basin and non-basin stations (B1 with NB2, B2 with NB3, and B3 with NB4), to control for differing distances from shore. The experiment is a two-way completely random analysis of variance (ANOVA) that is described by the following model:

$$Y_{ijk} = \mu + \alpha_j + \beta_k + \alpha\beta_{jk} + \varepsilon_{i(jk)}$$

where  $Y_{ijk}$  is the measurement for each individual replicate,  $\mu$  is the overall sample mean,  $\alpha_j$  is the main effect for treatments and  $j = 1-3$ ,  $\beta_k$  is the main effect for distance from shore and  $k = 1-3$ ,  $\alpha\beta_{jk}$  is the interaction term, and  $\varepsilon_{i(jk)}$  is the random error for each

replicate measurement and  $i = 1-5$ .

The canyon hypothesis ( $H_{04}$ ) was formulated to test for diversity differences between stations located in the Mississippi Trough (MT) compared to adjacent stations in the central transect (C) (Fig. 2.1, Table 1.1). Five MT stations were paired with five C stations at five common depth zones, thus removing the effect of depth. Canyon differences were tested using a two-way completely random analysis of variance (ANOVA) that is described by the following model:

$$Y_{ijk} = \mu + \alpha_j + \beta_k + \alpha\beta_{jk} + \varepsilon_{i(jk)}$$

where  $Y_{ijk}$  is the measurement for each individual replicate,  $\mu$  is the overall sample mean,  $\alpha_j$  is the main effect for canyon and  $j = 1-2$ ,  $\beta_k$  is the main effect for depths and  $k = 1-5$ ,  $\alpha\beta_{jk}$  is the interaction term, and  $\varepsilon_{i(jk)}$  is the random error for each replicate measurement and  $i = 1-5$ .

The escarpment hypothesis ( $H_{05}$ ) compared the escarpment transect to a northwestern Gulf transect (W) that experiences a gradual and relatively constant depth increase (Fig. 1, Table 1). Six stations per transect were paired at equal distance from shore to remove this effect. The experiment was tested using a two-way completely random analysis of variance (ANOVA) that is described by the following model:

$$Y_{ijk} = \mu + \alpha_j + \beta_k + \alpha\beta_{jk} + \varepsilon_{i(jk)}$$

where  $Y_{ijk}$  is the measurement for each individual replicate,  $\mu$  is the overall sample mean,  $\alpha_j$  is the main effect for transects and  $j = 1-2$ ,  $\beta_k$  is the main effect for distance from shore and  $k = 1-6$ ,  $\alpha\beta_{jk}$  is the interaction term, and  $\varepsilon_{i(jk)}$  is the random error for each

replicate measurement and  $i = 1-5$ .

### **Multivariate analysis**

Detailed methodology of the environmental principal components analysis and multidimensional scaling of biotic data can be found in chapter one of this dissertation. Briefly, matching species data with environmental variables requires multivariate analyses, and included parametric and non-parametric procedures. Parametric multivariate analysis (principal components analysis, PCA) is performed on environmental variables, creating new variables (principal components), that are uncorrelated. The new variables are extracted in decreasing order of variance, such that the first few principal components (PC) explain most of the variation in the data set. The contribution of each environmental variable to the new PC is called a load. Typically, the new PC loads can be interpreted to indicate structure in the data set. Each observation contributing to the PC is called a score. Thus, the main advantage of PCA is the generation of station scores, which are interpretable, and can subsequently be used in other analyses (i.e. correlation or regression with abundance). Non-parametric procedures (multidimensional scaling, MDS; and the BIOENV procedure) were used to compare station similarity based on species composition, and further for further comparison with environmental variables.

The 43 survey stations were also subjected to cluster analysis, based on Bray-Curtis Similarity, with 4<sup>th</sup> root transformation (Primer-E v.5). Stations were grouped into “zones” where station similarity was greater than or equal to 20% of the species

composition. Stations with less than 20% similarity to any other station were identified as unique. GIS-based analyses were performed (ArcView 8.0, ESRI) to analyze harpacticoid community zonation over the entire northern GOM. Stations were plotted and labeled with the appropriate “zone” to identify region-scale similarities in species composition.

ANOVA and PCA procedures were accomplished using SAS statistical software (SAS Institute Inc. 1991). Non-parametric MDS, cluster analysis, BIOENV procedures, were conducted with Primer 5.0 (Primer-E, 2000).

### **Diversity Estimates**

Harpacticoid diversity was calculated using several common ecological indices.

The Shannon index is the average uncertainty per species in an infinite community made up of species with known proportional abundances (Shannon and Weaver 1949).

The Shannon index is calculated by the following expression:

$$H' = - \sum_{i=1}^S \left[ \left( \frac{n_i}{n} \right) \ln \left( \frac{n_i}{n} \right) \right]$$

where  $n_i$  is the proportion of individuals belonging to the  $i$ th of  $S$  species in the sample and  $n$  is the total number of individuals in the sample.

Rarefaction was used to estimate the expected number of species, thus, accounting for differences in abundance due to bathymetric gradients. Hurlbert (1971)

describes the model as calculating the proportion of potential inter-individual encounters in a given sample. The model is described by the equation:

$$E(S_n) = \sum_{i=1}^S \left[ l - \frac{\binom{N - N_i}{n}}{\binom{N}{n}} \right]$$

$E(S_n)$  describes the expected number of species found in a sample of  $n$  individuals drawn from a population of  $N$  total individuals distributed among  $S$  species.

New diversity indices have been developed based on phylogenetic structure within the sample (Clarke and Warwick 2001), and therefore give a measure of relative functional diversity. Average taxonomic diversity is defined as (Warwick and Clarke 1995):

$$\Delta = \left[ \sum \sum_{i < j} \right] / [N(N - 1) / 2]$$

where the double summation is over all pairs of species  $i$  and  $j$ , and  $N$  is the total number of individuals in the sample. “Simply put, average taxonomic diversity can be thought of as the average taxonomic distance apart of every pair of individuals in the sample, or the expected path length between any two individuals chosen at random” (Clarke and Warwick 2001). Similarly, average phylogenetic diversity:

$$\Phi^+ = PD/S$$

is the cumulative branch length of a sample's phylogenetic tree (PD), divided by the number of species (S) in the sample (Clarke and Warwick 2001). Average phylogenetic diversity can be thought of as the "total evolutionary history, genetic turnover, or morphological richness" represented within the sample (Clarke and Warwick 2001). All diversity indices were calculated in Primer 5.0 (Primer-E Ltd.)

### **Regional and Global Biodiversity Estimates**

Regional and global species richness is by extrapolation. This method uses a single survey, from a single region of the world, to plot species found versus sample number (Lambshead and Boucher 2003). When the species number reaches a maximal accumulation rate it is possible to estimate the rate of encounter of new species with distance traveled. This rate can be expanded to the area of the geographic region sampled, allowing for further extrapolation to global scales. Extrapolation estimates generally require large data sets, preferably from the deep-sea, which accounts for the majority of marine surface area and probably the majority of benthic marine species. Harpacticoid copepod species abundance was analyzed for DGoMB stations along with a previous study on the Texas continental shelf (Montagna and Harper 1996) in order to estimate the entire northern Gulf of Mexico species pool. Species accumulations curves were constructed using Colwell's *EstimateS 6.1* program, with fifty randomized runs (<http://viceroy.eeb.uconn.edu/EstimateS>). A sigmoidal growth model [ $y = (ab + cx^d)/(b + x^d)$ ] was fitted to each data set in order to extrapolate regional diversity (Hyams *Curve*

*Expert 1.3*, <http://www.ebicom.net/~dhyams/cvxpt.htm>) (see also Lambshead, *in press*).

## **RESULTS**

### **General Results**

Harpacticoid copepods were collected from 423 samples at 43 locations in the northern Gulf of Mexico deep sea. In total 12,480 individuals were collected, of which 7667 were in the copepodite stage, 1159 were damaged adults (unidentifiable), and 3654 were adult specimens suitable for identification. Of 3654 individuals, 696 species were identified from 22 families and 175 genera (see Appendix for complete species list, grouped by family). Nine families accounted for approximately 93% of all harpacticoida (Table 2.1), and two, Tisbidae and Ectinosomatidae, accounted for 46%. Only 182 of these species (27%) have been formally described in the literature.

Average abundance over all stations (from five pooled replicate cores = 118.8 cm<sup>2</sup>) was  $172 \pm 94$ , with maximum and minimum values of 412 and 54, found at stations WC5 and MT6, respectively (Table 2.2). The average number of species was  $52 \pm 19$  (from pooled replicate cores) with maximum and minimum values of 104 and 23, found at stations WC5 and MT6, respectively (Table 2.2). Total abundance (N) and species richness (S) decrease significantly ( $R^2 = 0.466$  and  $0.495$ , respectively) with increasing water depth (Fig. 2.2A,B). The number of species is highly correlated to the number of individuals encountered ( $r = 0.91$ ). However, rate of decrease with water depth is approximately five times greater for abundance than species richness (slope =  $-0.068$  and  $-0.014$ , respectively).



Shannon-Wiener diversity ( $H'$ ) decreases in a strong relationship with depth ( $R^2 = 0.501$ ,  $P < 0.0001$ , Fig. 2.3).  $H'$  had a mean of 3.73 and standard deviation of 0.32 (calculated from Table 2.2). Maximum values of  $H'$  were found at stations S35, WC5, MT2 and MT1, while minimum values were found at stations NB2, NB4, B1, B2 and MT6 (Table 2.2). The expected number of species per 30 harpacticoid individuals [ES(30)] shows a moderate non-linear, unimodal relationship with depth ( $R^2 = 0.312$ ,  $P = 0.0006$ , Fig. 2.4). Mean ES(30) was 22.24 with standard deviation of 2.08 (calculated from Table 2.2). Maximum values of ES(30) are found at stations WC5 and W1, while minimum values are found at stations C12, C14, and W6. Although the relationship is moderately significant, ES(30) is highly variable at both shallow and deep stations (Fig. 2.4).

Average taxonomic diversity ( $\Delta$ ), the average taxonomic distance apart of any two individuals chosen at random within a sample, increases with increasing water depth ( $R^2 = 0.185$ ,  $P = 0.004$ , Fig. 2.5). Determination of average taxonomic diversity was based on a 4-level taxonomic scheme, from species to order.  $\Delta$  had a mean value of 98.76 and standard deviation of 4.24 (calculated from Table 2.2). Highest average taxonomic diversity was found at station MT6 (111.88), with lowest values at station MT1 (91.44). Although the relationship is moderately significant, variance in  $\Delta$  increases at deep stations (Fig. 2.5). Another index of taxonomic relatedness is average phylogenetic diversity ( $\Phi^+$ ), which is the cumulative branch length of the phylogenetic tree within each sample (Clarke and Warwick 2001). As with average taxonomic

diversity (above), average phylogenetic diversity was calculated with a 4-level taxonomic scheme, from species to order. Average phylogenetic diversity shows a strong, and highly significant, increasing trend with depth ( $R^2 = 0.500$ ,  $P < 0.0001$ , Fig. 2.6). The mean value of average phylogenetic diversity was 62.33 with standard deviation of 5.73 (calculated from Table 2.2). Maximum average phylogenetic diversity of 79.92 was found at station MT6, while the minimum was 54.62 at station C7 (Table 2.2). Both  $\Delta$  and  $\Phi^+$  suggest proportionally more higher order taxa (genera and families) per individual with increasing depth (see discussion). Therefore, the ratios of species (S), genera (G), and families (F) to individuals was compared over 1000-meter depth increments (Fig. 2.6). The ratios of S, G, and F to N, increase with depth (Fig. 2.6). Depth zones were significantly different ( $P < 0.01$ ) by two-way analysis of variance. Pairwise comparisons using Tukey's HSD test indicated significant differences only among the shallowest and deepest zones (i.e. 200-999 meters and >3000 meters).

### **Univariate Analysis**

*Hypothesis Testing* – In the test for differences between depth and longitude ( $H_{01}$  and  $H_{02}$ ), a highly significant depth main effect was observed ( $P < 0.0001$ , Table 2.3, Fig. 2.8), but a weak significant interaction was also observed ( $P = 0.0203$ , Table 2.3, Fig. 2.8). Overall, harpacticoid  $\Phi^+$  responded similarly over most of the transects with a small peak in  $\Phi^+$  at mid depths (approx. 1500 m) followed by relatively constant diversity until a second peak at depths greater than 3000 meters. The eastern stations (S transect) has a decrease in  $\Phi^+$  at shallow depths (S44 to S35), but then a constant

increase in  $\Phi^+$  with increasing depth.

In the test for differences in  $\Phi^+$  between basin and non-basin stations ( $H_{03}$ ) no significant differences were observed for main effects, and no interaction was observed (Table 2.3). Similarly, in the test for canyon effects ( $H_{04}$ ) no significant difference in  $\Phi^+$  was observed between canyon and non-canyon transects, but a significant depth effect was observed ( $P < 0.0001$ , Table 2.3, Fig. 2.9). No significant canyon by depth interaction was observed between (Table 2.3). In the test for escarpment effects on  $\Phi^+$ , a weak transect main effect was observed ( $P = 0.035$ , Table 2.3) but strongly significant interaction between transect and distance from first station was observed ( $P = 0.0003$ , Table 2.3, Fig. 2.10). There is a peak in diversity at the two deep stations below the Florida Escarpment (S40 and S41), and then a decrease in diversity moving away from the escarpment (S39). The western (W) transect had a peak in  $\Phi^+$  at approximately 1500 meters (W4), and a second peak at the deepest station (W6).

### **Multivariate Analysis**

*PCA* – The reader is referred to the environmental variable PCA in chapter one of this dissertation for complete details on variable loads and PC interpretation. Briefly, PC1 was interpreted as **sediment properties**. Highly positive station scores ( $>1$ ) on PC1 characterized stations near Mississippi River outflow with high silt, Cr, Sn and total PAH. Station scores between 1 and -1 represented the general offshore environment with moderate silt, clay, sand, Ca, and Sr. Highly negative station scores on PC1 ( $<-1$ )

represented stations with a high sand fraction relative to silt and clay. PC2 was interpreted as **POM flux**. Highly positive station scores on PC2 (>1) were those near Mississippi River outflow in the northeastern GOM. Stations scores <1 and moving in the negative direction were deeper and further away from Mississippi River outflow. PC1 through PC4 were regressed against average phylogenetic diversity ( $\Phi^+$ ) to determine the percentage of variance within the diversity data set that is accounted for by environmental variables. PC1 had a non-significant relationship with  $\Phi^+$  (Fig. 2.11A), but reveals the overall homogeneity in sediment properties in the northern GOM; with the exception of a few stations near Mississippi River outflow with high silt (MT1-3, C1), and a few stations in the west (W3, W4) and east (S43, S44) with high sand. Conversely, PC2 (POM flux) was strongly related to average phylogenetic diversity ( $\Phi^+$ ), with highest values of diversity corresponding to lowest values of POM flux (Fig. 2.11B,  $R^2 = 0.316$ ,  $P = 0.0002$ ).

*Multidimensional Scaling* – MDS was used to analyze harpacticoid species abundance from a multivariate perspective (Fig. 2.12 & 2.13). Depth zones of 1000 meter increments show clear separation at the 1000 meter threshold, with stations below 1000 meters showing considerable overlap. Stress, a measure of the ability of the analysis to display multidimensional differences in a two dimensional space, is high for the harpacticoid MDS ordination (Stress = 0.26). Any stress value greater than 0.2 is considered high, and thus the ordination is not appropriately displaying multidimensional station differences (Clarke and Warwick 2001). However, zones are significantly

different in a one-way analysis of similarity (ANOSIM) ( $P < 0.01$ ). Similarly, stations were grouped using longitudinal zones as a factor in the MDS plot (Fig. 2.13). Stations group together by longitudinal zone with little overlap, and zones are significantly different by one-way ANOSIM ( $P < 0.01$ ). Harpacticoid species abundance and environmental data were compared using the BIOENV analysis (Primer-E v.5). No strong correlations were observed between harpacticoid community structure and the environmental variables, but a weak correlation (0.228) was found between the biotic data and five environmental variables (%sand, %clay, %silt, ChlA, and OrgN).

*Spatial and Bathymetric Species Zonation* – The concept of geographic or bathymetric zonation was analyzed using cluster and subsequent GIS analysis (Figs. 2.14 & 2.15). Cluster analysis was performed on the harpacticoid data set implementing Bray-Curtis similarity and group average linking (Primer-E v.5.) (Fig. 2.14). Minimum Bray-Curtis similarity, i.e. the similarity of all 43 survey stations, was 8.4%. Groups, or “zones,” were chosen on the basis of  $>20\%$  similarity. A total of 17 zones were determined, with 1-7 stations per zone (Fig. 2.14). Stations that did not group with at least one other station at the 20% level were designated as unique zones. Highest zone similarity was found for stations MT1, MT2 and MT3 (36.8%), and highest similarity between any two stations was 48.4%, for stations MT2 and MT3. All other zones, that included at least two stations, had similarity values between 20 and 36%.

Harpacticoid species composition differs both longitudinally and bathymetrically (Fig. 2.15). Only three zones are found both east and west of  $90.5^\circ$  W longitude (groups

9, 11, and 13). All remaining groups are isolated to either the west or east of 90.5° W longitude. Bathymetrically, groups 4, 10, and 13 are found at shallow stations, groups 1, 12, and 6 are found at mid depths, groups 2, 3, 7, 8, 14, 15, 16, and 17 are found at deep stations and groups 5, 9, and 11 are found a virtually all depths. Seven stations are characterized as zone 5 in the northwestern GOM, but these stations are all less than 40% similar. In total, 77 species are found in zone 5, with 5 species accounting for 34% of the total richness (*Halectinosoma aff. gothiceps*, *Neozosime bisetosa*, *Neozosime trisetosa*, *Bradya aff. congenera*, *Ameira aff. parvula*). Four of the above species, *Neozosime bisetosa*, *Neozosime trisetosa*, *Halectinosoma aff. gothiceps*, and *Bradya aff. congenera*, are cosmopolitan over all stations, accounting for 25 % of all individual; and together with *Tachidiopsis aff. bozici*, *Halectinosoma aff. herdmani*, *Paraleptopsyllus sp.* *Zosime aff. mediterranea*, and *Zosime aff. incrassata*, account for 40% of the total abundance at all 43 stations.

*Regional and Global Biodiversity Estimates* – Two regional data sets were analyzed in order to extrapolate to regional and global scales. Species accumulation curves (Fig. 2.16) were constructed for each data set. The convex nature of the curves suggests that an asymptote exists, given an unlimited sample pool (Lambhead and Boucher 2003). The sigmoidal growth model parameters for the two data sets were as follows: NGOM,  $a = -7.5$ ,  $b = 499.4$ ,  $c = 2241.4$ , and  $d = 0.75$ ; NWGOM,  $a = -2.28$ ,  $b = 166.08$ ,  $c = 457.06$ , and  $d = 0.57$ . The models for both NGOM and NWGOM fitted the data very closely,  $R^2 = 0.99996$  and  $0.99980$ , respectively. The model interpolation

indicates that asymptotes exist at 2241 and 457 species for deep-sea (NGOM) and shallow (NWGOM) regions of the Gulf of Mexico respectively. Species accumulation curves become linear as they approach the asymptotes (estimates of regional diversity), and thus suggest the rate of encounter of new species is relatively constant with increasing geographic distance or area sampled. Summing the shelf and deep-sea estimates yields the regional biodiversity of the entire Gulf of Mexico at approximately 2700 species, assuming there is no overlap between shallow shelf and deep-sea species. The approximate area of the Gulf of Mexico is  $1.5 \times 10^6 \text{ km}^2$ , which is about 0.4 % of the world's oceans. Assuming the rate of increase of new species with area remains constant then extrapolation suggests a global species richness of  $6.5 \times 10^5$  for the Harpacticoida.

## **DISCUSSION**

Harpacticoid copepods are ubiquitous in deep-sea environments where they have been shown to have particular adaptations (Montagna 1982), are relatively successful compared to macrobenthos (Thistle 2001), and exhibit high diversity (Coull 1972; Thistle 1978). Although much work has been accomplished describing harpacticoid community structure on small spatial scales, few studies have addressed large region-scale patterns. More specifically, the knowledge of regional species pools, processes structuring communities on various scales, and the distributions of organisms and how they respond to topographic, geochemical, and physical oceanographic forcing is largely unknown for deep-sea environments (Etter and Mullineaux 2001). Therefore the purpose of the current study was to investigate harpacticoid species diversity with

respect to the complex interactions between Mississippi River outflow, physical oceanographic processes, and sea floor topography in the northern Gulf of Mexico deep sea.

Harpacticoida abundance (N) and species richness (S) decrease in strong linear relationships with depth (Fig. 2.2A,B), as observed in previous deep-sea investigations (Tietjen 1971; Coull *et al.* 1977; Shirayama 1984b; Soltwedel 2000, *and reference therein*). However, the rate of decrease is approximately five times greater for abundance than richness (comparison of slopes, N/S = -0.068/-0.014). Gray *et al.* (1997) reviewed several studies and found the number of macrofauna species per individual was comparable in coastal and deep-sea environments; with the exception of a deep-sea data set by Etter and Grassle (1992), which showed much higher S:N ratios in the deep sea. The overall ratio of species to individuals (696/3680) reveals a new species being encountered in one out of every five individuals.

Spatial and bathymetric trends in harpacticoid diversity exist in the northern Gulf of Mexico deep sea, as confirmed by the significant depth ( $H_{01}$ ) by longitude ( $H_{02}$ ) interaction ( $P = 0.0203$ , Table 2.2). Bathymetric patterns of average phylogenetic diversity ( $\Phi^+$ ) indicate that communities are structured differently with increasing depth and distance from the Mississippi River (Fig. 2.8). However, this difference is mainly due to low mid-depth diversity along the S transect, compared to the other four transects; as well as a deep diversity maximum for station MT6 compared with other stations at approximately 3000 meters depth. Average phylogenetic diversity is a measure of higher



taxonomic, or morphological richness (Clarke and Warwick 2001). Therefore, harpacticoid copepod communities have increased morphological complexity with increasing water depth.

Average phylogenetic diversity was not significantly different between basin and adjacent non-basin stations ( $H_{03}$ ), suggesting communities located in the west-central Gulf have similar morphological complexity. Although they reside in contrasting topographic environments, basin and non-basin stations have comparable sediment structure (William Behrens, personal communication) and receive comparable POM flux (see chapter one of this dissertation). Average phylogenetic diversity is not significantly different between canyon and non-canyon stations ( $H_{04}$ ) (Table 2.3, Fig. 2.9), however, a significant depth effect does suggest that morphological complexity increases similarly with depth along the MT and C transects (Fig. 2.9). Average phylogenetic diversity changed differently with depth between escarpment ( $H_{05}$ ) and non-escarpment transects ( $P = 0.0003$ ). Strong hydrodynamic regimes can significantly alter abundance and diversity of meiofauna (Thistle *et al.* 1985, 1991, 1999). Stations along the Florida Escarpment transect S39-S44, especially S40-S42, experience strong current regimes due to impingement by the loop current (see chapter one discussion), and also have a high sand fraction within the sediment structure, compared to other DGoMB stations. In a study of the Fieberling Guyot, a physically reworked site, Thistle *et al.* (1999) found lower abundance of surface-dwelling harpacticoids, a higher proportion of interstitial harpacticoids, and a higher harpacticoid to nematode ratio. Sediments at the Fieberling

Guyot are dominated by sand (greater than 90% by mass), whereas sediments along the Florida Escarpment transect are comprised of 20% to 50% sand mass. However, sediments at the majority of station in the northern GOM are comprised of 2 to 20% sand mass. The dynamic conditions associated with loop current interaction with the Florida escarpment, rapid increase in water column depth, and high sand fraction are likely responsible for the increase in harpacticoid diversity at stations S41 and S40.

Diversity can be estimated by either species dependent or species independent indices. Species independent indices (Shannon-Weiner, Hill's  $N_1$ , etc.) are useful for generally describing diversity; however, they do not represent the structure of the community. For example two communities may have the same number and relative abundance of species, but have completely different sets of species present. In this situation the two communities would have the same diversity value according to Shannon's (or Hill's) index when in reality they look very different. Ecological diversity indices (e.g.  $H'$  and  $J$ ) are not commonly used to analyze community structure over bathymetric gradients because of strong dependence on sample size. For example, harpacticoid diversity ( $H'$ ) decreases strongly, and significantly, with depth (Fig. 2.3) in a linear relationship that strongly reflects decreasing harpacticoid abundance. Because the number of species encountered is strongly related to the number of individuals in a sample ( $r = 0.91$ ), diversity must be analyzed by indices that are independent of sample size.

The most common abundance-independent index used in deep-sea studies is

Hurlbert Rarefaction (Hurlbert 1971), which is the expected number of species encountered per number of individuals ( $E_{Sn}$ ). The expected number of harpacticoid species per 30 individuals follows the typical parabolic relationship (Paterson and Lambshead 1995; Etter and Mullineaux 2001; Lambshead *et al.* 2002; and others) with a maximum diversity found at approximately 1200 meters water depth and decreasing diversity moving into deeper water (Fig. 2.6,  $R^2 = 0.312$ ,  $P = 0.0006$ ). Coull (1972) used rarefaction curves to compare continental shelf and deep-sea harpacticoid species in the north Atlantic and found maximum diversity at 3000 meters, with decreasing diversity thereafter. Macrofaunal diversity in the north Atlantic has been shown to peak at 1250 meters using the Hurlbert rarefaction method (Maciolek-Blake *et al.* 1985; Maciolek *et al.* 1987). Similarly, polychaete diversity in the northeast Atlantic peaks between 1000 and 2000 meters (Paterson and Lambshead 1995).

Alternatively, species dependent measures of biodiversity take into consideration the taxonomic composition calculate diversity based on multi-level phylogenetic trees (Warwick and Clarke 1995; Clarke and Warwick 1999; Clarke and Warwick 2001); with the only disadvantage being the semi-arbitrary nature of taxonomy. Perhaps the best approach to comparing community structure over large spatial scales is by a measure of taxonomic distances (Warwick and Clarke 1995), such as average taxonomic diversity ( $\Delta$ ) and average phylogenetic diversity ( $\Phi^+$ ) (Clarke and Warwick 2001). Average taxonomic diversity is sample size independent, and reflects the average branch length between any two individuals chosen at random from, provided they are not from the

same species (Clarke and Warwick 2001). Average phylogenetic diversity (the total branch length of the phylogenetic tree) is not sample size independent, but corrects for sample size differences by dividing by the number of species in the sample. Harpacticoid average taxonomic and average phylogenetic diversity both increase linearly increasing water depth (Figs. 2.5 & 2.6), although average taxonomic diversity shows considerably more variance at stations at depths of approximately 3000 m. Taken together, these indices suggest an increase in harpacticoid diversity with increasing depth and proportionally more genera and families per individual with increasing water depth. This hypothesis was tested by comparing ratios of species, genera, and families per individual, pooling stations into 1000-meter depth zones, in a 2-way analysis of variance. ANOVA indicated significant differences, with pairwise tests (Tukey's) indicating differences between shallowest (200-999 m) and deepest (>3000 m) zones (Fig. 2.9). Thus, dominance by particular species, genera or families seems to decrease with increasing water depth in the northern Gulf of Mexico, which is partially reflected in the pattern of decreasing  $H'$  (a dominance index) with increasing depth (Fig. 2.5).

Phylogenetic-based diversity indices are useful for understanding higher taxonomic, or morphological diversity, but do not differentiate on the basis of actual species composition. Stations could conceivably have identical  $\Delta$  values, but have entirely different species present. Therefore, to compare many stations on a regional scale it is necessary to employ multivariate procedures to analyze similarities between stations, based on their species composition (Warwick and Clarke 1991; Montagna and

Harper 1996). Cluster analysis of stations based on species similarity revealed 17 distinct zones (Figs. 2.10 & 2.11). However, relatively small similarity between stations (20-40%) could justify assigning every station to a unique zone, especially since every fifth individual encountered is a new species. However, the 20% benchmark was sufficient to differentiate between the northeastern and northwestern Gulf of Mexico, with only three similar zones found on both sides of the 90.5° W longitude boundary (Zones 9, 11 & 13; Fig. 2.11). Common zones over bathymetric and longitudinal gradients are explained by the existence of a few cosmopolitan species, and a higher percent similarity benchmark would have likely eliminated common zones over large longitudinal and bathymetric distances. Hence, most stations are very different with respect to harpacticoid species composition in the northern Gulf of Mexico. On the contrary, recent analysis of nematode diversity from the north-central equatorial Pacific revealed 71% of all species being found at four stations spanning more than 3000 km of abyssal plain (Brown 1998, Lamshead *et al.* 2003, Lamshead and Boucher 2003), suggesting an increase in cosmopolitan species at abyssal depths. This is consistent with previously observed bathymetric diversity patterns where diversity is maximized in the bathyal and decreases in the abyssal (Maciolek-Blake *et al.* 1985; Maciolek *et al.* 1987; Paterson and Lamshead 1995; Etter and Mullineaux 2001; Lamshead *et al.* 2002).

Species extinction associated with habitat loss and fragmentation on a global scale has led to increased interest in regional and global scale biodiversity studies in both the terrestrial and marine environments (Wilson 1985, 1988; May 1988) as well as

associated studies attempting to understand the connection between natural biodiversity and ecosystem function (Emmerson and Raffaelli 2000; Rothman 2001; Loreau *et al.* 2001; Raffaelli *et al.* 2003). Regional and global diversity of deep-sea soft sediments has received increasing attention since the discovery that this environment is generally more species rich than coastal systems (Hessler and Sanders 1967). On global scales, macrobenthos diversity has been estimated to be at least  $5 \times 10^5 - 10 \times 10^7$  species (Grassle and Maciolek 1992; May 1992, Poore and Wilson 1993), with meiofauna diversity equaling or exceeding that estimate by one to two orders of magnitude (potentially  $10^9$  species) (Lamshead, *in press*). It is estimated that harpacticoid regional species richness within the northern Gulf of Mexico is approximately 2700 species. Zonation results suggest very little overlap between stations in the northern GOM, therefore a regional diversity estimate of 2700 species is not unreasonable. Furthermore, estimates of global species richness, by extrapolation from regional species accumulation (*sensu* Lamshead and Boucher 2003) of Harpacticoida suggest between  $10^5$  and  $10^6$  harpacticoid species. Although estimates are dramatically higher than the number of described species (4500, for marine and freshwater species), they are in line with global estimates of other highly diverse taxa, e.g., Nematoda (May 1988, Lamshead and Boucher 2003).

Given what we know of harpacticoid ecology (Hicks and Coull 1983), and their ubiquity and abundance, the potential for speciation is high in this taxa. Harpacticoida, and other meiofauna, have shorter generation times than macrofauna or megafauna, have

slower movement, have non-planktonic larvae, and with smaller body sizes live on ecologically smaller scales (Hicks and Coull 1983; Higgins and Thiel 1988; Giere 1993; Thistle 2003). Without planktonic larval stages, harpacticoid (meiofauna in general) dispersal is dependent upon suspension and transport by current flow, turbidity currents, or some other transport mechanism.

The deep-sea is known to have dynamic current regimes, which have been shown to alter meiofauna abundance and diversity at locations such as the HEBBLE site (High Energy Benthic Boundary Layer Experiment) (Thistle *et al.* 1985, 1991; Aller 1997), the Rockall Trough (Gage 1977; Patterson and Lamshead 1995), and the Setubal Canyon (Gage 1977; Gage *et al.* 1995). The rate of dispersal of meiofaunal organisms on a global scale is unknown. Limited evidence suggests harpacticoid patchiness on 100-meter, meter, and centimeter scales (Thistle 1978) is consistent with Jumar's (1975) grain matching hypothesis (microhabitat specialization), and such patchiness should result in species dispersions on these scales (Thistle 1978). Furthermore, genetic evidence suggests the existence of cryptic species within previously assumed cosmopolitan populations (Schizas *et al.* 1999; Rocha-Olivares *et al.* 2001), and small-scale (100 m) dispersion patterns of genetic haplotypes within populations (Street and Montagna 1996). Therefore, if rates of speciation in the deep sea exceed rates of dispersal, then high regional and global species richness will be purely a function of the deep sea's vast area (*sensu* Abele and Walters 1979).

Parametric and non-parametric multivariate analyses yield contrasting results,

with respect to environmental variables that affect diversity, but together give a complete picture. Comparing environmental principal components (PC1 & PC2) to a single diversity index ( $\Phi^+$ ) reveals no relationship with sediment characteristics (PC1), but an inverse relationship between POM flux (PC2) and functional diversity (Figs. 2.11A&B). The availability of food resources has been used to explain both bathymetric (Rex 1981; Levin *et al.* 1994) and geographic (Levin *et al.* 1991; Rex *et al.* 1993; Lamshead *et al.* 2000; Lamshead *et al.* 2002) diversity patterns. Because deep-sea communities are reliant upon sinking POM derived from surface water production, it is logical that food resources play a significant role in the number and types of species present in a community. The general consensus is that increased POM flux results in increased abundance, a shift towards dominance, and therefore a decrease in diversity. Short term laboratory experiments of organic enrichment (Grassle and Morse-Porteous 1987; Snelgrove *et al.* 1996) confirm what has been observed in several field experiments (Rex 1983; Schaff *et al.* 1992; Rex *et al.* 1993; Levin *et al.* 1994; Levin and Gage 1998), that diversity is maximized at moderate levels of organic enrichment. Large scale bathymetric and latitudinal diversity patterns are generally unimodal, with highest diversity at intermediate levels of production (depth, latitude, etc.) (Rex 1981; Levin and Gage 1998), which is confirmed here (Fig. 2.6). The mechanism for decrease in diversity at high levels of production appears to result from competitive exclusion due to increased dominance (Levin and Gage 1998), but could also result from chemical stress associated with increased biological oxygen demand (Levin *et al.* 2000).



Microelectrode profiles of stations MT1 and MT3 in this study (John Morse, DGoMB data) indicate oxygen penetration depths of 2 mm, compared to 8 cm at deeper more oligotrophic stations, further evidence supporting decreased functional diversity in areas of high organic enrichment. On the other side of the unimodal diversity/production curve is a decrease in diversity at lower bathyal and abyssal depths. This has been hypothesized to occur as a result of a chronic allee effect, or a point at which populations are no longer reproductively viable due to death rates exceeding birth rates (M.A. Rex, personal communication).

Multidimensional scaling plots confirm significant differences in harpacticoid community structure with depth and longitude in the northern GOM deep sea (Figs. 2.12 & 2.13). Comparison of harpacticoid species abundance and environmental data with the BIOENV gives only weak Spearman Rank Correlations with grain size and chl-a biomass. PC1 (sediment properties) was not correlated with average taxonomic diversity in the parametric analysis, but is important with respect to the actual species list as reflected by stations similarities in the MDS analysis. But, the amount of variance explained by the BIOENV procedure is low. Many studies have shown that soft-sediment community structure is related to sediment characteristics (Sanders 1958; Rhoads 1974; Gray 1981), but as emphasized by Etter and Mullineaux (2001), the relationships between diversity and sediment properties remain numerous and often controversial. In the current study, most stations were characterized by high silt and clay fractions, with little sand. Only 10 stations (MT5, MT6, S38-S44, and W1) had greater

than 30% sand, and were all located in the northeastern GOM, except station W1. Therefore, grain size may partially explain longitudinal variability in harpacticoid diversity within the northern GOM.

Several hypotheses have been formulated to explain the mechanisms regulating high deep-sea diversity, but they fall under two broad categories: 1) small-scale patch dynamics and 2) large-scale regional processes. In general, diversity is highly related to bathymetric and regional variation in POM flux, as confirmed here by a significant relationship with PC2 (Fig. 2.11B). However, a wealth of literature has focused on small-scale processes creating spatial sediment heterogeneity (Jumars 1975, 1976; Gage 1977), particularly biogenic structures (Thistle 1979; 1983; Thistle and Eckman 1988, 1990; Eckman and Thistle 1991; Thistle *et al.* 1993), which can exist for large periods of time and provide distinct microhabitats. Small scale heterogeneity in sediment grain size has been hypothesized to provide diverse food resources, because the majority of deep-sea species are deposit feeders (Sanders 1958; Rhoads 1974; Gray 1981). However, perhaps the most convincing and unifying argument comes from patch dynamics theory; small-scale disturbances creating a network of patches in multiple stages of succession (Grassle and Sanders 1973; Caswell 1978; Connell 1978; Sousa 1979; Paine and Levin 1981; reviewed by Etter and Mullineaux 2001). Highly variable life history characteristics in the deep sea (Gage and Tyler 1991) may therefore enable multiple inferior species to colonize patches, and slower dynamics in deep water may reduce the rate at which these inferior species are excluded (Caswell and Cohen 1991;

Caswell and Etter 1999).

Although the current study was not specifically designed to test small-scale hypotheses, it is possible to assess within versus between-station variability. For example, cluster analysis of all replicates at stations NB3 and NB4 (Fig. 2.18) reveals as much within-station similarity as between-station similarity. Replicates three and five at station NB4 are approximately 40% similar, but are, at most, 10% similar to other NB4 replicates. At station NB3, replicates one and two are approximately 20% similar. However, replicate two from station NB3 is 30% similar to replicate two at station NB4; likewise replicate two at NB3 and replicate two at NB4 are 30% similar. This pattern of within-station variability equaling or exceeding between-station variability allows for at least three conclusions to be made. First, the harpacticoid species pool in the northern GOM is large, and this study only captured a small percentage of the total. This reinforces our regional diversity estimate of at least 2700 species. Second, there are a few cosmopolitan species that are observed Gulf-wide, producing small between-station similarities. Third, processes maintaining harpacticoid diversity in the northern GOM rely on both small-scale and large-scale mechanisms.

## CONCLUSION

The northern Gulf of Mexico deep sea is a dynamic environment, with the complex morphology of the Texas/Louisiana continental slope, dramatic canyon features such as the Mississippi Trough, and the precipitous Florida escarpment. Inflow from the Mississippi River interacts with the Loop Current to enhance POM flux, which strongly influences diversity. The harpacticoid community shows remarkable diversity with approximately one in five individuals belonging to a different species. With the exception of a few cosmopolitan species, most stations have different species compositions, which suggests high regional (2700 species) and global ( $10^5$  -  $10^6$  species) diversity by extrapolation. Although highest diversity, with respect to the expected number of species (rarefaction), is found at approximately 1200 meters, average taxonomic and average phylogenetic diversity continue to increase with depth. Multivariate analysis reveals significant inverse relationships between diversity and production, which are confirmed by a significant region-scale depth and longitude differences. However, within versus between station variability suggests an interaction between small and region-scale processes maintaining diversity. Low rates of dispersion, coupled with high local diversity, result in high regional and global diversity, thus, speciation in the deep-sea likely exceeds dispersion. Therefore, global species richness of the Harpacticoida is likely a function of the vast area of deep-sea soft sediments, in agreement with Abele and Walter's (1979) hypothesis.

Table 2.1: Results of SIMPER analysis (Primer 5.0) indicating family percent

contributions to total harpacticoid abundance. AA = Average abundance, Contrib.% = percent contribution of family, T% = cumulative percent contribution of families.

<b>Family</b>	<b>AA</b>	<b>Contrib.%</b>	<b>T%</b>
Tisbidae	40.19	32.98	32.98
Ectinosomatidae	24.12	13.27	46.24
Diosaccidae	19.74	9.84	56.09
Ameiriidae	15.71	8.24	64.33
Argestidae	11.00	8.08	72.41
Paranannopidae	9.15	6.50	78.91
Canthocamptidae	12.38	6.03	84.95
Paramesochriidae	6.73	4.15	89.10
Cletodidae	6.62	3.42	92.52
Neobryidae	2.73	1.39	93.91
Thalestridae	2.34	1.09	95.00
Normanellidae	2.41	1.09	96.08
Cerviniidae	2.55	1.05	97.13
Danielssenidae	3.55	0.93	98.06
Huntemannidae	1.70	0.93	98.99
Unid. family	1.79	0.61	99.60
Ancorabolidae	1.21	0.32	99.93
Laophontidae	0.42	0.03	99.96
Canuellidae	0.28	0.03	99.99
Darcythompsonidae	0.19	0.01	100.0
Longipediae	0.16	0.00	100.0
Euterpinidae	0.05	0.00	100.0

Table 2.2: Total species (S) and total individuals (N) per five pooled replicates cores (= 118.8 cm<sup>2</sup>). Species diversity indices: expected species per 30 individuals [ES(30)], Shannon-Wiener diversity (H'), average taxonomic diversity ( $\Delta$ ), and average phylogenetic diversity ( $\Phi^+$ ) at each of the 43 stations where harpacticoid copepods were identified to species.

Station	Depth	S	N	ES(30)	H'	$\Delta$	$\Phi^+$
AC1	2440	51	114	24.91	3.90	102.14	59.79
B1	2253	27	74	19.56	3.21	105.25	70.97
B2	2635	32	90	20.27	3.33	102.51	62.74
B3	2600	37	108	21.00	3.46	96.59	64.92
C1	336	51	195	19.70	3.73	96.85	58.63
C12	2924	34	125	17.34	3.31	95.37	70.14
C14	2495	33	118	17.37	3.31	93.49	66.12
C4	1463	56	148	23.98	3.91	101.77	63.23
C7	1066	74	212	24.64	4.14	96.27	54.62
MT1	482	69	322	22.68	3.95	91.44	57.51
MT2	677	67	338	21.45	3.82	92.72	53.06
MT3	990	81	418	21.68	3.92	92.99	55.02
MT4	1401	53	144	23.80	3.87	101.76	63.93
MT5	2267	44	110	23.35	3.71	102.31	62.27
MT6	2743	23	54	18.92	3.04	111.88	79.92
NB2	1530	40	112	22.14	3.59	99.71	64.78
NB3	1875	50	120	24.02	3.83	101.57	63.81
NB4	2020	39	108	21.76	3.54	100.51	63.91
NB5	2065	36	94	21.90	3.50	101.88	65.86
RW1	212	66	240	23.54	3.99	95.83	57.38
RW2	950	57	178	23.41	3.89	97.50	59.27
RW3	1340	61	174	23.47	3.92	95.49	57.34
RW4	1575	57	148	24.28	3.94	101.27	65.85
RW5	1620	43	112	22.56	3.64	101.49	66.40
RW6	3000	49	130	22.99	3.74	96.16	61.75
S35	668	89	388	23.02	4.10	93.75	54.72
S36	1826	74	306	23.14	4.02	95.58	56.98
S37	2387	70	198	24.49	4.09	99.48	60.17
S38	2627	44	108	23.36	3.71	100.96	63.09
S39	3000	38	96	21.85	3.50	102.23	66.89
S40	2972	30	78	19.94	3.24	105.63	71.18
S41	2974	31	84	20.69	3.35	104.42	72.10

<b>Station</b>	<b>Depth</b>	<b>S</b>	<b>N</b>	<b>ES(30)</b>	<b>H'</b>	<b><math>\Delta</math></b>	<b><math>\Phi^+</math></b>
S42	763	58	178	23.33	3.89	98.33	57.55
S43	362	57	178	23.17	3.87	95.31	56.08
S44	212	41	133	20.14	3.64	99.64	64.76
W1	420	94	306	25.46	4.37	96.45	56.50
W2	625	65	214	23.12	3.93	97.02	56.36
W3	875	65	212	23.55	3.98	96.13	57.16
W4	1460	52	146	23.79	3.86	100.75	66.58
W5	2750	35	86	22.10	3.49	101.27	64.93
W6	3150	33	108	17.39	3.02	90.01	68.15
WC12	1175	52	180	21.75	3.71	98.55	62.62
WC5	348	104	412	25.26	4.42	96.28	55.24

Table 2.3: ANOVA results of test for differences in Harpacticoida diversity. Dependent variable is average phylogenetic diversity ( $\Phi^+$ ). DFS = distance from shore; DFFS = distance from first station.

Source	DF	SS	MS	F Value	Pr > F
<b>H<sub>01&amp;02</sub></b>					
Transect	4	110.02	27.51	0.50	0.7332
Depth	4	2198.28	549.57	10.06	<.0001
T*Depth	16	1749.36	109.34	2.00	<b>0.0203</b>
Error	96	5243.96	54.62		
<b>H<sub>03</sub></b>					
Treatment	1	16.45	16.45	0.18	0.6711
DFS	2	109.87	54.93	0.62	0.5479
T*DFS	2	57.33	28.67	0.32	0.7277
Error	23	2045.74	88.95		
<b>H<sub>04</sub></b>					
Transect	1	2.67	2.67	0.05	0.8312
Depth	4	1870.96	467.74	8.08	<b>&lt;.0001</b>
T*Depth	4	302.41	75.60	1.31	0.2855
Error	37	2141.06	57.87		
<b>H<sub>05</sub></b>					
Transect	1	241.31	241.31	4.73	0.0347
DFFS	5	56.15	11.23	0.22	0.9521
T*DFFS	5	1450.89	290.18	5.69	<b>0.0003</b>
Error	47	2396.81	50.99		



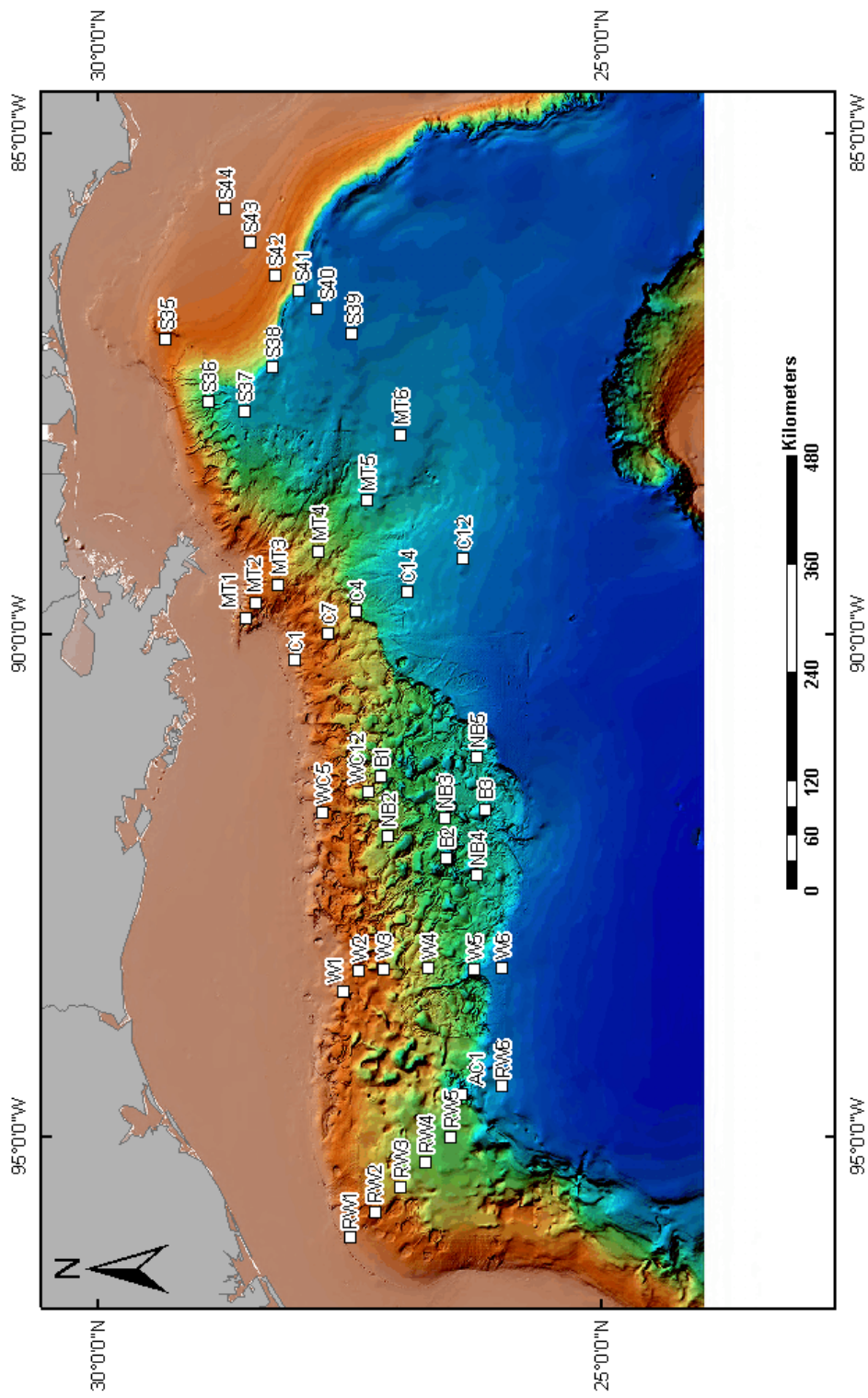


Figure 2.1: Harpacticoid copepods were identified to species at a total of 43 stations in the northern Gulf of Mexico deep sea.

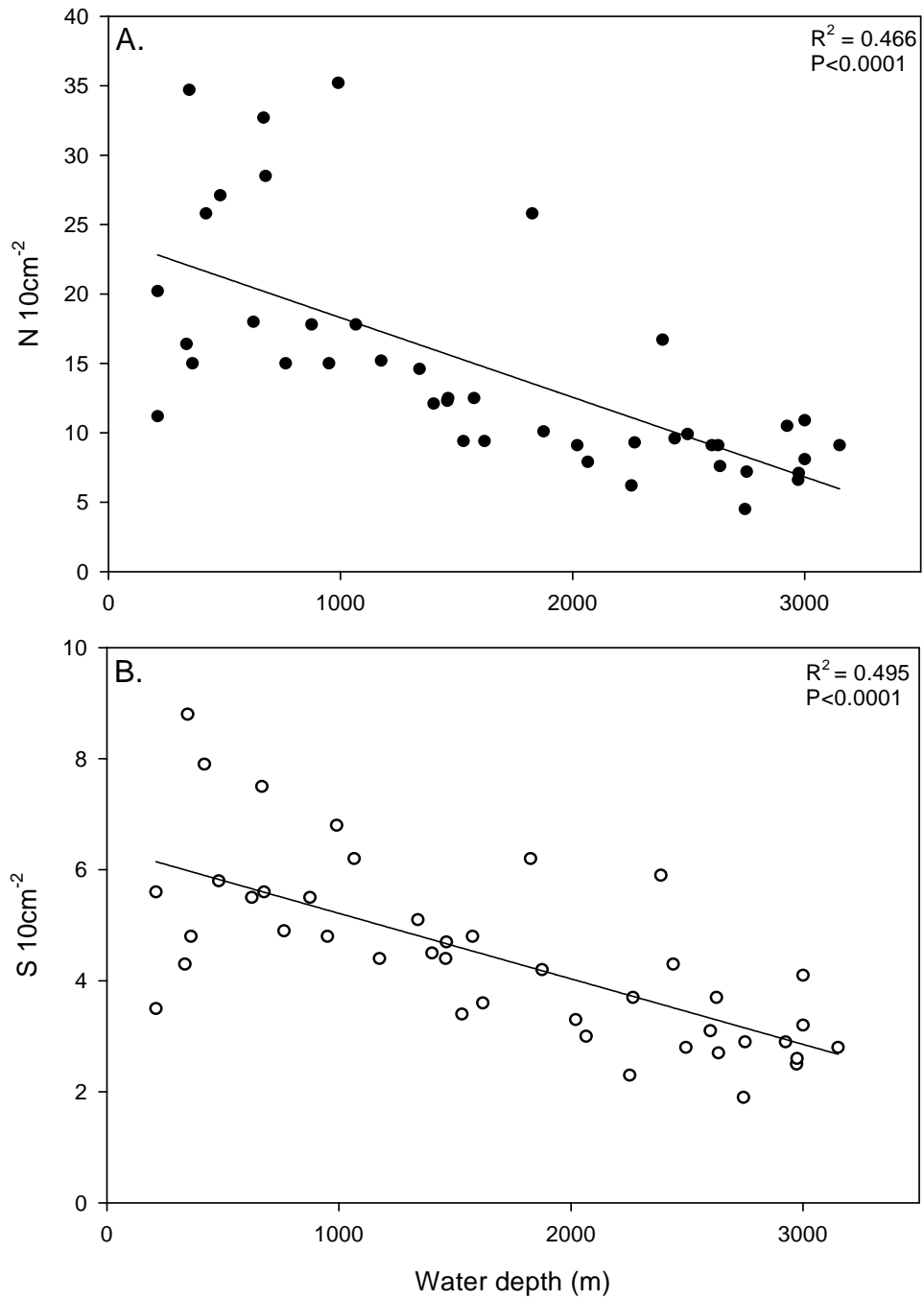


Figure 2.2: Harpacticoid copepod abundance (N) and species richness (S), adjusted to the number per  $10\text{ cm}^2$ , as a function of depth. Abundance and richness are highly correlated ( $r = 0.91$ ).

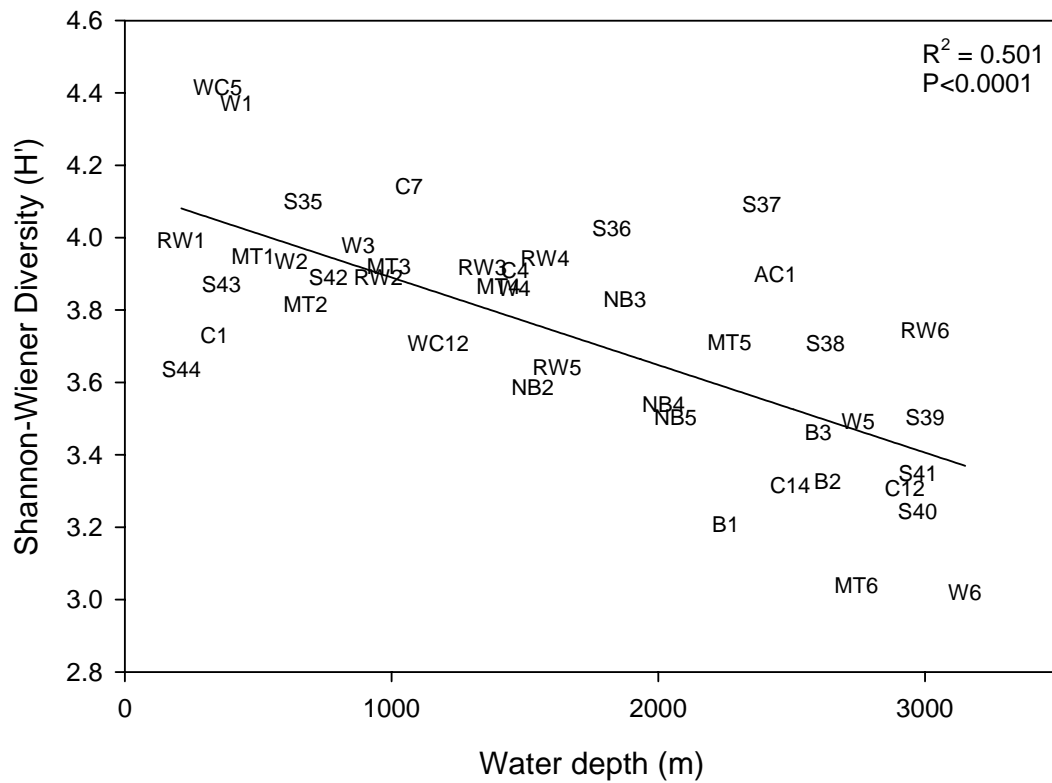


Figure 2.3: Shannon-Wiener diversity index ( $H'$ ) as a function of depth for pooled replicate core samples of harpacticoid copepods.

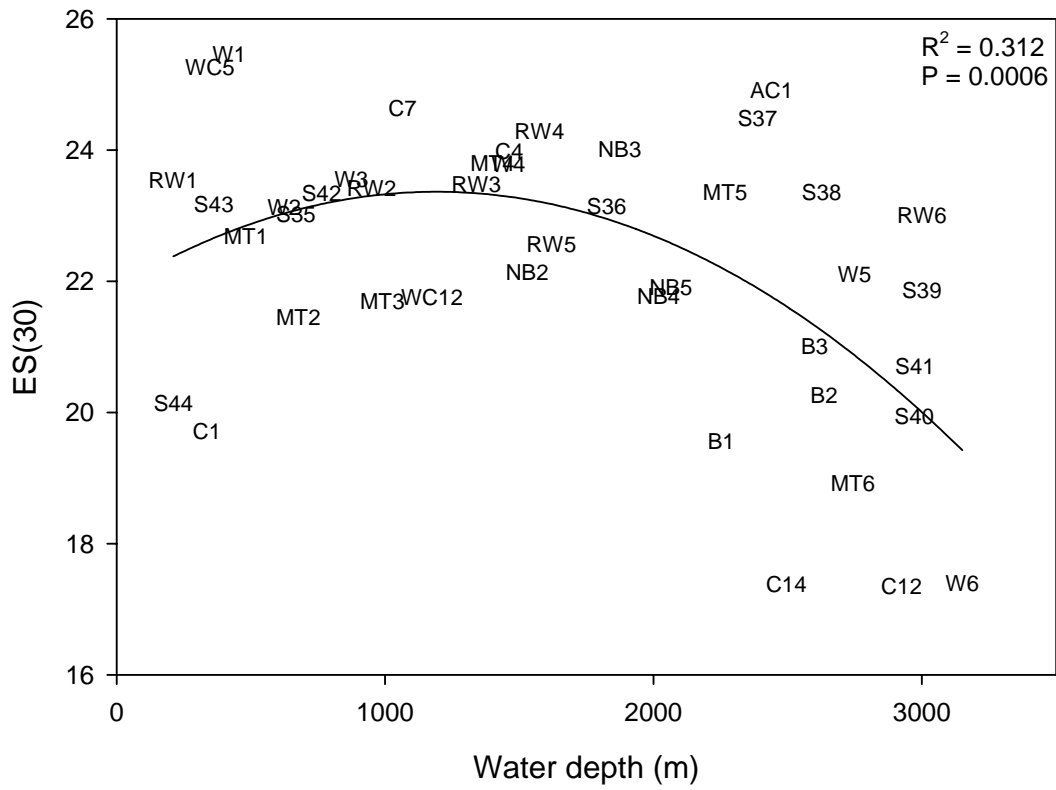


Figure 2.4: Expected number of harpacticoid species per 30 individuals [ES(30)], for pooled replicate core samples of harpacticoid copepods.

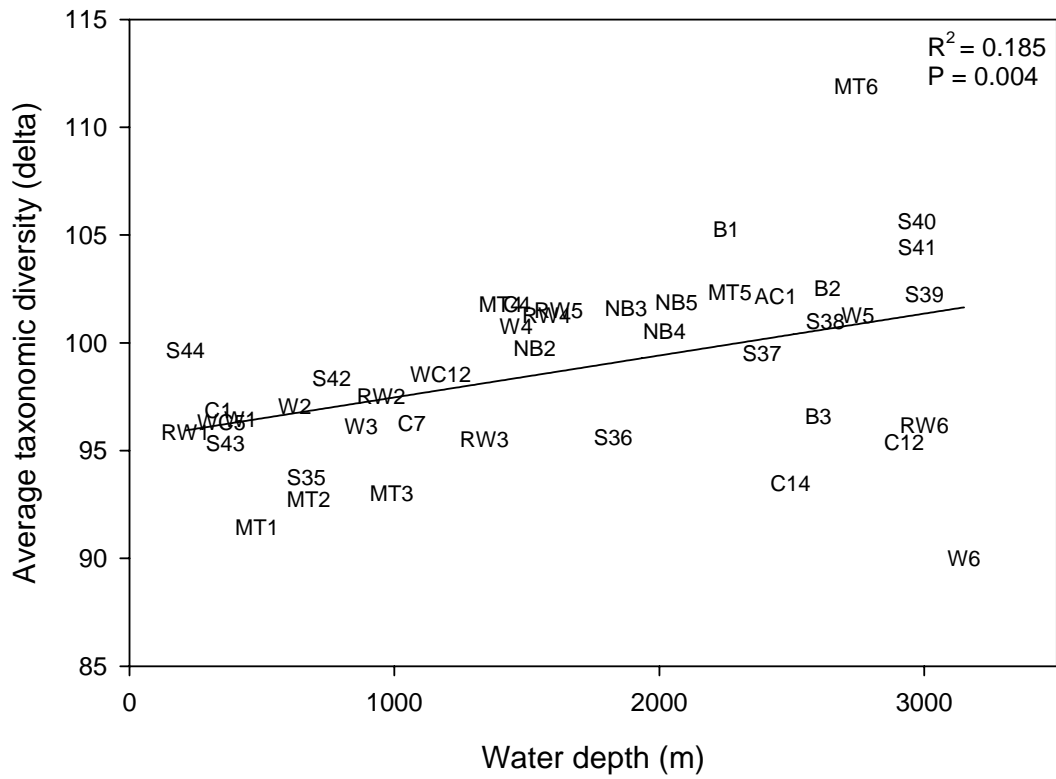


Figure 2.5: Average taxonomic diversity ( $\Delta$ ) for pooled replicate core samples of harpacticoid.

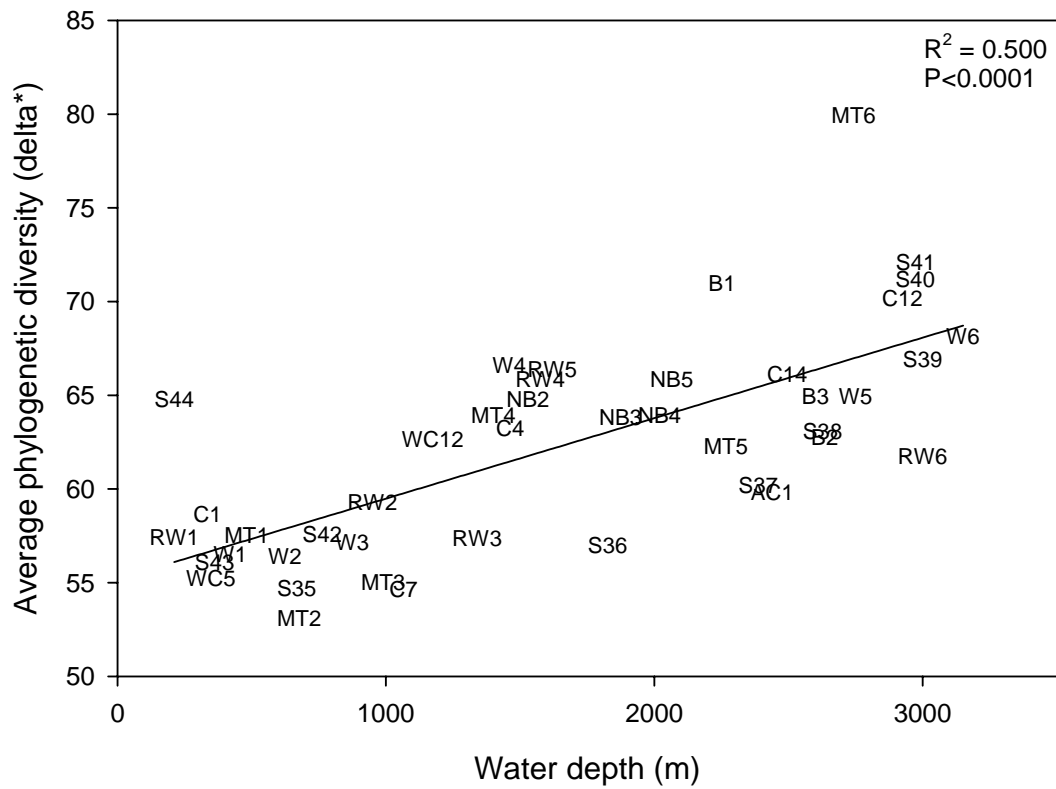


Figure 2.6: Average phylogenetic diversity ( $\Phi^+$ ) for pooled replicate core samples of harpacticoid copepods.

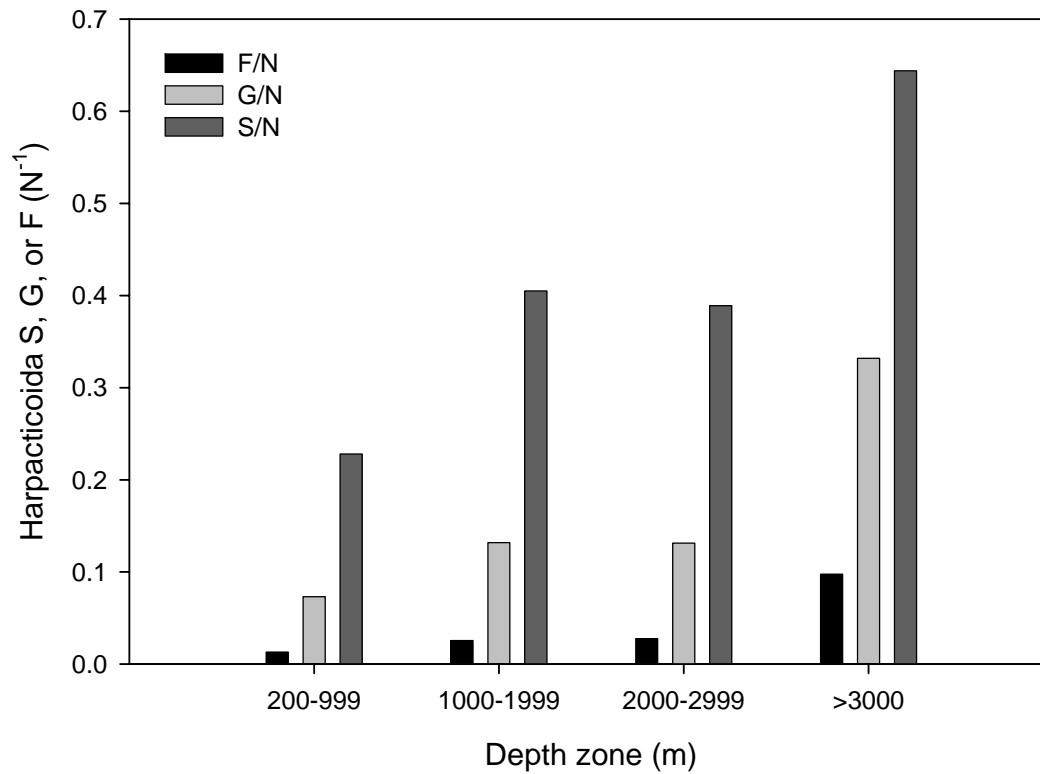


Figure 2.7: The ratio of harpacticoid copepod species (S), genera (G), and families (F) per total individuals (N) in each depth zone. Zones are significantly different ( $P < 0.01$ ), with pairwise comparisons indicating differences among shallowest and deepest zones only.

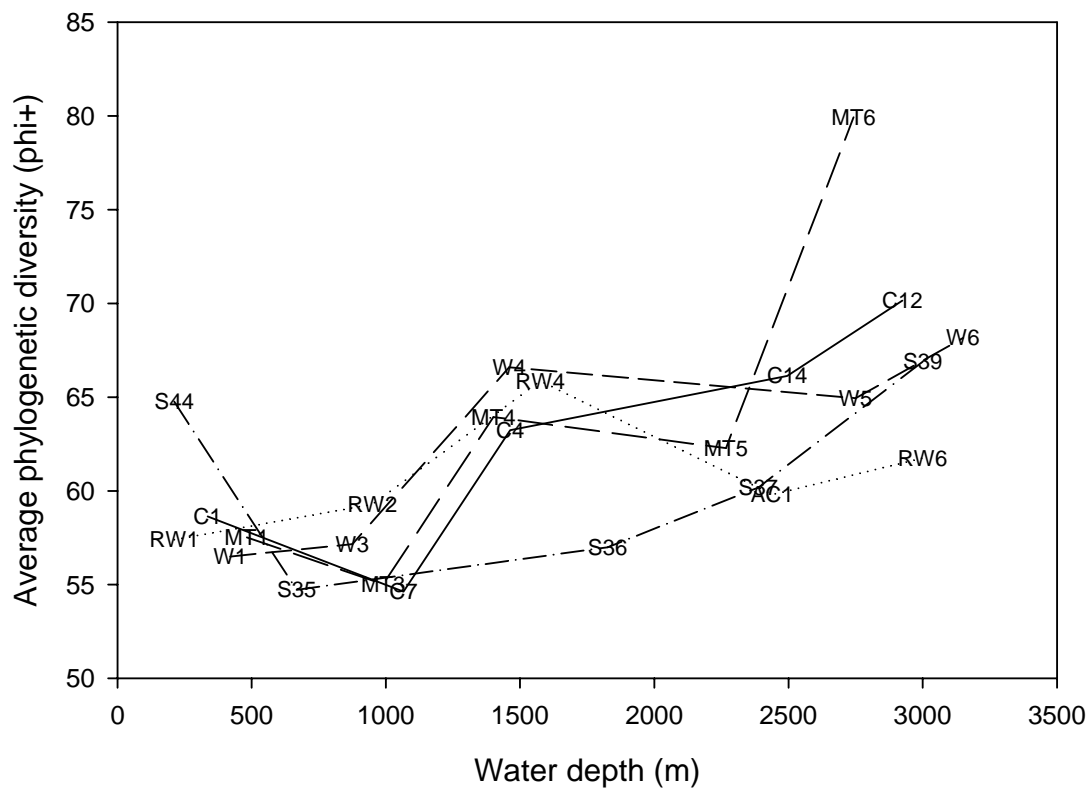


Figure 2.8: Average phylogenetic diversity ( $\Phi^+$ ) as a function of depth for transects included in the test for depth and longitude differences ( $H_{01}$  and  $H_{02}$ ).



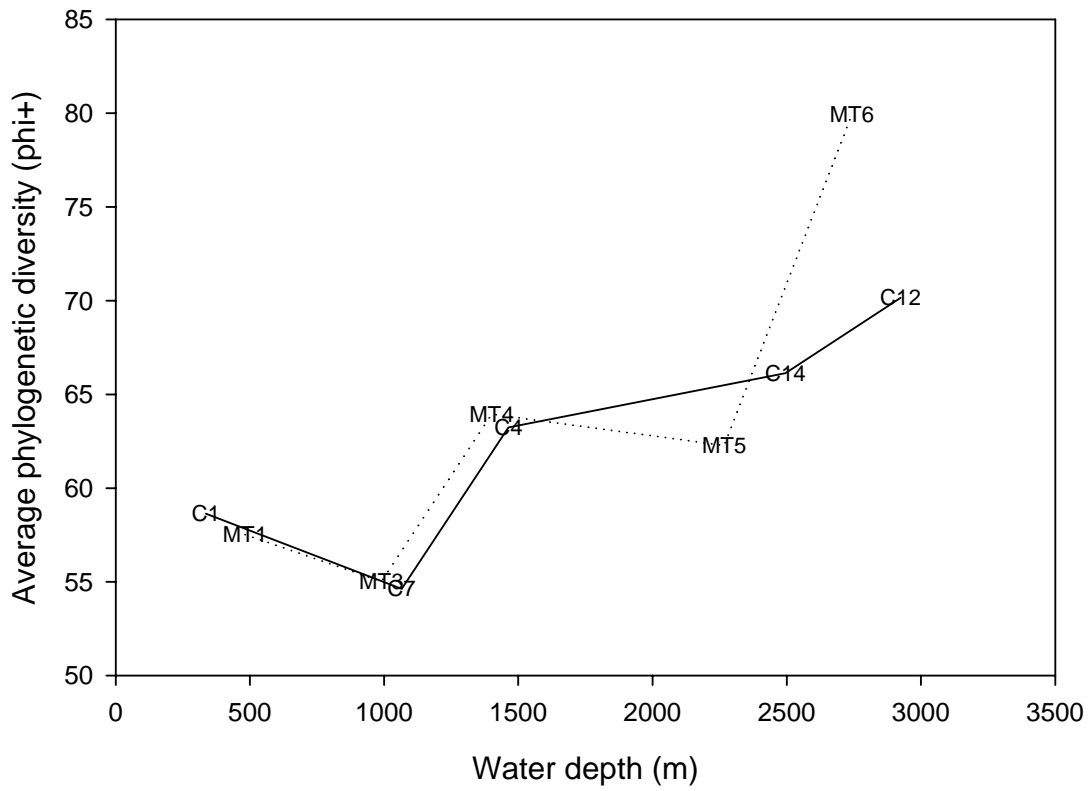


Figure 2.9: Average phylogenetic diversity ( $\Phi^+$ ) as a function of depth for transects included in the test for diversity differences between canyon (MT) and non-canyon (C) areas ( $H_{04}$ ).

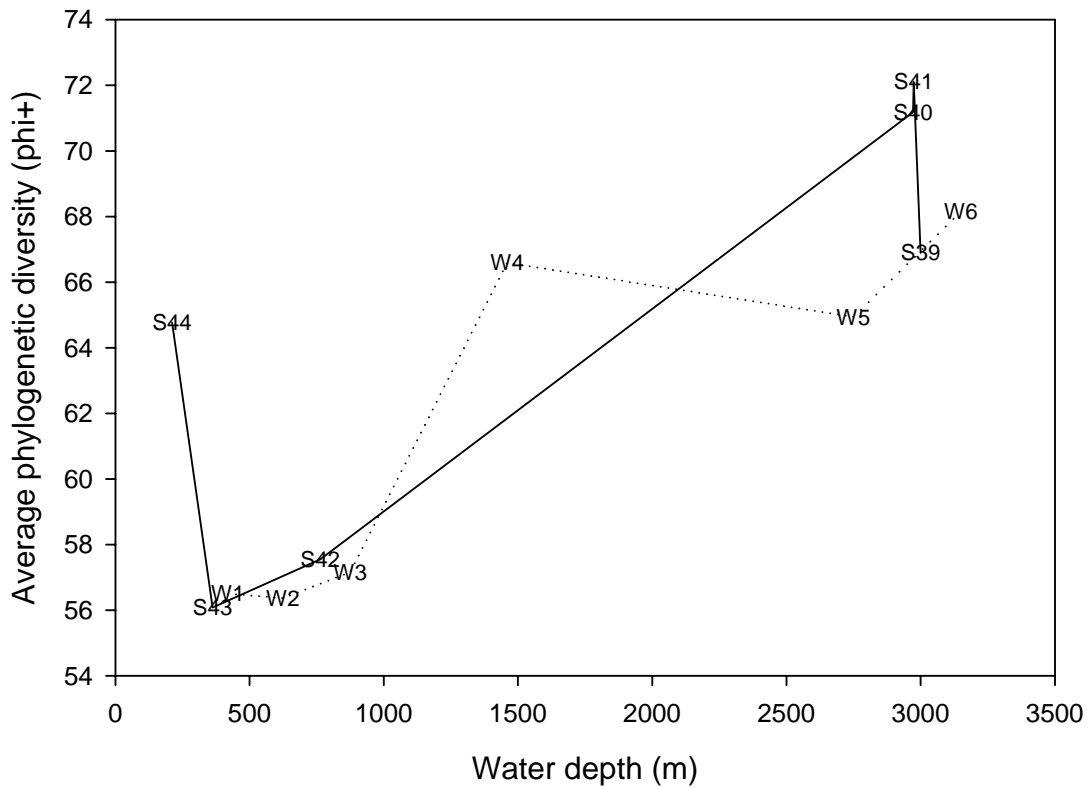


Figure 2.10: Average phylogenetic diversity ( $\Phi^+$ ) as a function of depth for transects included in the test for escarpment (S transect) effects on diversity ( $H_{05}$ ).

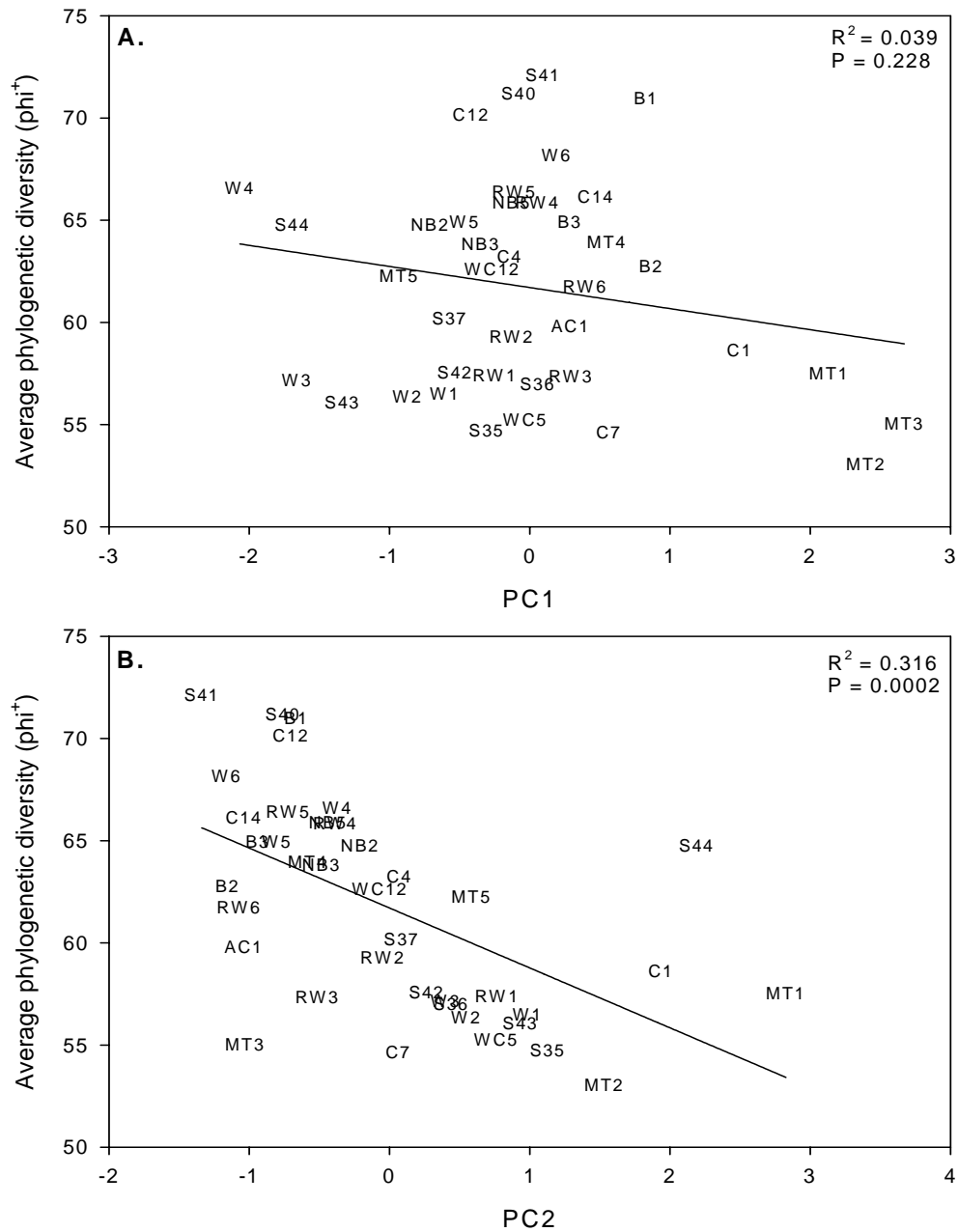


Figure 2.11: Regression of average phylogenetic diversity ( $\Phi^+$ ) as a function of **A)** environmental PC1 and **B)** PC2.  $\Phi^+$  is not significantly related to sediment properties (PC1), but is significantly related to POM flux (PC2).

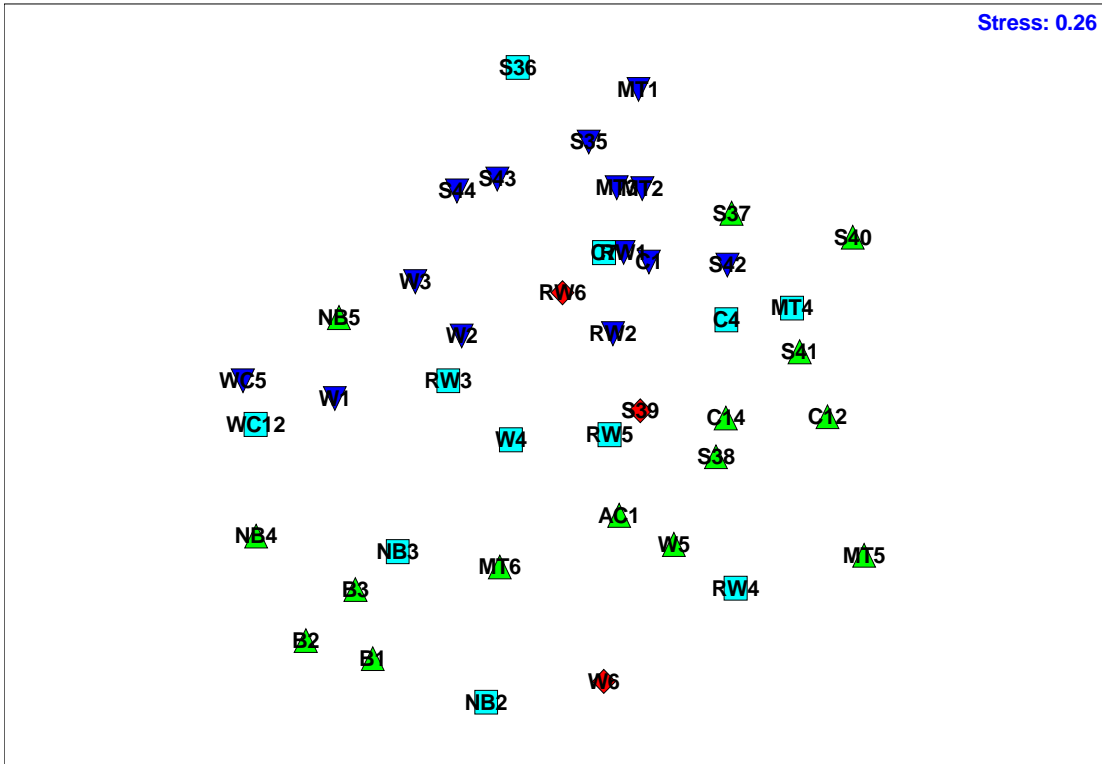


Figure 2.12: MDS orientation of stations based on harpacticoid species abundance. Symbols indicate depth zone: ▼ = 200-1000 meters, ■ = 1000-2000 meters, ▲ = 2000-3000 meters, ◆ > 3000 meters. One-way analysis of similarity (ANOSIM) indicates significant depth differences (P<0.01).



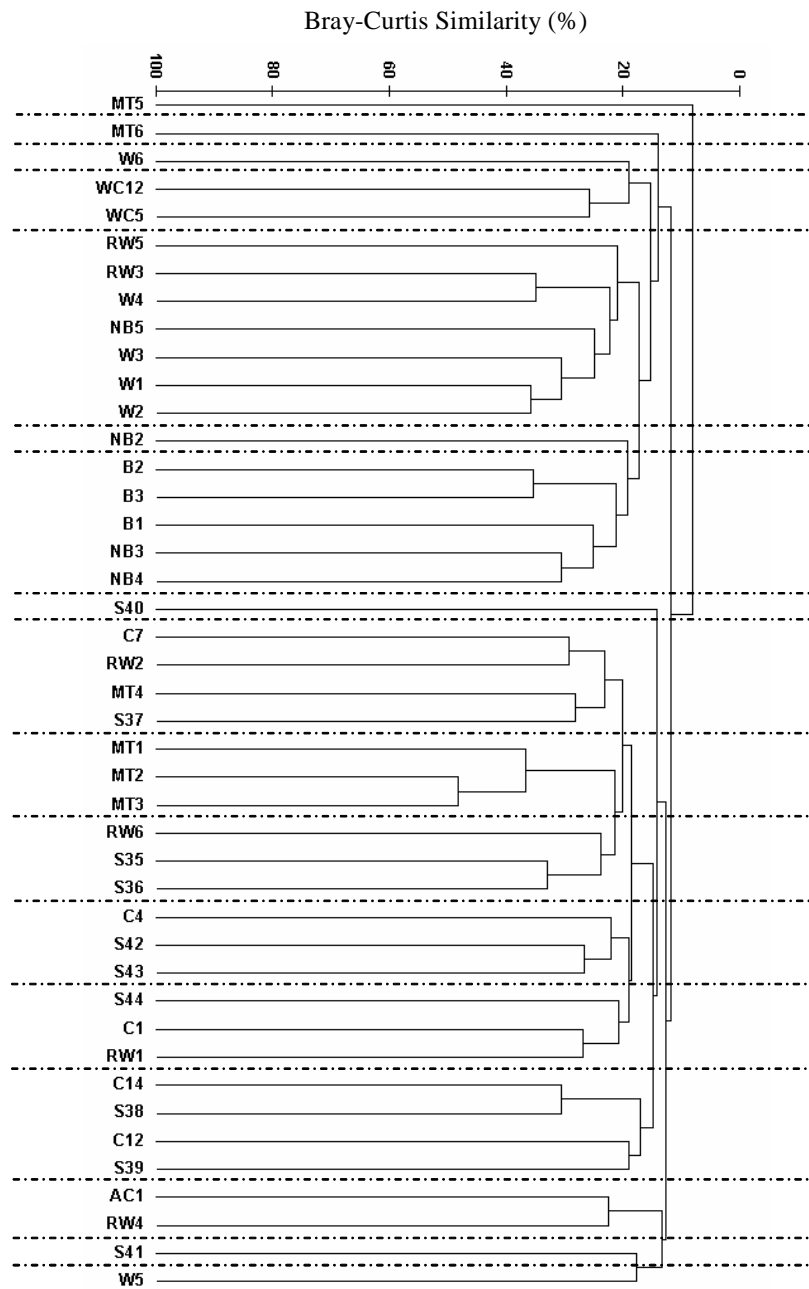


Figure 2.14: Cluster analysis of Harpacticoid community composition, created using Bray-Curtis similarity, and group average linking. Zonation determined on basis of >20% similarity.

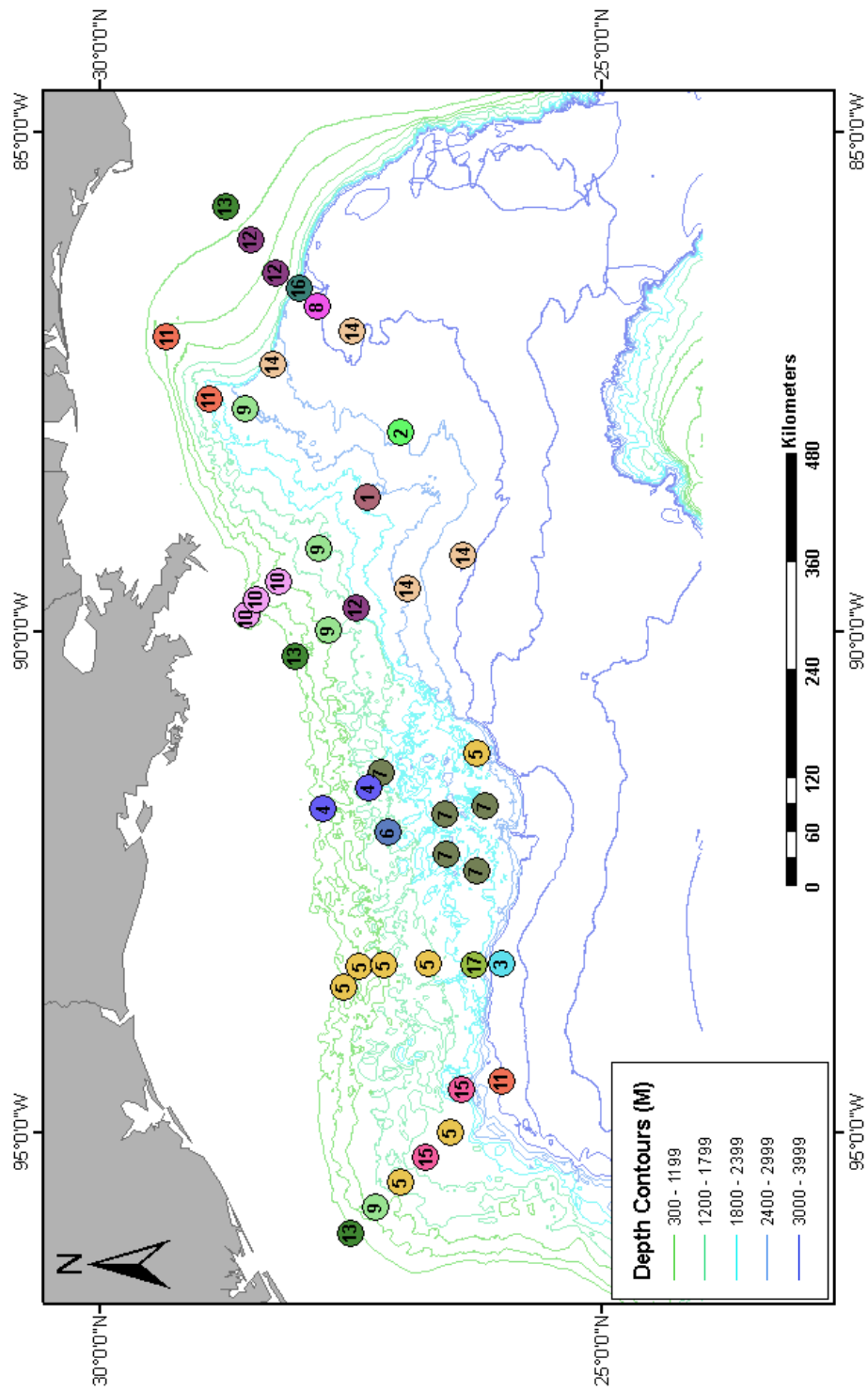


Figure 2.15: Harpacticoid copepod species zonation in the northern Gulf of Mexico deep sea. Zones were chosen on the basis of >20% similarity using the Bray-Curtis similarity index.

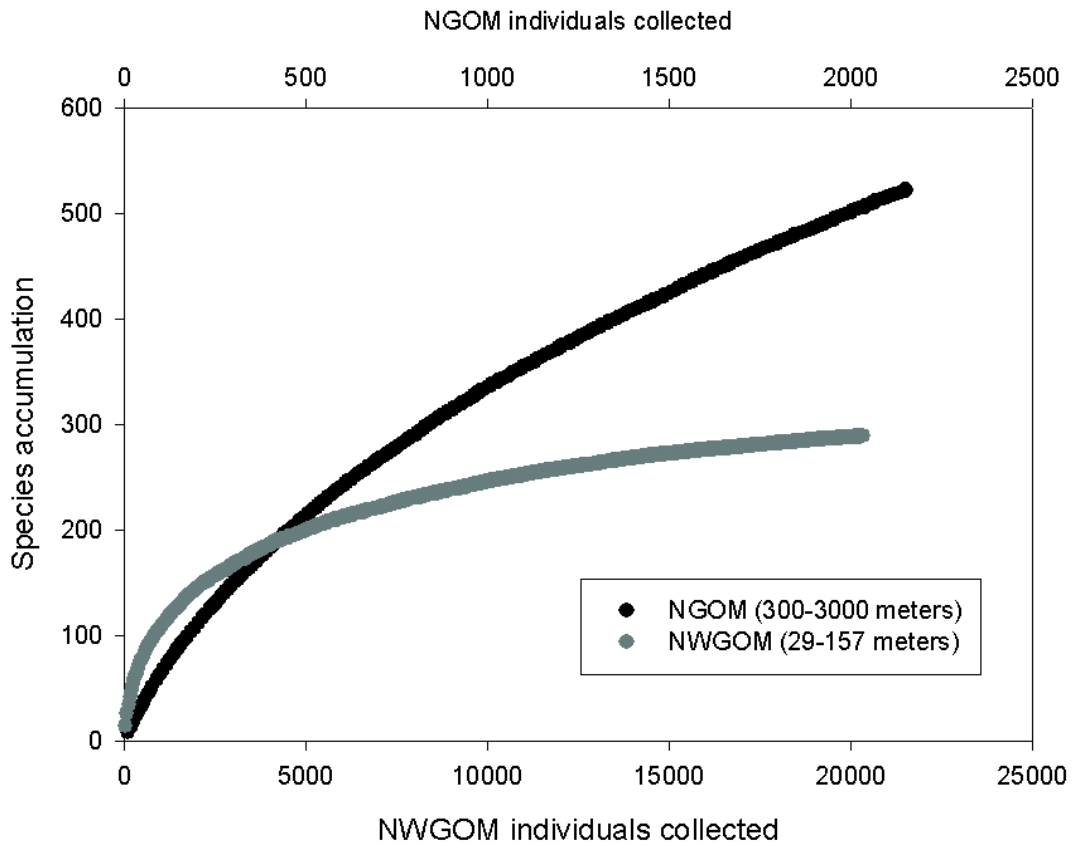


Figure 2.16: Species accumulation curves used to estimate regional Harpacticoida species abundance in the Gulf of Mexico (extrapolation).



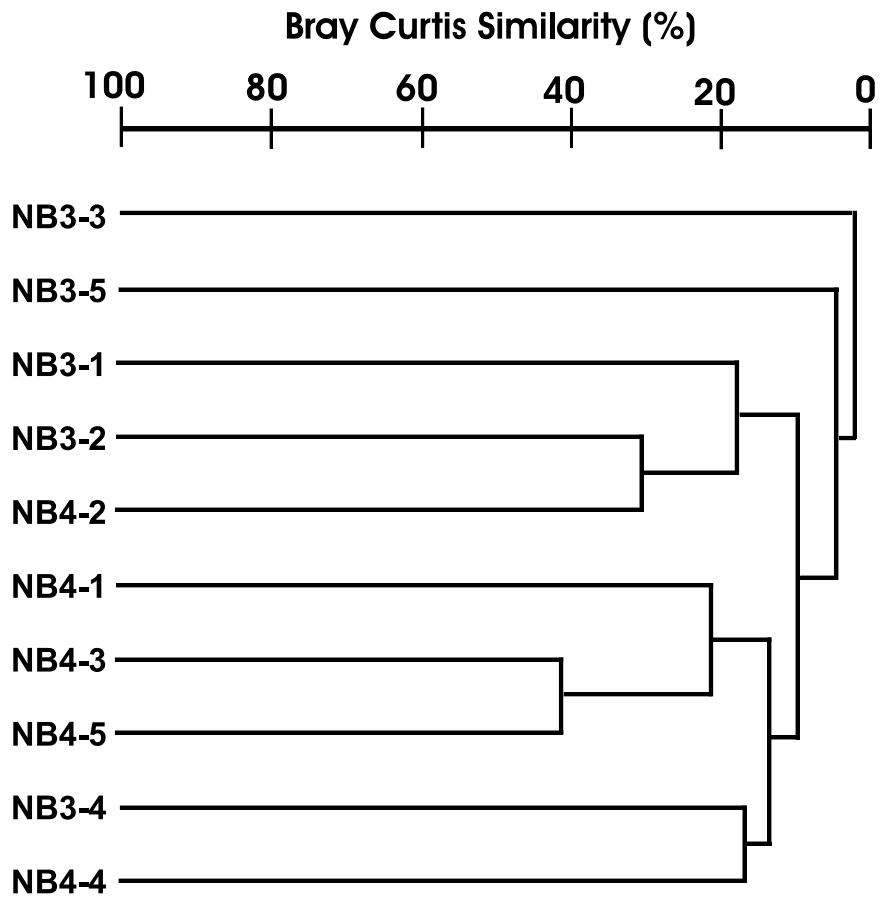


Figure 2.17: Cluster analysis illustrating within versus between station differences in harpacticoid community structure for all replicates at stations NB3 and NB4.

### **CHAPTER 3: MEIOFAUNA BIOMASS AND WEIGHT-DEPENDANT RESPIRATION IN THE NORTHERN GULF OF MEXICO DEEP SEA**

#### **ABSTRACT**

Meiofauna exhibit high biomass in deep-sea soft sediments, compared to larger invertebrates (e.g. macro- and megafauna), and play an important role in the global carbon cycle. However, deep-sea meiofauna community function (grazing, respiration, etc.) has only been sparsely investigated. In the present study, meiofauna biomass was calculated at 51 stations using a newly developed, semi-automated, digital microphotographic method; grazing rates on bacteria were measured at four stations using radiotracer techniques in controlled temperature and pressure shipboard experiments; and meiofauna mass-dependent respiration was estimated at 51 stations using an allometric power law. Strong relationships exist between biomass and meiofauna community respiration with depth. Highest biomass and respiration occurred in the proximity of high particulate organic matter flux; where surface currents interact with Mississippi River inflow complex slope topography. Allometric estimates indicate that meiofauna require 7% of their biomass per day to meet their metabolic energy budget, and are therefore not food limited with respect to sediment bacterial biomass. Meiofauna account for 10-25% of whole sediment community respiration indicating their importance in global biogeochemical cycles.

## INTRODUCTION

Meiofauna are ubiquitous in marine soft-sediment communities (Coull and Bell 1979; Hicks and Coull 1983; Soltwedel 2000), and are an important link in transferring carbon primary and secondary production to higher trophic levels (Montagna 1984, 1995). Meiofauna ubiquity extends into deep-sea environments, with greater (Pequegnat *et al.* 1990), or proportionally greater (Rowe *et al.* 1991), biomass compared to mega- and macrofauna-sized invertebrates. However, meiofauna trophic interactions as well as community respiration in the deep-sea are poorly understood. Rates of meiofauna grazing (Montagna 1984, 1993, 1995) as well as accurate biomass measurements (Baguley *et al.* 2004) are necessary to validate deep-sea trophic structure models and gain understanding of meiofauna community function.

Prior to the 1980's little was known of meiofauna trophic interactions with the microflora (i.e. bacteria and microphytobenthos); specifically, whole community grazing rates. Although, it had been discovered that meiofauna (Nematoda and Harpacticoida) are largely selective feeders (Marcotte 1977; Hicks and Coull 1983; Jensen 1987). Food particle selectivity, or grazing, was first measured by Montagna (1984) using radio-labeled tracer experiments originally designed for planktonic food web studies (Daro 1978), which subsequently spawned extensive investigation in shallow-water estuarine and coastal environments (Carman and Thistle 1985; Decho 1988; Decho and Fleeger 1988; Montagna and Bauer 1988; Carman 1990; Blanchard 1991; Montagna and Yoon 1991; Montagna *et al.* 1995; Pace and Carman 1996; Carman *et al.* 1997; Buffan-Dubau

and Carman 2000; Pinckney *et al.* 2003). Stable isotope chemistry has also been applied to shallow water benthic studies to identify natural food sources (Couch 1989; Riera *et al.* 1996; Peterson 1999) and trace food movement through two or more trophic levels (Peterson 1999; Middelburg *et al.* 2000; Herman *et al.* 2000; Moens *et al.* 2002; Carman and Fry 2002).

An understanding of deep-sea metabolic rates, in the context of whole-community respiration, evolved parallel to meiofauna grazing studies, beginning in the 1970's, and continuing to the present (Smith and Teal 1972; Smith *et al.* 1979; Smith 1987, 1992; Rowe *et al.* 1994; Smith *et al.* 2001, 2002). However, contribution of the meiofaunal component to whole-community respiration has only been sparingly studied (Shirayama 1992; Mahaut *et al.* 1995). Deep-sea floor carbon budgets (Smith *et al.* 1992; Rowe *et al.* 1994; Anderson *et al.* 1994), and trophic structure models (Rowe 1996), have been constructed to explain soft-sediment community function. However, meiofauna grazing on bacteria, phytodetritus, or any other food source, has never been empirically measured. Therefore the meiofauna contribution to deep-sea food webs, carbon cycling, and whole community respiration is largely unknown. Given the vast size of the deep-sea, the ubiquity of meiofauna in this environment, and the dominance of meiofauna biomass, it is imperative that meiofauna trophic interactions be understood.

Meiofauna are an important, but often ignored, component of deep-sea soft sediments, and although meiofauna biomass often exceeds macrofaunal biomass (Pequegnat *et al.* 1990), their contribution to whole-community metabolism is largely

unknown. Additionally, trophic interactions in the deep sea, and dynamics that structure deep-sea communities have not been elucidated (Etter and Mullineaux 2001). To gain an understanding of deep-sea meiofauna community function, a carbon budget is needed in which both standing stocks and fluxes are quantified. The purpose of this study was to determine meiofaunal biomass, meiofauna contribution to whole-community respiration, and to quantify meiofaunal-bacterial trophic linkages in the northern Gulf of Mexico deep sea.

## **METHODS**

Biomass and mass-dependent respiration were estimated at 51 stations (Fig. 3.1), and shipboard grazing experiments were conducted at four experimental stations (Fig. 3.2). The stations were sampled as part of a larger, comprehensive study of deep Gulf of Mexico benthos (DGoMB). For complete field and laboratory methods associated with sample collection and processing see chapter one of this dissertation.

*Biomass* – Meiofauna biomass was calculated using a newly-developed digital microphotographic approach (Baguley *et al.* 2004) for all samples at all DGoMB stations (Fig. 3.1). Typically, meiobenthic samples are dominated by two taxa: Harpacticoida and Nematoda. Nematodes generally dominate the sample contributing 70 to 95% of total individuals while harpacticoids constitute a lesser proportion ranging from 5 to 20%. Other taxa usually comprise a minor proportion of individuals ranging from 5 to 20%. For this reason, meiofaunal biomass is frequently based on harpacticoid and nematode values alone (Montagna 2002). All harpacticoids and a subsample of 30 nematodes were

digitally photographed using a compound microscope. Area and width measurements were calculated using Sigma Scan Pro 4.0, analytical graphics software (Baguley *et al.* 2004).

Nematode biovolume (V, in nL units) was estimated *sensu* Baguley *et al.* (2004) by assuming nematode body shape is approximately cylindrical:

$$V \text{ (nL)} = \pi r^2 L / 10^6$$

where, L equals the total length of the nematode (area/width), and r equals the radius (mid- body width/2). Nematode biovolume estimates by the above equation have are not significantly different from direct measurement with analytical balance or elemental analyzer (Baguley *et al.*, 2004).

Harpacticoid biovolume calculation relied on area and width measurements along with two conversion factors ( $C_{bf}$  = body form and  $C_o$  = orientation). Body volume was estimated from a formula used by Feller and Warwick (1988) and Warwick and Price (1979) to measure harpacticoid biovolume:

$$V \text{ (nl)} = [A \text{ (mm)} \times W \text{ (mm)}](C_{bf} \times C_o) / 10^9$$

Harpacticoid body volume estimates relied on eight body type-specific conversion factors ( $C_{bf}$ ) derived from volumetric displacement of plasticene scale models (McIntyre and Warwick 1984, Warwick and Gee 1984). Application of these factors required matching SigmaScan images of individual harpacticoids to line-drawings of different body forms (cylindrical, semi- cylindrical compressed, semi-cylindrical, semi-cylindrical depressed, fusiform, pyriform, pyriform depressed, and scutelliform) and their

corresponding conversion factors (McIntyre and Warwick 1984, Warwick and Gee 1984). Photographic images that did not approximate one of these eight body forms because of variable axial orientation and rotation were assigned a default value ( $C_{bf} = 440$ ). The default value was derived from average conversion factors of five of the most commonly encountered body forms (semi-cylindrical, semi-cylindrical depressed, fusiform, pyriform, pyriform depressed).  $C_{bf}$  values for all minor taxa were taken from Feller and Warwick (1979).

One additional conversion factor was required to account for the average loss of image area resulting from variable body orientations. The longitudinal axis of most animals was generally parallel ( $\sim 0^\circ$ ) to the photographic plane displaying a ventral, dorsal or lateral aspect, as desired. However, individuals were frequently oriented at an angle to the photographic plane ( $1 - 90^\circ$ ), yielding underestimates of biovolume. A correction factor ( $C_o = 1.5$ ) was determined by comparing the average biovolume of 90 harpacticoids photographed in the standard mode (avg. biovolume =  $1.17 \pm 1.09$  nL) to the biovolume of the same individuals after being manipulated into a flat, non-compressed, dorsal orientation (avg. biovolume =  $1.75 \pm 2.19$  nL).

Nematode and harpacticoid wet mass was calculated from biovolume using a specific gravity of 1.13, and wet mass was converted to dry mass assuming a ratio of 25% (Weiser 1960; Feller and Warwick 1988). Previous studies have used a carbon to dry mass ratio of 40% (Feller and Warwick 1988; Warwick and Price 1979; Danovaro *et al.* 1995; and others), which was estimated for chaetognaths by Steele (1974).

Baguley *et al.* (2004) found carbon to dry mass ratios of 51.4% for nematodes and 45.8% for harpacticoids by direct measurement. These empirically measured values were used to convert dry mass to carbon mass.

For the less abundant taxa, a sub-sample of at least 10 individuals (taken from random samples) was digitally photographed under a compound microscope, and biomass was calculated as described above for the harpacticoid copepods. However, taxon-specific conversion factors were applied for different body forms ( $C_{bf}$ ), as proposed by Feller and Warwick (1988). For these taxa, a uniform conversion factor of 48% was used to convert dry mass to carbon mass, but specific gravity (1.13), and dry to wet mass (0.25) were assumed to be uniform (Feller and Warwick 1988).

Bacterial biomass was estimated by Jody Deming (unpublished DGoMB data) using epifluorescence microscopy for enumeration of Acridine Orange and DAPI-stained cells (Deming *et al.* 1997; Schmitt *et al.* 1998), and a conversion factor of 10 fg C cell<sup>-1</sup> was used to determine estimate (Alongi 1990; Relaxans *et al.* 1996). For more detailed information regarding bacterial abundance and biomass methodology, see the above references and Rowe *et al.* (in prep). The complete bacterial abundance and biomass data set can be accessed, with permission, from the DGoMB database at <http://www.gerg.tamu.edu>.

*Grazing Experiments* – Meiofauna grazing experiments were carried out using radiolabeled tritiated thymidine (<sup>3</sup>HTdr) to measure feeding rates on bacteria (Montagna 1984, 1993). Grazing experiments were conducted at four experimental stations (Fig.



3.2) during June 2001. The experimental design for all grazing studies included 6 replicates per station, with 3 replicates designated as experimental and 3 as killed controls.

Core tubes (5.5 cm i.d.) were mounted inside the GOMEX boxcore (Boland and Rowe 1991) and removed immediately upon return to the ship's deck. The top centimeter of each core was extruded (in a shaded area of the ship's deck), rinsed into pre-sterilized 50 ml polypropylene centrifuge tubes with ice-cold 0.2 micron-filtered bottom water (obtained from CTD cast). Samples were placed immediately on ice, and transported to the refrigerated van where all experiments took place. The refrigerated van was kept at in situ temperature (4-7° C), as determined from a CTD cast prior to sampling.

To test for meiofauna grazing on bacteria, 5  $\mu\text{Ci}$  of  $^3\text{HTdr}$  was added by pipetting 1 ml of  $^3\text{HTdr}$  stock solution (5  $\mu\text{Ci}/\text{ml}$ ) into each centrifuge tube. Control samples were immediately fixed with 10 ml of 10% buffered formaldehyde solution. Any remaining headspace in tubes was eliminated by adding 0.2 micron-filtered bottom water, and tubes were then sealed with two layers of Parafilm® (making sure no air bubbles remained in tubes). Both experimental and control samples were placed in stainless steel vessels (Deming 1997, 2001) and pressurized to *in situ* conditions. Incubations were run for 24 hours, after which time experimental samples were fixed with 50 ml of 10% buffered formaldehyde solution. An equal volume of 10% buffered formaldehyde solution was added to control tubes to maintain volume proportions.

Estimation of bacterial label uptake was accomplished by taking 1.0 ml aliquots from both experimental and control tubes and rinsing over 0.2  $\mu\text{m}$  Millipore® filters. Aliquots were rinsed three times with de-ionized (DI) water to ensure removal of free label. Filters were placed into 20 ml glass scintillation vials and stored under refrigeration and returned to The University of Texas Marine Science Institute (UTMSI), Port Aransas, Texas, USA for analysis. The remaining sample was pre-sieved shipboard over a 45  $\mu\text{m}$  Nitex® mesh and rinsed thoroughly with DI water until the entire silt and clay fractions were removed. An equal volume of 10% buffered formaldehyde and DI water were added to samples making the final formaldehyde concentration 5%. Samples were frozen, to prevent isotope leakage from animals (Moens *et al.* 1999), and returned to UTMSI for sorting and analysis.

Laboratory analysis of grazing samples includes extraction of meiofauna from sediments and counting of animal and bacterial radiolabel uptake (disintegrations per minute, DPM). The 1.0 ml aliquot sub-sample is used to measure bacterial uptake of  $^3\text{H}$ Tdr. The subsample was dispersed and suspended in 5 ml of distilled water and 15 ml ScintiVerse BOA™ (Fisher) scintillation cocktail. Meiofauna were separated from sediments by isopycnic centrifugation with Ludox-AM™ (DuPont). Animals were then picked and sorted into four groups using a dissecting microscope: Nematoda, Harpacticoida, Polychaeta, and other taxa. Animals were placed in 7 ml glass scintillation vials with 1 ml of DI water. The meiofauna are then dried at 60 °C for 24 hours and then solubilized in 200  $\mu\text{l}$  Hemo-De™ (Fisher) tissue solubilizer for 24 h.

Samples were counted by scintillation spectrophotometry in 5 ml of ScintiVerse BOA™ (Fisher) scintillation cocktail. Liquid scintillation analysis was carried out using a Beckman LS5801 liquid scintillation spectrophotometer (Beckman Instruments Inc., Fullerton, CA, USA). Quenching was corrected for by using external standards.

Meiofauna grazing rates are calculated by the following model (Montagna 1984, 1993):

$$G = 2F/t$$

$$F = M/B$$

Where G is the grazing rate expressed in units of  $d^{-1}$ , F is the fraction of label uptake in meiofauna (M), relative to bacteria (B), at time, t (days). M and B are both in units of disintegrations per minute (DPM).

*Allometric Respiration Estimates* – Meiofauna mass-dependent respiration rate (R, in units of  $d^{-1}$ ) was estimated by an allometric law which is described by the following power function:

$$R = aW^b$$

where W is the mean weight of the organism ( $\Sigma\text{Biomass}/\Sigma\text{Abundance}$ ),  $a = 7.4 \cdot 10^{-3}$ , and  $b = -0.24$ . The constants,  $a$  and  $b$ , were determined by Mahaut *et al.* (1995) by regressing published respiration values for metazoan invertebrates and fish in both deep-sea and shallow water environments. In their deep-sea regression, the correlation coefficient was -0.94, and the 95% confidence interval of  $b$  was -0.263 to -0.228. Thus, the mass-dependent respiration rate (R) is a rate constant relating to the average

individual biomass. Therefore, total community respiration, in terms of CO<sub>2</sub> mass (mg) released per meter squared per day, can be estimated by multiplying the total biomass ( $\Sigma B_i$ , mg C m<sup>-2</sup>) by the mass-dependent rate constant (R<sub>i</sub>, d<sup>-1</sup> units):

$$CO_2 = (\Sigma B_i \times R_i)$$

The total metabolic organic carbon (OrgC) requirement was estimated by assuming respiration is only 80% of consumption. Consumption (C) is the sum of respiration (R), secondary production (P), and egestion (E), following the equation reviewed by Valiela (1995):

$$C = R + P + E$$

*GIS Analysis of Regional Biomass and Respiration* – GIS-based analyses were performed (ArcView 9.0, ESRI) to further examine spatial trends in the data set. The relative biomass at each station was compared by generating bubble values, where bubble size is relative to the standing stock. Biomass was interpolated to raster using the inverse distance weighted model, with variable search radius, and cell size of 2.8 km<sup>2</sup>. The interpolated raster was fixed to the extent of Northern Gulf of Mexico bathymetry (courtesy of Bill Bryant, TAMU), ranging from 200 to 3600 meters. The total meiofauna standing stock within the model study area (kg Carbon ± 1 st. dev.) was calculated by multiplying the average cell value (32 kg C km<sup>-2</sup>) by the total area (6.6 10<sup>5</sup> km<sup>2</sup>), both generated by the model. Meiofauna respiration in the sampling region was also interpolated using the inverse distance weighted model. Total meiofauna respiration within the model study area (kg O<sub>2</sub> ± 1 st. dev.) was calculated by multiplying the

average cell value ( $2.3 \text{ kg C km}^{-2}$ ) by the total area ( $6.6 \cdot 10^5 \text{ km}^2$ ), both generated by the model.

## RESULTS

*Meiofauna Biomass* – Meiofauna biomass is dominated by the two dominant taxa, Nematoda and Harpacticoida (Table 3.1). Mean biomass per station was  $273 \text{ mg wet weight m}^{-2}$  ( $43.3 \text{ mg C m}^{-2}$ ). Maximum and minimum biomass values of  $157.1$  and  $3.5 \text{ mg C m}^{-2}$  were found at stations S42 and JSSD3, respectively (Table 3.2). A strong linear relationship exists between log meiofauna biomass ( $R^2 = 0.726$ ,  $P < 0.0001$ ) and water depth (Fig. 3.3). A general trend of decreasing biomass per individual with increasing water depth was observed for Nematoda ( $R^2 = 0.125$ ,  $P = 0.0202$ , Fig. 3.4), while Harpacticoida had a general increasing trend of biomass per individual with increasing water depth ( $R^2 = 0.167$ ,  $P = 0.0066$ , Fig. 3.5).

Spatial trends in meiofauna biomass (Fig. 3.6) closely parallel those observed with abundance (Chapter one, Fig. 1.4). However, highest biomass was observed at station S42 (Table 3.2, Fig. 3.6). High biomass at station S42 reflects proportionally larger nematode individuals at this location (Fig. 3.4). At the four experimental stations (MT3, MT6, S36, S42) meiofauna biomass decreased in a general linear relationship with depth (Table 3.3, Fig. 3.6). Nematodes and harpacticoids account for 95-98% of meiofaunal biomass at the four experimental stations (calculated from Table 3.1).

*Allometric Respiration Estimates* – The mean mass-dependent respiration rate of meiofauna was estimated using the average individual biomass at each DGoMB

station (Table 3.2, Fig. 3.7A). Mean respiration ( $d^{-1}$ ) increases as function of depth, in a weak, but significant linear relationship (Fig. 3.7A,  $R^2 = 0.256$ ,  $P < 0.0001$ ). Mean respiration ( $d^{-1}$ ) increases with decreasing average biomass (Table 3.2). Meiofauna community respiration ( $mg\ C\ m^{-2}\ d^{-1}$ ) decreases in a strong linear relationship with depth (Fig. 3.7B,  $R^2 = 0.598$ ,  $P < 0.0001$ ). Variance in community respiration is higher in shallower water (200-1500 meters; Fig. 3.10). Community respiration ranges from a low of  $0.3\ mg\ C\ m^{-2}\ d^{-1}$  at stations JSSD2-4 to a high of  $6.3\ mg\ C\ m^{-2}\ d^{-1}$  at S36 and S42.

*Grazing Experiments* – Grazing rates by all four meiofauna taxa exhibited significant treatment by station interactions in two-way block analysis of variance (Table 3.4). Polychaetes and others accounted for the majority of label uptake (Fig. 3.8), with harpacticoid grazing only measured at one station (S36), and nematode grazing was measurable at one station, but was sufficiently small that it was not comparable in magnitude to the other taxonomic groups (Fig. 3.8). The average grazing rate for pooled taxonomic groups at each of the experimental stations ranges from a high of  $4.6 \times 10^{-4}\ d^{-1}$  at station S36 to a low of  $1.1 \times 10^{-9}$  at station MT6. This rate ( $d^{-1}$ ) reflects a total carbon flux from bacteria to meiofauna ranging from  $1.0 \times 10^{-6}$  to  $7.7 \times 10^{-1}\ mg\ C\ m^{-2}\ d^{-1}$ , when multiplied by bacterial biomass ( $mg\ C\ m^{-2}$ ), and is between 0.0001 and 9.8% of the theoretical carbon requirement (Table 3.5).

*Regional Biomass and Community Carbon Requirement Estimates* – The general relationship of decreasing meiofauna biomass with water depth is seen over the entire northern GOM deep-sea. Variance from this pattern is observed primarily in the

northeastern GOM (Fig. 3.6), where highest biomass is often observed at mid-depth stations (S36, S42, MT3). Interpolated biomass estimates over the entire sampling region, and to the extent of the available bathymetry, illustrates the general pattern of decreasing biomass with depth, and also highlights biomass hot spots (Fig. 3.9). Average biomass per 2.8 km<sup>2</sup> cell, as calculated by the model, was  $2.7 \times 10^5 \pm 1.6 \times 10^5$   $\mu\text{g}$  wet mass m<sup>-2</sup>. A total of 83,844 cells (each 2.8 km<sup>2</sup>) were created by the model, equaling a total area of  $6.57 \times 10^5$  km<sup>2</sup>. Total meiofaunal biomass within the region was found to be  $2.1 \times 10^7 \pm 1.2 \times 10^7$  kg Carbon (wet mass converted to carbon using conversion factors of 0.25 dry/wet mass, and 0.48 carbon/dry mass, Baguley *et al.* 2004). Geographic variation in community organic carbon requirement (assuming respiration = 80% of total metabolic requirement) is observed mainly at water depths less than 1500 meters (Fig. 3.10). Stations MT1 and MT3 in the Mississippi Trough, station S36 located in the De Soto Canyon, and station S42 directly above the Florida Escarpment, have the highest community organic carbon requirement. These four stations are located in the northeastern Gulf of Mexico and also have highest biomass. Stations in the western Gulf of Mexico have comparably lower community respiration and lower biomass (Fig. 3.13 and 3.14). The theoretical organic carbon requirement over the northern GOM deep sea study area was estimated to be  $1.5 \times 10^6 (\pm 8.4 \times 10^5)$  mg C km<sup>-2</sup> d<sup>-1</sup>. The ratio of total estimated organic carbon requirement to total estimated biomass is 0.07 ( $1.5 \times 10^6$  kg C d<sup>-1</sup> /  $2.1 \times 10^7$  kg C) in units of d<sup>-1</sup>; which equals 7% of the community biomass.

## DISCUSSION

Meiofauna are an important, but often ignored, organisms living within deep-sea soft sediments, and although meiofauna biomass often exceeds macrofaunal biomass (Pequegnat *et al.* 1990), their contribution to whole-community metabolism is largely unknown. Additionally, trophic interactions in the deep sea, and community dynamics that structure deep-sea communities have not been elucidated (Etter and Mullineaux 2001). To gain an understanding of deep-sea meiofauna community function, a carbon budget is needed in which both standing stocks and fluxes are quantified. The purpose of this study was to determine meiofaunal biomass, meiofauna contribution to whole-community respiration, and to quantify meiofaunal-bacterial trophic linkages in the northern Gulf of Mexico deep sea.

Meiofauna biomass was strongly related to water depth (Fig. 3.3), and highest values occur in the northeastern GOM (Fig. 3.6). As previously discussed for the meiofauna abundance pattern (chapter one), interactions with Mississippi River outflow, the Loop Current, and complex slope topography in the northeast GOM worked to enhance biomass. Highest biomass above the Florida Escarpment at station S42 was due primarily to greater average body size by the nematodes (Fig. 3.4). Meiofauna biomass was found to be roughly equivalent to benthic foraminiferal biomass, but exceeded foram biomass at 5 of 10 stations sampled by Bernhard *et al.* (submitted manuscript). However, meiofauna biomass was one to two orders of magnitude lower than bacterial biomass (Deming, unpublished DGoMB data). Interpolation of point data over the entire



sampling region (approx. 2/3 of the GOM deep-sea) gave a conservative estimate of the total meiofaunal standing stock of  $2.1 \times 10^7$  kg C (Fig. 3.13). The model could not accurately estimate biomass of the Florida and Campeche escarpments due to a lack of sampling over most of this area, thus regional biomass estimates are conservative. However, if converted to units of energy  $2.1 \times 10^7$  kg C could provide roughly enough energy to power one million houses for a month. Meiofauna respiration over the sampling area (Fig. 3.14) is responsible for processing approximately  $1.5 \times 10^6$  kg C  $d^{-1}$ , or 7% of the total biomass.

Observed meiofauna grazing rates on heterotrophic aerobic bacteria (Table 3.5) were extremely low, and likely due to the lack of measured grazing by nematodes and harpacticoids (Fig. 3.7), which account for 95-98% of meiofaunal biomass at the four experimental stations (Table 3.1). Overall, grazing rates on bacterial carbon ranged from  $7.7 \times 10^{-1}$  to  $1.0 \times 10^{-6}$  mg C  $m^{-2} d^{-1}$  (Table 3.5), corresponding to removal of  $1.1 \times 10^{-7}$  to  $5.0 \times 10^{-2}$  % of the bacterial standing stock, which equals  $1.0 \times 10^{-4}$  to 9.8 % of the meiofauna metabolic requirement (Table 3.5) per day. In shallow water systems meiofauna consume approximately 1% of microfaunal standing stocks on a daily basis (Montagna 1984, 1995). Grazing rates measured here were at least one and a half orders of magnitude less than rates observed in shallow water. Additionally, the huge variability in the measurements suggest both poor precision and accuracy.

The radiotracer grazing method (Montagna 1993) is limited and has large sources of variability (Montagna *et al.* 1995), which are exacerbated when attempting

shipboard incubations for deep-sea samples. The single-label approach limits the types of prey items that can be labeled (aerobic heterotrophic bacteria), although <sup>3</sup>H-Thymidine appears to be the most robust choice for labeling bacteria due to incorporation via DNA synthesis (Montagna 1993). However, variability in natural communities can affect the types of food eaten and rates of meiofauna grazing (Montagna *et al.* 1995). Species specific (Carman and Thistle 1985) and ontogenetic feeding preferences exist (Decho and Fleeger 1988), but error associated with label uptake by epicuticular bacteria can be a major source of experimental error (Carman 1990). However, the most likely sources of error within the current study arise from depressurization and subsequent re-pressurization for incubation, as well as thermal shock during core extrusion and pre-incubation processing. Although meiofauna (mainly nematodes and harpacticoids) appeared to survive after core extrusion (Baguley, personal observation), animals may not have survived rapid re-pressurization for incubation at *in situ* conditions, or may have been sufficiently stressed that natural grazing processes were disrupted. Additionally, label loss occurs unless samples are analyzed immediately after sampling (Moens *et al.* 1999). Even with ideal sample processing (i.e., preservation using ice cold formalin, immediate freezing, and analyzing samples less than 2 hours after thawing), average label loss of 50% still occurs (Moens *et al.* 1999). However, even if this adjustment was made, it does not account for the order of magnitude, or greater, discrepancy in measured grazing rates of this study.

Although measured grazing rates were unreasonable, it was possible to estimate

a whole-community metabolic budget using allometry. Allometric respiration measurements require only abundance and biomass to determine mean respiration rate (Mahaut *et al.* 1995). Whole-community respiration (Smith 1978a; Reimers and Smith 1986; Smith 1992; Smith *et al.* 1997; Drazen *et al.* 1998; Smith *et al.* 2001; Smith *et al.* 2002), and respiration of various macro- and megafaunal organisms (Smith and Hessler 1974; Smith 1978b; Smith and Laver 1981; Smith 1983; Childress *et al.* 1990), have been documented in previous deep-sea investigations but the contribution of meiofauna has only been sparsely investigated (Shirayama 1992; Mahaut *et al.* 1995). A general allometric equation for the calculation of weight-dependent respiration of deep-sea organisms (Mahaut *et al.* 1995) was used to calculate meiofaunal respiration at all DGoMB stations (Table 3.2). However, the total metabolic budget for all consumers includes secondary production and egestion (Valiela 1995, and references therein), yet these processes are often ignored in the estimation of deep-sea whole-community metabolism. Respiration generally accounts for 40-80% of total consumption, with 0-30% of consumed energy being allocated to secondary production (Valiela 1995, and references therein). Therefore, as a conservative estimate, respiration was assumed to account for 80% of the total metabolic budget (Table 3.2). The mean meiofaunal respiration rate increases with increasing water depth, reflecting overall decrease in animal size with depth (Fig. 3.7A), although harpacticoids show an opposing trend (Fig. 3.5) (Baguley *et al.* 2004). Meiofauna community respiration decreases with depth (Fig. 3.7B) reflecting a decrease in overall biomass.

Geographic variation in community respiration, and therefore the overall metabolic budget, is greatest at depths less than 2000 meters (Figs. 3.8B, 3.11). Highest respiration is found at stations near Mississippi River outflow, and where there is an interaction between the Loop Current and canyon (MT1-3, S36) and escarpment (S42) features (see chapter one). A comparison of experimentally measured consumption versus allometrically-derived requirements (Table 3.5), indicates poor agreement by measured grazing, confirming poor results from the grazing study (Table 3.5). Alternatively, it is possible that there is a lack of trophic linkage between bacteria and meiofauna, and that deep-sea meiofauna depend heavily on surfaced-derived detritus. Compared to total bacterial biomass, meiofauna only require approximately 0.1 to 0.7% of the bacterial standing stock to meet their theoretical metabolic requirements (Table 3.5). But, grazing rates were, at most, 10% of the theoretical metabolic requirement (Table 3.5).

If bacteria are a primary food source for meiofauna in deep-sea sediments, then the standing stock does not appear to be food limited. Although multiple feeding types exist within the meiofauna (Hicks and Coull 1983; Jensen 1987), most metazoan meiofauna selectively feed on microalgae, bacteria, and protists (Montagna 1995). In deep-sea sediments, microalgal cells are in the form of partially or highly remineralized phytodetritus, derived from surface primary production. It is likely that deep-sea meiofauna are largely dependent upon phytodetrital flux from surface waters, and are therefore food-limited with respect to overlying water column primary production, as

suggested by modeling studies (Rowe 1996), bathymetric gradients of abundance and biomass (Soltwedel 2000), and strong dependence on POM flux as outlined in chapter one of this dissertation.

Shallow-water meiofauna have been shown to increase feeding rates in response to increased microphytobenthos stocks (Montagna *et al.* 1995). Deep-water communities likely exhibit similar functional responses (Taghon and Green 1990) to seasonal phytodetrital pulses, as suggested by trophic structure models (Rowe 1996). Deep-sea communities do respond to seasonally varying fluxes of organic matter (see Gooday 2002 for a thorough review). Meiofauna may be slow to respond to fresh phytodetritus inputs compared to single-celled Foraminifera or bacteria (Gooday *et al.* 1996; Gooday 2002), with lagged increases in standing stocks due to slower rates of somatic growth and high energetic costs of gamete production (Graf 1992; Eckelbarger 1994; Gooday *et al.* 1996). However, a recent shallow water (20 m) investigation on the North Sea continental shelf demonstrated temporal changes in abundance, biomass, and diversity of nematodes, in response to the spring bloom and flux of fresh phytodetrital cells to the sea floor (Vanaverbeke *et al.* 2004).

In comparison to total benthic community respiration ( $\text{CO}_2$ , converted from sediment community oxygen consumption, G. Rowe, unpublished DGoMB data), meiofauna are responsible for approximately 10-25 % of the total benthic community  $\text{CO}_2$  flux (Table 3.6). Total global oxygen utilization in the deep sea has been estimated to be  $1.2 \times 10^{14}$  mol  $\text{O}_2$   $\text{yr}^{-1}$  (Jahnke *et al.* 1996), which equals approximately  $1.22 \times 10^{15}$

g C yr<sup>-1</sup> (converted to units of carbon using a respiratory quotient of 0.85, and stoichiometric conversion of 12g C per mole O<sub>2</sub>). If meiofauna are responsible for 10 % of this flux (conservative) then they are responsible for processing 1.2x10<sup>14</sup> g C yr<sup>-1</sup>, and are therefore a globally significant component of the carbon cycle.

Many questions remain unanswered, particularly with respect to deep-sea trophic interactions. A conceptual model of meiofaunal community trophic interactions in the deep-sea (adapted from Rowe 1996) reveals just a small portion of the complexity within this system (Fig. 3.11). Although meiofaunal standing stocks can now be more easily and accurately estimated (Baguley *et al.* 2004), the relative importance of bacterial, protist, phytodetrital, or recycled detrital carbon in sustaining meiofaunal metabolic demands remains enigmatic. However, the total theoretical consumption (metabolic requirement as a function of respiration) can be estimated based on accurate estimates of meiofaunal biomass. Although specific trophic interactions were not elucidated here, changes in community structure have been demonstrated with temporal changes in quality and quantity of food supply to the benthos (Vanaverbeke *et al.* 2004). Areas of high POM flux (e.g., the Mississippi Trough region) likely have higher proportions of selective deposit feeding (pick specific bacterial or detrital cells) and epistrate feeding (suck the juice out of cells) nematodes, as observed during spring bloom conditions by Vanaverbeke *et al.* (2004). Similar feeding types (Marcotte 1977) would be expected among the harpacticoid copepods (point feeders = selective epistrate feeders; line feeders = selective deposit feeders). Increased dominance by two of the four general feeding

types (see Marcotte 1977; Jensen 1987) in areas of high POM flux would be consistent with low observed average phylogenetic diversity (functional diversity) at these stations (chapter two of this dissertation). Conversely, high average phylogenetic diversity observed at deeper stations suggests more functional diversity, and therefore more complicated trophic interactions with increasing depth.

Future investigation of deep-sea meiofauna community function (respiration, trophic interactions, etc.) should seek to elucidate specific meiofaunal-microbial trophic interactions, or quantify the relative importance of microbial versus phytodetrital or recycled detrital food sources (Fig. 3.11). Analysis of natural carbon and nitrogen stable isotopes may be useful in uncovering these interactions. Recent developments have allowed for increased sensitivity in stable isotope analysis of meiofaunal samples (Carman and Fry 2002). Grazing studies may also prove useful, specifically stable isotope enrichments (Carman and Fry 2002). Radioisotope studies (Montagna 1993) may still have utility in uncovering bacterial-meiofaunal trophic interactions, or uptake of pre-labeled ( $^{14}\text{C} - \text{HCO}_3^-$ ) phytodetrital carbon, but I must stress that grazing studies should be done *in situ* using a remotely operated vehicle (ROV) or deep sea research vessel (DSRV). Understanding temporal dynamics associated with seasonal POM flux, trophic interactions, etc., is essential and must be further investigated (Smith *et al.* 2002).

## **CONCLUSION**

A carbon budget was created for 51 stations in the northern Gulf of Mexico deep sea by determination of standing stocks and estimates of total metabolic requirement, as

a function of respired carbon. Empirical measurements of meiofauna grazing rates on bacteria were unsuccessful. Biomass, respiration, and grazing all decreased with increasing water depth. Regional variation in biomass and respiration indicated highest values in the northeastern Gulf of Mexico, where the Loop Current interacts with Mississippi River outflow and topo-geographic features such as the Mississippi Trough, DeSoto Canyon, and Florida Escarpment. Estimates of total meiofaunal biomass and respiration in the northern Gulf of Mexico indicate that meiofauna require 7% of their own biomass on a daily basis (which equals, at most, 0.7% of the bacterial standing stock) to meet their metabolic needs. Meiofauna account for 10-25 % of total sediment community respiration and are therefore a significant component of the global carbon cycle. Lack of food limitation with respect to bacterial carbon, and may suggest preferential reliance upon other carbon sources, such as surface-derived phytodetritus.



Table 3.1: Biomass contribution of the major taxonomic groups to total meiofaunal biomass (mg C m<sup>-2</sup>) at each DGoMB station. NEMA = Nematoda, HARP = Harpacticoida, NAUP = Harpacticoida nauplii, POLY = Polychaeta, OSTR = Ostracoda, CYCL = Cyclopoida, TANA = Tanaidacea, ISOP = Isopoda, KINO = Kinorhyncha.

STA	NEMA	HARP	NAUP	POLY	OSTR	CYCL	TANA	ISOP	KINO
AC1	17.52	6.83	0.18	0.20	0.08	0.09	0.30	0.00	0.01
B1	23.97	8.60	0.36	0.22	0.31	0.05	0.10	0.07	0.02
B2	12.50	3.52	0.34	0.25	0.12	0.00	0.20	0.07	0.00
B3	11.88	5.41	0.55	0.28	0.04	0.00	0.22	0.00	0.01
BH	23.31	20.80	0.98	1.42	0.48	0.16	0.50	0.40	0.02
C1	89.37	8.04	0.64	1.27	0.24	0.24	0.38	0.00	0.04
C12	12.83	7.27	0.54	0.17	0.10	0.04	0.13	0.00	0.01
C14	14.30	7.45	0.32	0.17	0.12	0.02	0.38	0.00	0.01
C4	60.26	9.12	0.79	0.36	0.44	0.07	0.30	0.13	0.01
C7	69.86	10.97	0.68	0.81	0.33	0.09	0.45	0.00	0.02
GKF	3.20	2.87	0.13	0.10	0.00	0.00	0.00	0.00	0.01
HIPRO	9.24	8.88	0.44	1.71	0.25	0.37	0.30	0.07	0.00
JSSD1	1.76	2.32	0.30	0.13	0.00	0.00	0.00	0.00	0.00
JSSD2	1.90	1.57	0.26	0.14	0.02	0.00	0.00	0.13	0.00
JSSD3	1.51	1.54	0.13	0.13	0.06	0.00	0.00	0.07	0.00
JSSD4	1.28	1.87	0.22	0.13	0.07	0.00	0.00	0.00	0.00
JSSD5	3.51	2.71	0.25	0.13	0.15	0.00	0.20	0.00	0.00
MT1	110.02	6.44	0.56	1.32	0.74	0.40	0.29	0.05	0.02
MT2	45.12	8.22	0.82	3.07	0.33	0.94	1.70	0.20	0.05
MT3	87.39	15.57	0.76	1.43	0.75	0.34	0.60	0.20	0.04
MT4	33.69	9.46	0.51	0.75	0.21	0.16	0.60	0.07	0.01
MT5	24.92	4.38	0.33	0.42	0.23	0.09	0.50	0.00	0.01
MT6	9.99	1.37	0.18	0.17	0.03	0.04	0.05	0.03	0.00
NB2	15.55	6.24	0.43	0.36	0.17	0.02	0.20	0.35	0.01
NB3	17.31	8.12	0.91	0.42	0.04	0.00	0.20	0.00	0.01
NB4	10.23	6.51	0.46	0.21	0.04	0.02	0.30	0.07	0.00
NB5	10.63	9.68	0.35	0.15	0.15	0.02	0.30	0.07	0.01
RW1	66.47	9.47	1.06	1.04	0.50	0.39	0.10	0.20	0.03
RW2	23.33	7.96	0.56	0.53	0.30	0.24	0.56	0.07	0.02
RW3	36.20	7.45	0.53	0.59	0.38	0.10	0.45	0.00	0.01
RW4	37.36	7.74	0.53	0.61	0.02	0.19	0.70	0.00	0.03
RW5	24.12	8.61	0.35	0.29	0.12	0.05	0.10	0.13	0.01
RW6	16.95	10.46	0.28	0.25	0.06	0.02	0.20	0.00	0.01

<b>STA</b>	<b>NEMA</b>	<b>HARP</b>	<b>NAUP</b>	<b>POLY</b>	<b>OSTR</b>	<b>CYCL</b>	<b>TANA</b>	<b>ISOP</b>	<b>KINO</b>
S35	49.83	14.81	1.34	1.59	0.67	0.58	1.00	0.47	0.05
S36	98.41	11.48	0.89	0.83	0.43	0.09	0.70	0.20	0.02
S37	20.51	10.73	0.71	0.53	0.33	0.16	0.40	0.20	0.01
S38	9.70	6.46	0.48	0.38	0.15	0.11	0.20	0.00	0.01
S39	6.37	3.10	0.21	0.25	0.04	0.05	0.20	0.07	0.00
S40	9.82	5.95	0.31	0.35	0.15	0.19	0.30	0.07	0.00
S41	23.79	5.33	0.27	0.21	0.10	0.04	0.22	0.04	0.00
S42	141.54	12.92	0.68	0.72	0.17	0.22	0.30	0.13	0.02
S43	36.72	6.98	0.37	0.95	0.19	0.30	0.50	0.07	0.03
S44	29.38	7.48	0.69	1.83	0.38	0.60	0.50	0.00	0.02
W1	46.80	17.31	1.16	1.19	0.33	0.37	0.50	0.07	0.04
W2	41.97	10.77	0.62	0.62	0.13	0.32	1.00	0.07	0.01
W3	58.87	10.97	0.95	0.55	0.33	0.35	0.50	0.07	0.02
W4	16.81	8.73	0.56	0.55	0.15	0.18	0.40	0.00	0.00
W5	10.23	4.50	0.19	0.09	0.04	0.00	0.30	0.00	0.01
W6	15.95	5.94	0.27	0.28	0.02	0.05	0.10	0.07	0.01
WC12	61.48	14.56	0.57	0.53	0.37	0.02	0.80	0.07	0.00
WC5	81.55	13.25	1.04	1.00	0.15	0.41	0.80	0.20	0.03

Table 3.2: Allometric estimations of the mass-dependent meiofauna respiration rate ( $R$ , in  $d^{-1}$  units) and meiofauna community respiration ( $CO_2$ ,  $mg\ C\ m^{-2}\ d^{-1}$ ) and total organic carbon demand ( $OrgC$ ,  $mg\ C\ m^{-2}\ d^{-1}$ ). Mass-dependent respiration was calculated using an allometric rate law (*sensu* Mahaut et al. 1995) which is dependent upon the ratio ( $W$ ) of biomass ( $B$ ,  $mg\ C\ m^{-2}\ d^{-1}$ ) to abundance ( $A$ ,  $N\ m^{-2}$ ). Respiration ( $CO_2$ ,  $mg\ C\ m^{-2}\ d^{-1}$ ) is the product of the mass-dependent rate ( $R$ ) and the total biomass ( $B$ ), and total carbon demand ( $OrgC$ ) was calculated under the assumption that respiration equals 80% of the total metabolic budget (see discussion).

Sta	Lat.	Long.	Depth	B	A	W	R	$CO_2$	OrgC
AC1	26.3936	-94.5731	2440	25.2	129974	1.9E-04	0.06	1.5	1.8
B1	27.2025	-91.4052	2253	33.8	157417	2.1E-04	0.06	1.9	2.4
B2	26.5500	-92.2151	2635	17.1	139907	1.2E-04	0.06	1.1	1.4
B3	26.1644	-91.7351	2600	18.5	155817	1.2E-04	0.06	1.2	1.5
BH	27.7800	-91.5000	545	48.4	407852	1.2E-04	0.06	3.1	3.9
C1	28.0598	-90.2499	336	100.4	369129	2.7E-04	0.05	5.3	6.7
C12	26.3797	-89.2403	2924	21.2	138792	1.5E-04	0.06	1.3	1.6
C14	26.9382	-89.5725	2495	22.8	146578	1.6E-04	0.06	1.4	1.7
C4	27.4532	-89.7631	1463	71.6	273585	2.6E-04	0.05	3.8	4.8
C7	27.7304	-89.9820	1066	83.3	542119	1.5E-04	0.06	5.1	6.3
GKF	27.0000	-90.2500	2460	6.4	84348	7.6E-05	0.07	0.5	0.6
HIPRO	28.5500	-88.5800	1565	21.8	343118	6.3E-05	0.08	1.6	2.0
JSSD1	25.0000	-92.0000	3545	4.5	87547	1.3E-05	0.11	0.5	0.6
JSSD2	23.5000	-92.0000	3725	4.1	87295	4.6E-05	0.08	0.3	0.4
JSSD3	24.7500	-90.7500	3635	3.5	60441	4.0E-05	0.08	0.3	0.4
JSSD4	24.2500	-85.5000	3400	3.6	63451	5.9E-05	0.08	0.3	0.3
JSSD5	25.5000	-88.2500	3350	7.0	135698	1.1E-04	0.07	0.5	0.6
MT1	28.5411	-89.8250	482	119.9	945657	8.8E-04	0.04	4.8	6.0
MT2	28.4479	-89.6719	677	60.9	535216	6.4E-05	0.08	4.6	5.7
MT3	28.2215	-89.4940	990	107.4	885995	2.0E-04	0.06	6.1	7.7
MT4	27.8276	-89.1661	1401	45.5	246058	5.1E-05	0.08	3.6	4.5
MT5	27.3328	-88.6561	2267	31.0	128964	1.3E-04	0.06	2.0	2.5
MT6	27.0016	-87.9991	2743	12.0	155312	9.3E-05	0.07	0.8	1.0
NB2	27.1348	-92.0001	1530	23.4	168276	1.5E-04	0.06	1.4	1.8
NB3	26.5580	-91.8226	1875	27.0	165245	1.6E-04	0.06	1.6	2.0
NB4	26.2468	-92.3923	2020	17.9	148409	1.1E-04	0.07	1.2	1.5
NB5	26.2454	-91.2099	2065	21.4	117263	1.4E-04	0.06	1.3	1.7
RW1	27.5001	-96.0028	212	79.6	411809	6.8E-04	0.04	3.4	4.2
RW2	27.2540	-95.7468	950	33.7	219457	8.2E-05	0.07	2.4	3.0

<b>Sta</b>	<b>Lat.</b>	<b>Long.</b>	<b>Depth</b>	<b>B</b>	<b>A</b>	<b>W</b>	<b>R</b>	<b>CO<sub>2</sub></b>	<b>OrgC</b>
RW3	27.0084	-95.4924	1340	45.9	248752	2.1E-04	0.06	2.6	3.2
RW4	26.7514	-95.2502	1575	47.4	232842	1.9E-04	0.06	2.7	3.4
RW5	26.5075	-94.9967	1620	33.8	170633	1.5E-04	0.06	2.1	2.6
RW6	25.9973	-94.4956	3000	28.3	144453	1.7E-04	0.06	1.7	2.1
S35	29.3352	-87.0464	668	70.5	501629	4.9E-04	0.05	3.3	4.1
S36	28.9185	-87.6722	1826	113.2	799963	2.3E-04	0.06	6.3	7.9
S37	28.5536	-87.7668	2387	33.6	291179	4.2E-05	0.08	2.8	3.5
S38	28.2799	-87.3276	2627	17.5	157164	6.0E-05	0.08	1.3	1.7
S39	27.4837	-86.9998	3000	10.5	83170	6.7E-05	0.07	0.8	1.0
S40	27.8395	-86.7514	2972	17.3	99501	2.1E-04	0.06	1.0	1.2
S41	28.0136	-86.5733	2974	30.2	181408	3.0E-04	0.05	1.6	2.0
S42	28.2510	-86.4193	763	157.1	492537	8.7E-04	0.04	6.3	7.9
S43	28.5029	-86.0768	362	46.4	276279	9.4E-05	0.07	3.2	4.0
S44	28.7500	-85.7477	212	41.1	318516	1.5E-04	0.06	2.5	3.2
W1	27.5772	-93.5510	420	68.7	387228	2.2E-04	0.06	3.9	4.8
W2	27.4139	-93.3403	625	55.7	263315	1.4E-04	0.06	3.4	4.3
W3	27.1724	-93.3233	875	72.7	262642	2.8E-04	0.05	3.8	4.8
W4	26.7308	-93.3197	1460	27.5	187806	1.0E-04	0.07	1.8	2.3
W5	26.2678	-93.3327	2750	15.4	104552	8.2E-05	0.07	1.1	1.4
W6	26.0028	-93.3203	3150	22.7	124166	2.2E-04	0.06	1.3	1.6
WC12	27.3232	-91.5558	1175	78.5	218447	6.3E-04	0.04	3.4	4.3
WC5	27.7759	-91.7657	348	98.9	412061	4.5E-04	0.05	4.6	5.8

Table 3.3: Mean meiofaunal (MB) and bacterial (BB) biomass for pooled replicates and pooled taxonomic groups at the four experimental stations. Bacterial biomass courtesy of Jody Deming, University of Washington (unpublished DGoMB data).

<b>Station</b>	<b>Depth (m)</b>	<b>Latitude (N)</b>	<b>Longitude (W)</b>	<b>MB (mg C m<sup>-2</sup>)</b>	<b>BB (mg C m<sup>-2</sup>)</b>
S42	768	28.2565	86.4284	157	1180
MT3	985	28.2170	89.5106	107	2320
S36	1838	28.9118	87.6773	113	1680
MT6	2737	26.9956	88.0090	12	920

Table 3.4: ANOVA results of the test for differences in grazing rate between treatments (experimental vs. control) and stations, separated by taxonomic group. Significant treatment by station interactions were observed for all taxa ( $\alpha = 0.05$ ). Polychaetes were the only taxa to show consistent grazing, and overall grazing rates for all taxa were low (refer to Table 3.5 & Fig. 3.9 below).

<b>Taxa</b>	<b>Source</b>	<b>DF</b>	<b>SS</b>	<b>MS</b>	<b>F value</b>	<b>P</b>
Nematoda	Treatment	1	16.48	16.48	3.43	0.0825
	Station	3	49.43	16.48	3.43	0.0425
	TRT *STA	3	49.43	16.48	3.43	0.0425
Harpacticoida	Treatment	1	119.50	119.50	25.86	0.0001
	Station	3	134.30	44.77	9.69	0.0007
	TRT *STA	3	134.30	44.77	9.69	0.0007
Polychaeta	Treatment	1	511.71	511.71	35.16	<0.0001
	Station	3	161.28	53.76	3.69	0.0341
	TRT *STA	3	161.28	53.76	3.69	0.0341
Others	Treatment	1	120.47	120.47	10.68	0.0048
	Station	3	233.87	77.96	6.91	0.0034
	TRT *STA	3	175.91	58.64	5.20	0.0107

Table 3.5: Measured meiofaunal grazing on bacteria is only 9.8 to 0.0001% of their theoretical required consumption. Measured meiofauna grazing rate (GR, d<sup>-1</sup> units), bacterial biomass (BB, mg C m<sup>-2</sup> d<sup>-1</sup>), measured grazed bacterial carbon (GC = GRxBB, mg C m<sup>-2</sup> d<sup>-1</sup>), allometric carbon requirement (OrgC, mg C m<sup>-2</sup> d<sup>-1</sup>), and the ratio of measured grazing to the allometric requirement (GC/OrgC), expressed as a percent.

<b>STA</b>	<b>GR</b>	<b>BB</b>	<b>GC</b>	<b>OrgC</b>	<b>GC/OrgC (%)</b>
S42	7.8E-05	1180	9.2E-02	7.9	1.2
MT3	1.1E-06	2320	2.6E-03	7.7	0.03
S36	4.6E-04	1680	7.7E-01	7.9	9.8
MT6	1.1E-09	920	1.0E-06	1.0	0.0001

Table 3.6: Comparison of whole community respiration (CR, mg C m<sup>-2</sup> d<sup>-1</sup>) to meiofauna allometric respiration estimates (MR, mg C m<sup>-2</sup> d<sup>-1</sup>). Meiofauna account for 10-25% of whole community respiration. Note: whole community respiration (mg C m<sup>-2</sup> d<sup>-1</sup>), converted from sediment community oxygen consumption (SCOC) as measured by the Benthic Lander (Gil Rowe, unpublished DGoMB data). SCOC (mmol O<sub>2</sub> m<sup>-2</sup> d<sup>-1</sup>) was converted to carbon using a respiratory quotient of 0.85 and stoichiometric conversion factor of 12 mg C/mmol O<sub>2</sub>.

<b>Station</b>	<b>Depth</b>	<b>CR</b>	<b>MR</b>	<b>%MR</b>
S42	763	41	6.3	15.4
S36	1826	26	6.3	24.2
MT1	482	40	4.8	12.0
MT3	990	28	6.1	21.8
C7	1066	49	5.1	10.4
JSSD1	3545	4	0.5	12.5
JSSD4	3400	2.6	0.3	11.5



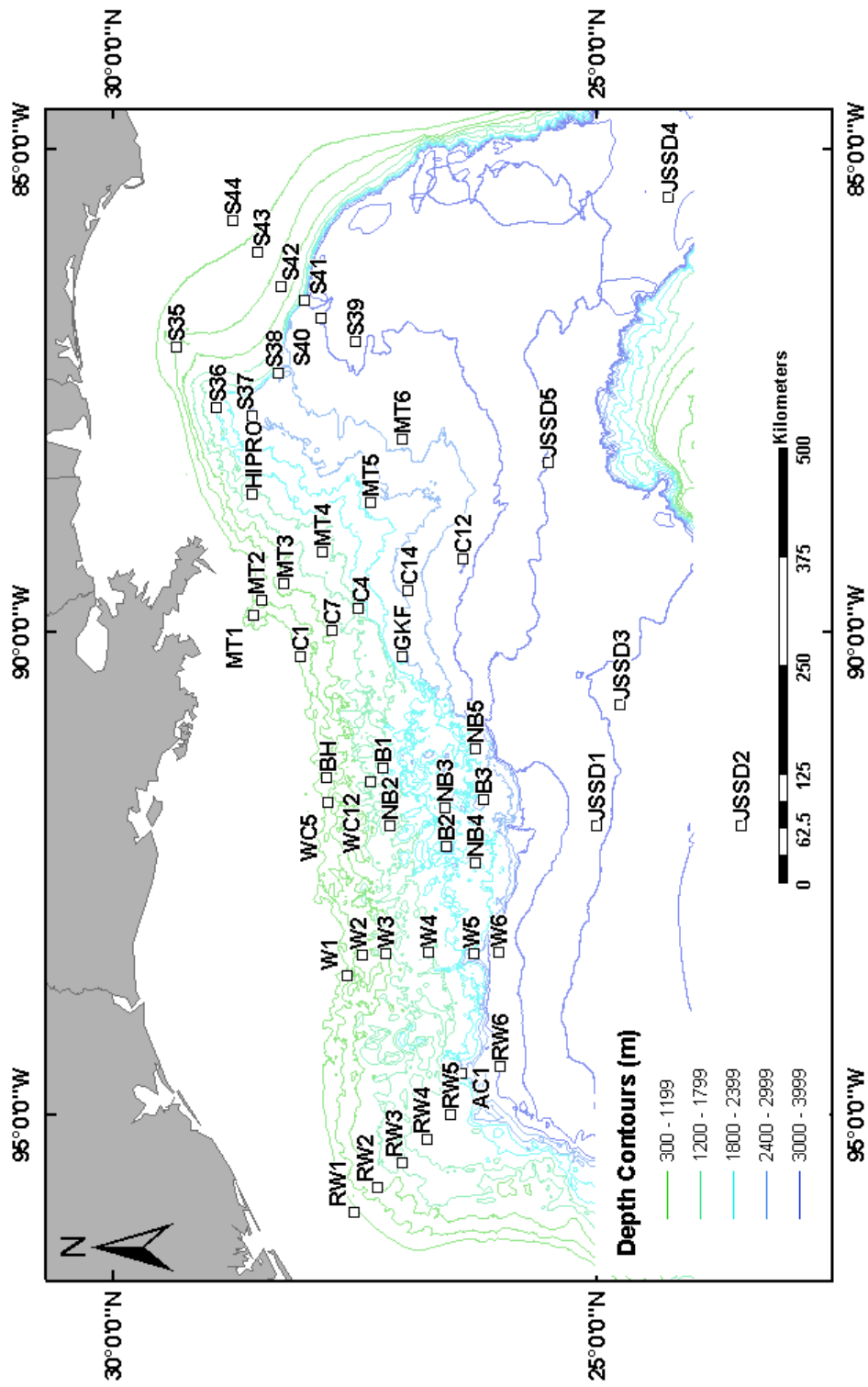


Figure 3.1: DGoMB station locations in the northern Gulf of Mexico deep-sea where meiofauna community biomass (*sensu* Baguley et al. 2004) and allometric respiration (*sensu* Mahaut et al. 1995) were estimated.

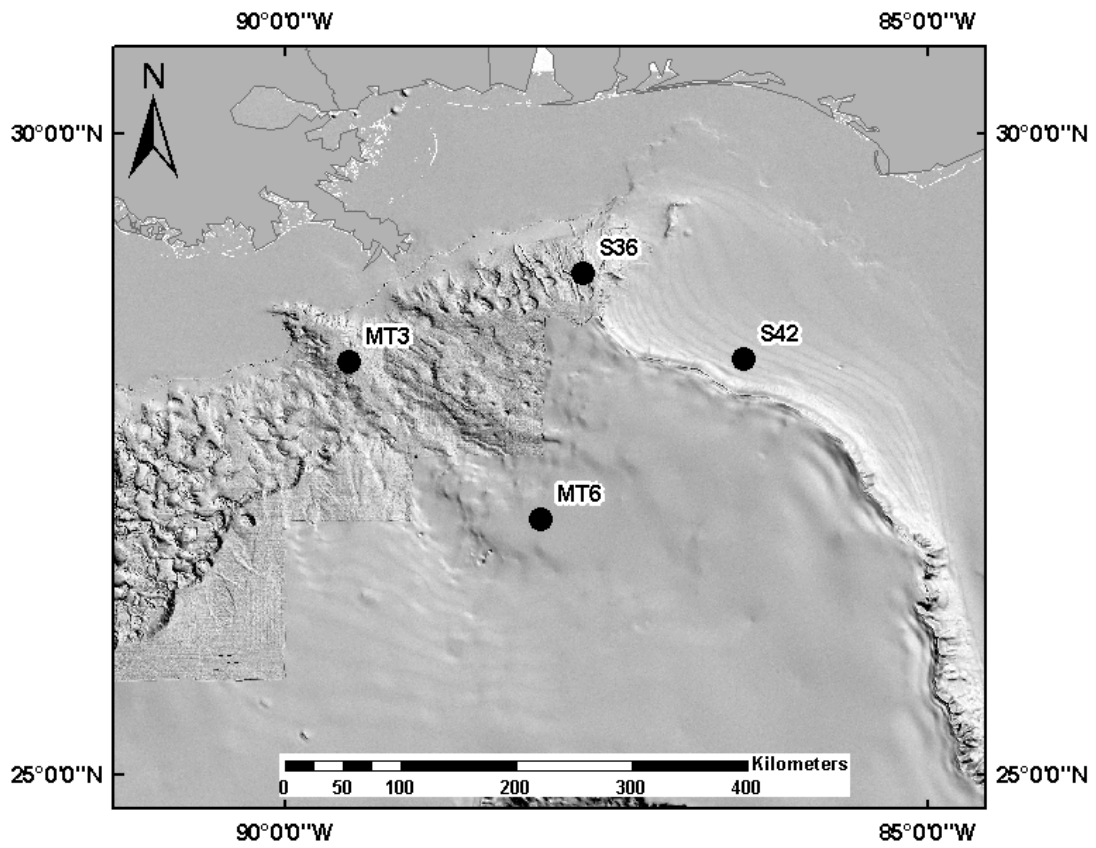


Figure 3.2: Process station locations for 2001 cruise. MT1 = 482 m; S42 = 763 m; S36 = 1826 m; MT6 = 2643 m.

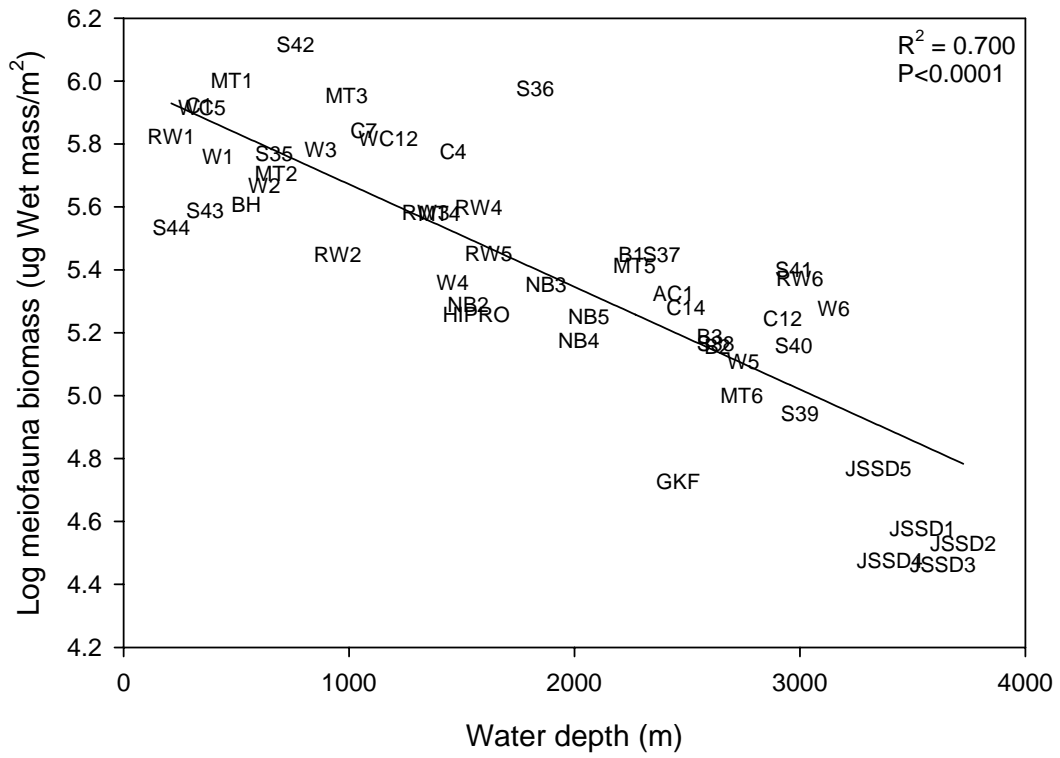


Figure 3.3: Meiofauna biomass ( $\mu\text{g wet wt/m}^2$ ) versus water depth at all DGoMB station.

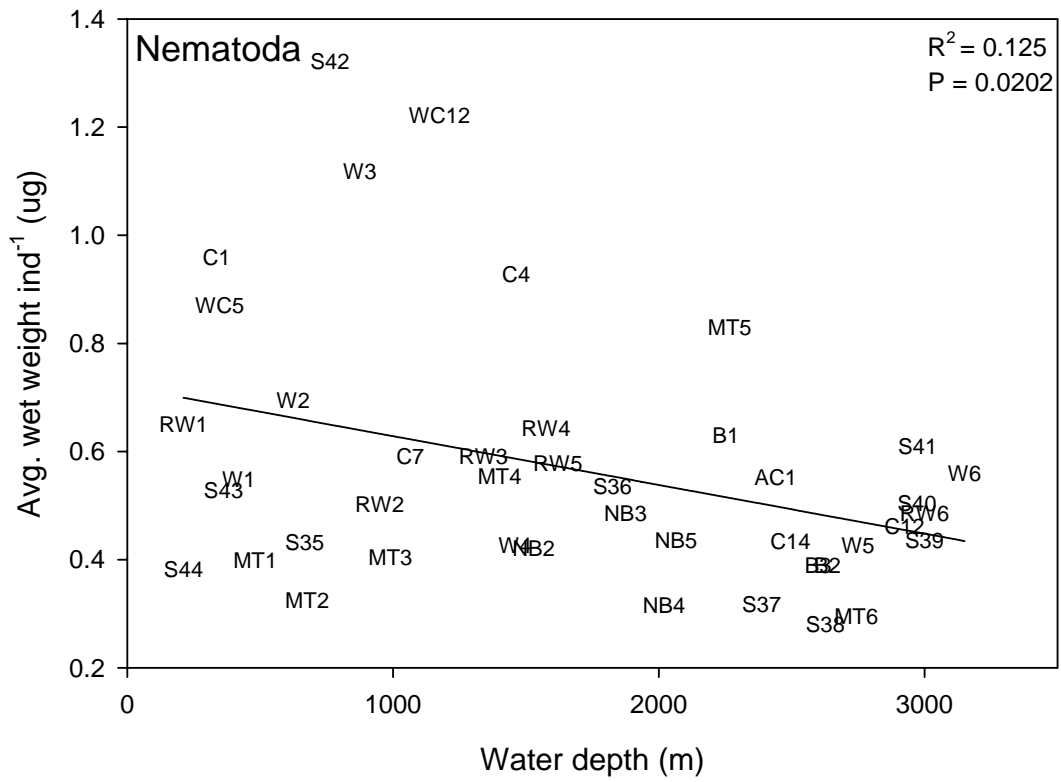
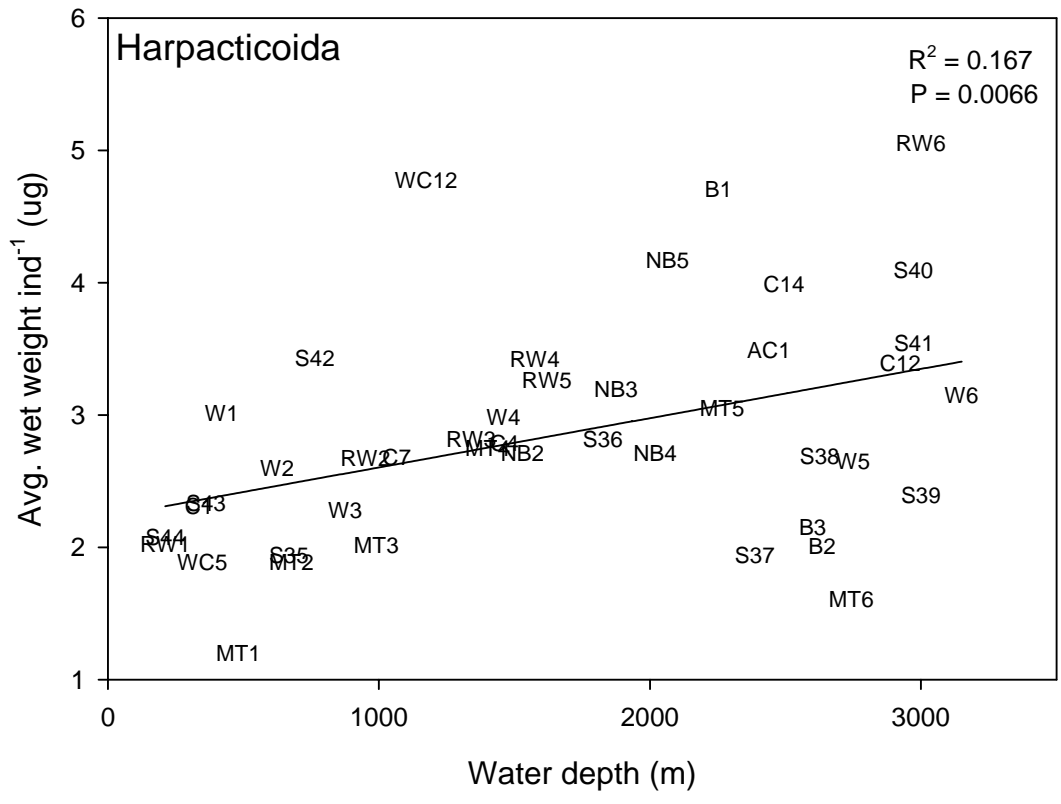


Figure 3.4: Average nematode wet weight ( $\mu\text{g}$ ) per individual versus depth.



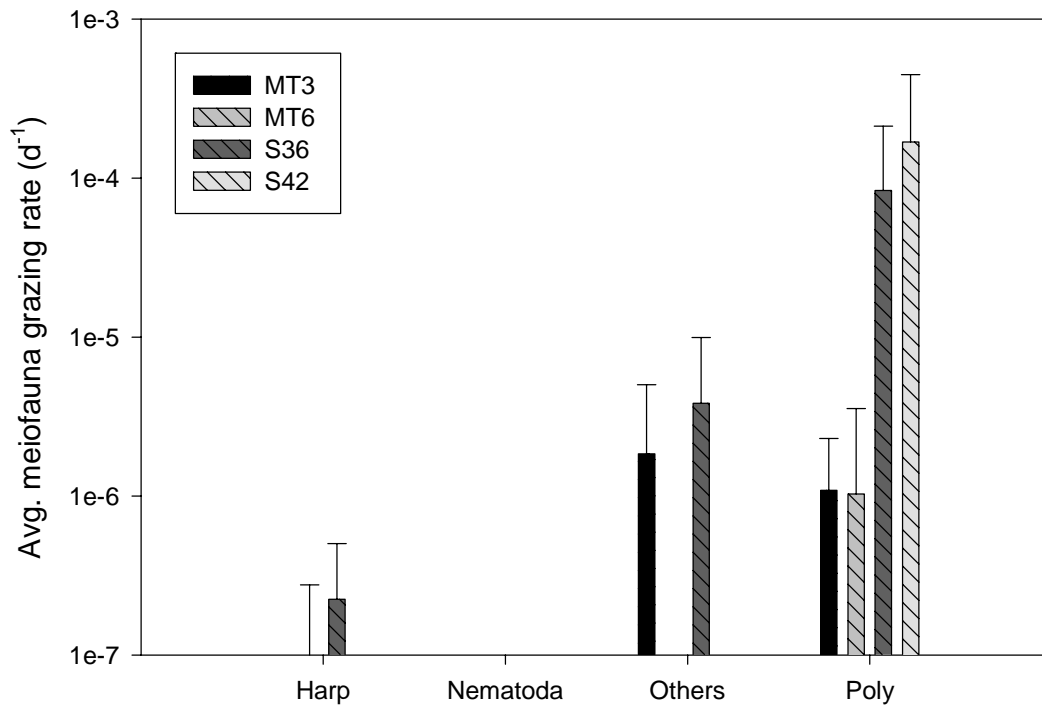


Figure 3.6: Meiofauna grazing rates by taxonomic group for the four experimental stations.

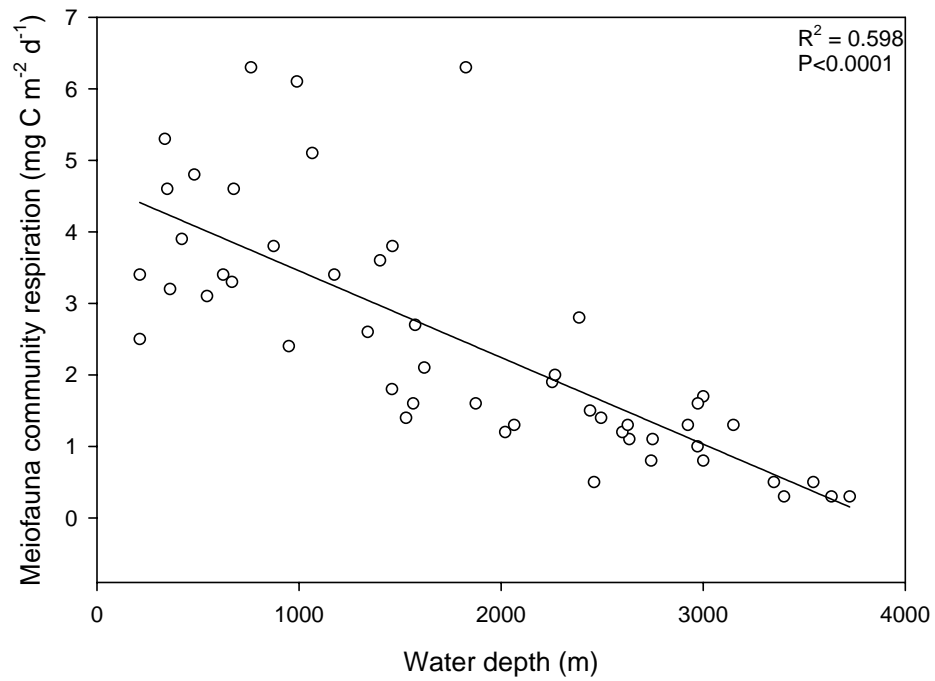
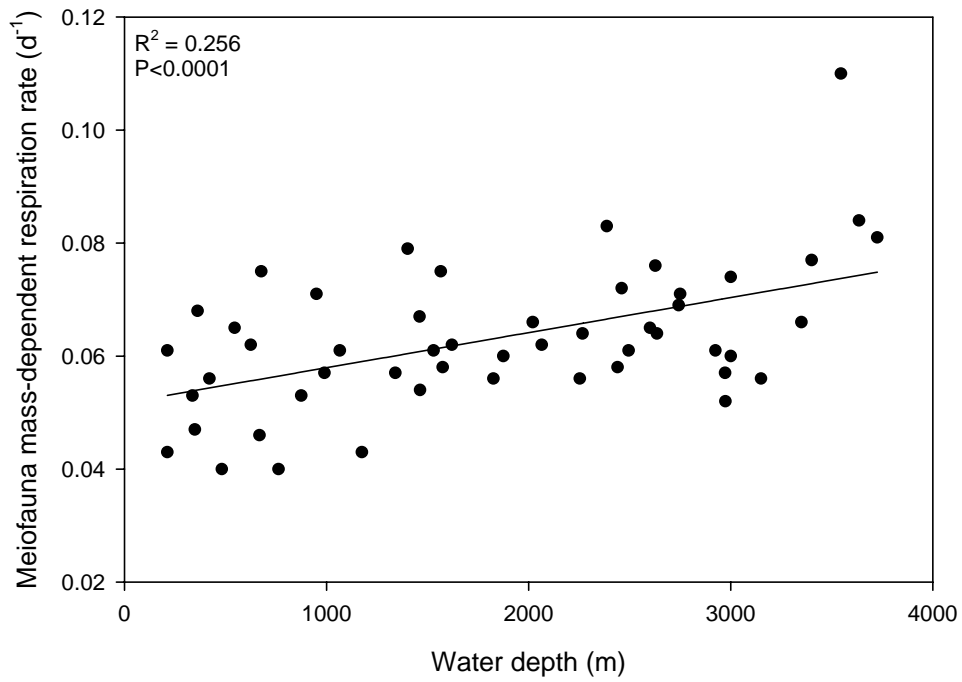


Figure 3.7: A) Meiofauna mass-dependent respiration rate ( $d^{-1}$ ) and B) meiofauna community respiration ( $mg\ C\ m^{-2}\ d^{-1}$ ) at each of the 51 DGoMB stations in the northern Gulf of Mexico deep-sea.

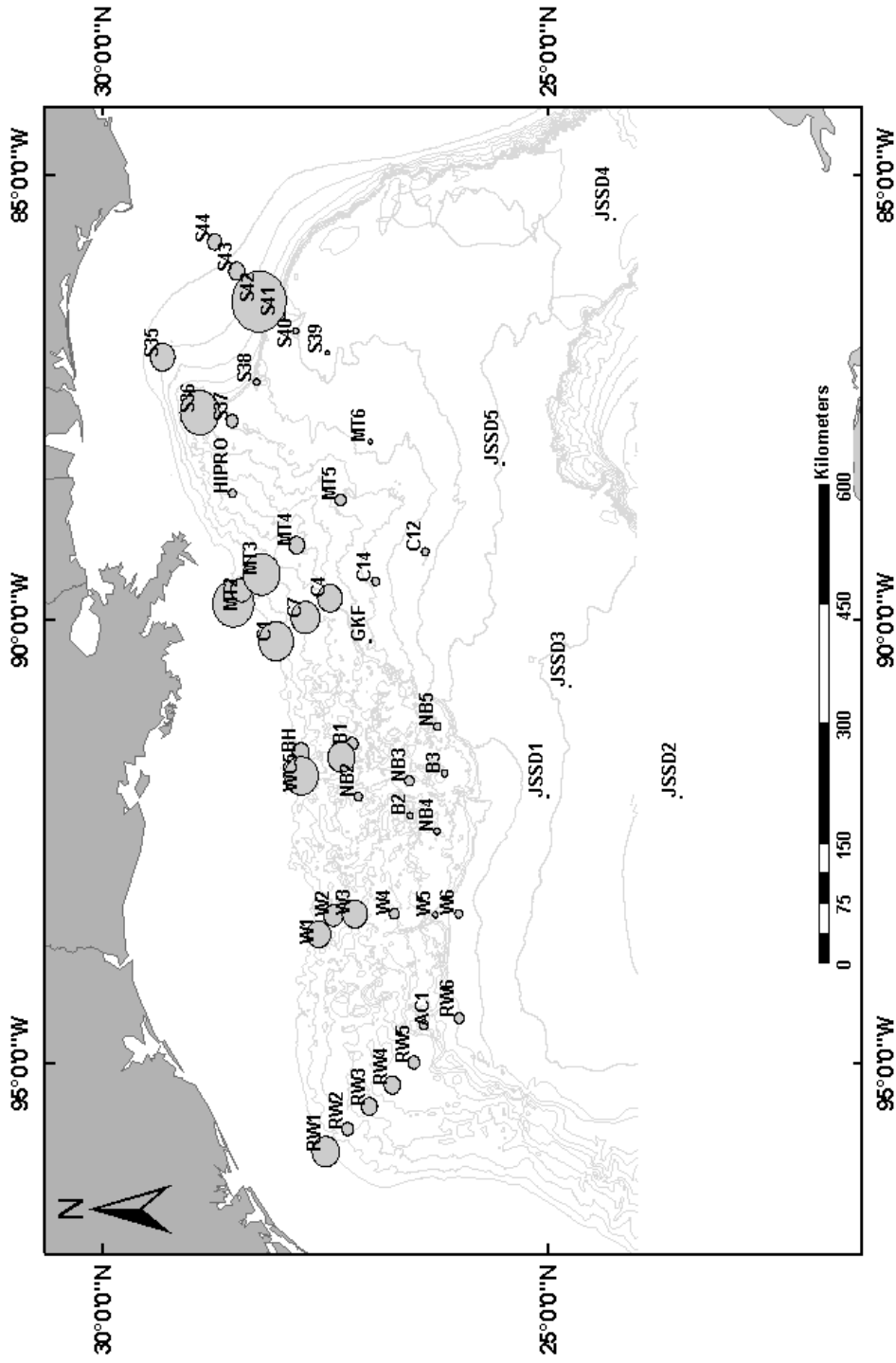


Figure 3.8: Spatial comparison of relative meiofauna biomass ( $\mu\text{g wet wt. m}^{-2}$ ), where bubbles size is proportional to biomass.



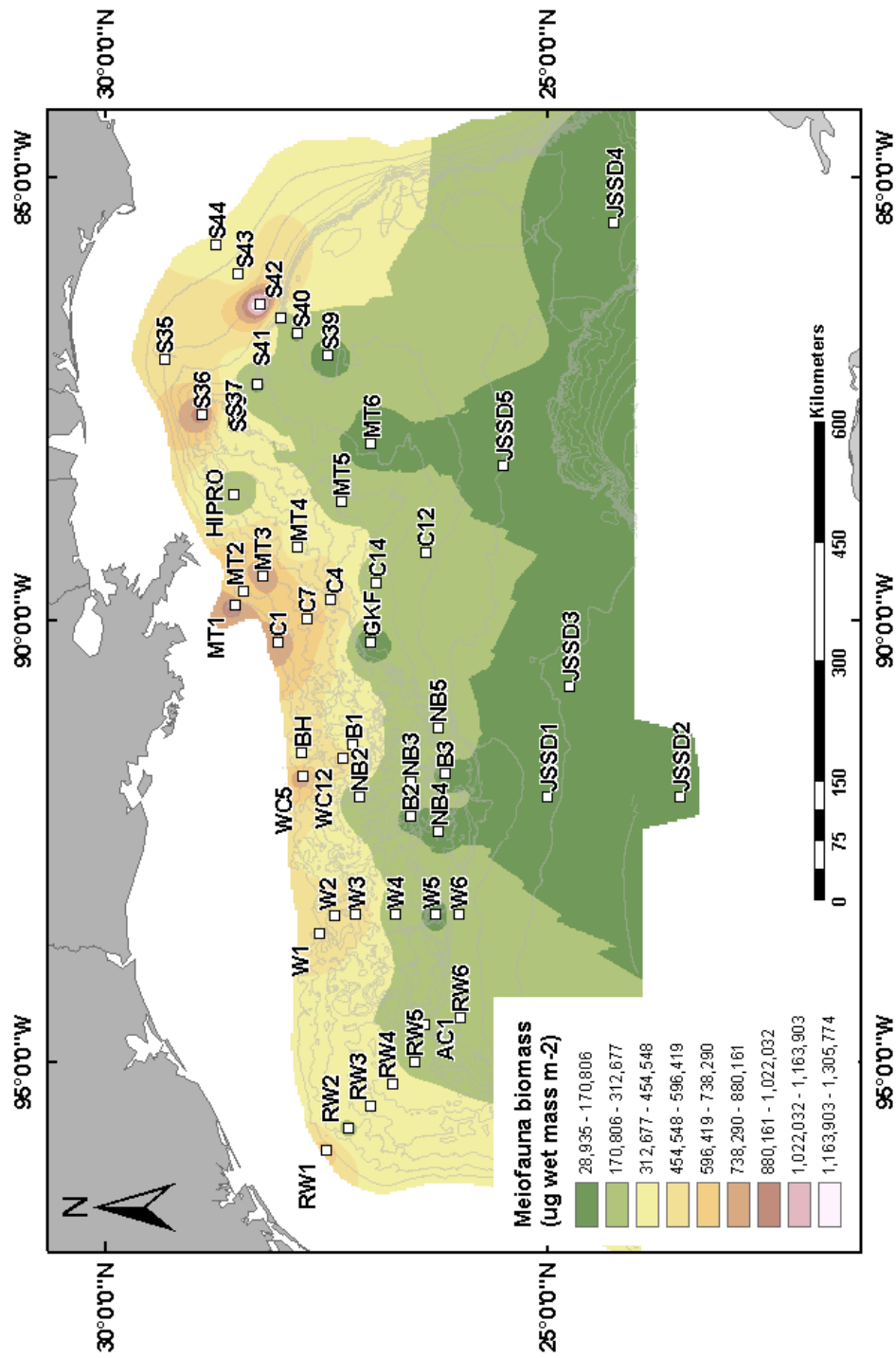


Figure 3.9: Spatial interpolation of meiofauna biomass ( $\text{mg wet mass m}^{-2}$ ) in the northern Gulf of Mexico deep sea.

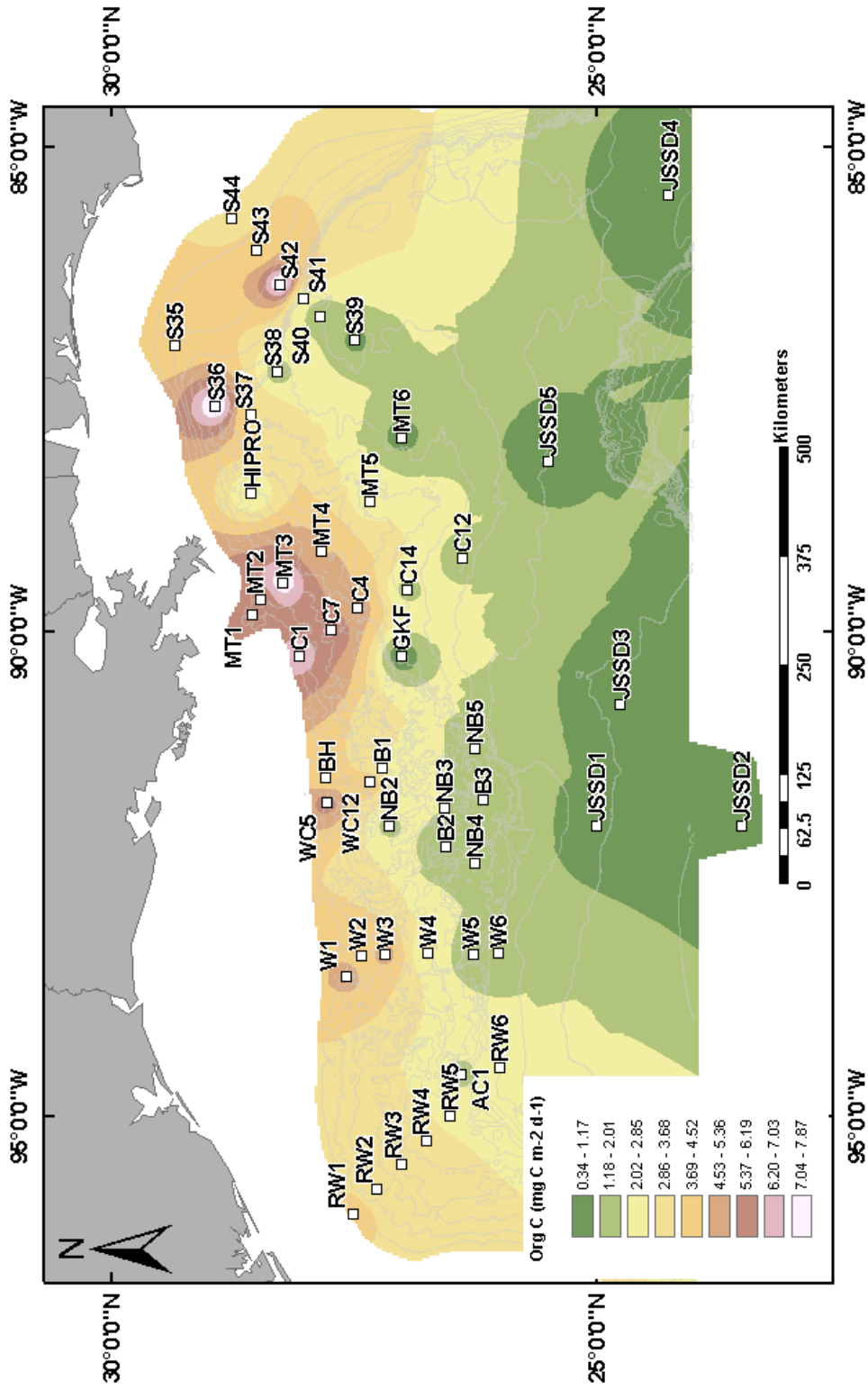


Figure 3.10: Spatial interpolation of the meiofaunal organic carbon requirement ( $\text{mg C m}^{-2} \text{d}^{-1}$ ), assuming respiration equals 80% of total metabolism.

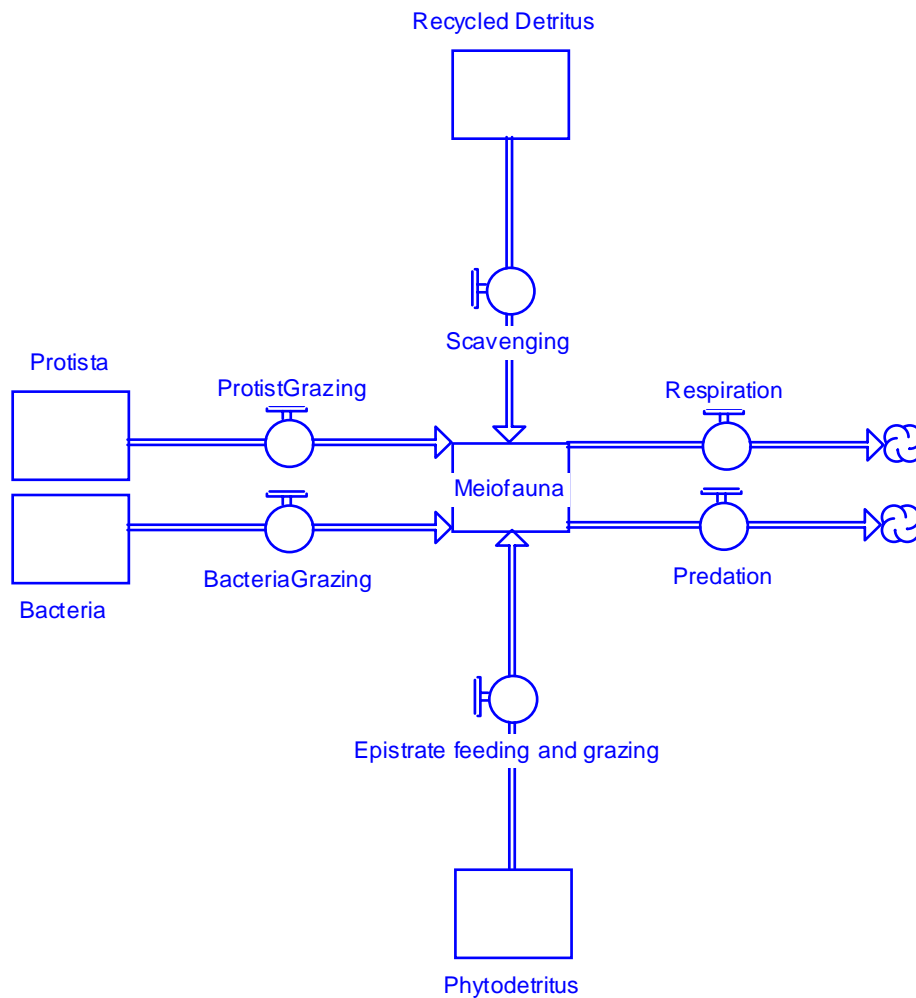


Figure 3.11: Conceptual model of complex meiofaunal trophic interactions with microfauna (bacteria and protists) and two different detrital pools (phytodetritus, and recycled detritus). Not shown are predatory meiofauna (prey upon other meiofauna) or meiofaunal deposit feeders that ingest whole sediment particles and obtain carbon from one or more of the above standing stocks. Carbon is lost via respiration transfer to higher trophic levels via predation (cloud symbols).

## APPENDIX

### (HARPACTICOIDA SPECIES LIST)

The species list is separated by family (in bold text), and includes the total number of individuals (N) identified per species (S). Species designated as sp., *aff.*, or *not* are not described in the scientific literature. The abbreviations *aff.* and *not* denote that the individual most closely resembles, but is not, that species. For example *Cervinia aff. bradyi* most closely resembles the described species *Cervinia bradyi*, but is actually a new species within the genus *Cervinia*.

S	N
<b>Longipedidae</b>	
<i>Longipedia</i> sp.	3
<b>Canuellidae</b>	
<i>Ellucana</i> sp.	1
<i>Canuella</i> sp.	3
<i>Ceratonus crownius</i>	1
<i>Intersunaristes</i> sp.	1
<b>Cerviniidae</b>	
<i>Cervinia aff. bradyi</i>	5
<i>Cervinia aff. synarthra</i>	1
<i>Cerviniopsis</i> sp.	5
<i>Cerviniopsis breviseta</i>	1
<i>Cerviniopsis inermis</i>	1
<i>Cerviniopsis aff. breviseta</i>	1
<i>Cerviniopsis aff. langi</i>	1
<i>Cerviniopsis aff. longicaudata</i>	7

S	N
<i>Cerviniopsis aff.stylicaudata</i>	2
<i>Cerviniella</i> sp.1	2
<i>Cerviniella</i> sp.2	1
<i>Cerviniella</i> aff. <i>hamata</i>	2
<i>Cerviniella</i> aff. <i>langarderei</i>	1
<i>Cerviniella</i> aff. <i>langi</i>	6
<i>Cerviniella</i> aff. <i>talpa</i>	3
<i>Hemicervinia</i> sp.	2
<i>Pontostratiotes</i> sp.	2
<i>Pontostratiotes</i> aff. <i>denticalatus</i>	1
<i>Pontostratiotes</i> aff. <i>horida</i>	3
<i>Pontostratiotes</i> aff. <i>pori</i>	2
<i>Pontostratiotes</i> <i>texanus</i>	2
<i>Neopontostratiotes</i> <i>typica</i>	1
<i>Tonpostratiotes</i> sp.	1
 <b>Ectinosomatidae</b>	
<i>Ectinosoma</i> aff. <i>compressum</i>	4
<i>Ectinosoma</i> aff. <i>califormicum</i>	1
<i>Ectinosoma</i> aff. <i>litorale</i>	1
<i>Ectinosoma</i> aff. <i>melaniceps</i>	6
<i>Ectinosoma</i> aff. <i>normani</i>	2
<i>Ectinosoma</i> aff. <i>reductum</i>	1
<i>Ectinosoma</i> aff. <i>tenerum</i>	1
<i>Ectinosoma</i> aff. <i>tenuipes</i>	2
<i>Ectinosoma</i> sp.	1
<i>Halectinosoma</i> aff. <i>anglifrons</i>	43
<i>Halectinosoma</i> aff. <i>arenical</i>	2
<i>Halectinosoma</i> aff. <i>armiferum</i>	17
<i>Halectinosoma</i> aff. <i>barroisis</i>	11
<i>Halectinosoma</i> aff. <i>curticorne</i>	8
<i>Halectinosoma</i> aff. <i>chrystalli</i>	13
<i>Halectinosoma</i> aff. <i>distinctum</i>	5
<i>Halectinosoma</i> aff. <i>elongatum</i>	4
<i>Halectinosoma</i> aff. <i>finmarchicum</i>	4
<i>Halectinosoma</i> aff. <i>gothiceps</i>	86
<i>Halectinosoma</i> aff. <i>herdmani</i>	52
<i>Halectinosoma</i> <i>longisegmenta</i>	1

S	N
<i>Halectinosoma aff.littorale</i>	1
<i>Halectinosoma aff.mixtum</i>	1
<i>Halectinosoma aff. neglectum</i>	5
<i>Halectinosoma aff propinquum</i>	18
<i>Halectinosoma aff propinquum II</i>	3
<i>Halectinosoma aff.proximum</i>	1
<i>Halectinosoma aff.sarsi</i>	2
<i>Halectinosoma aff.tenerum</i>	23
<i>Halectinosoma aff.conccinum</i>	2
<i>Halctinosoma hyalinus</i>	1
<i>Halectinosoma longiseta</i>	2
<i>Halectinosoma oligosegmenta</i>	1
<i>Halectinosoma oligoseta</i>	3
<i>Halectinosoma quatra</i>	1
<i>Halectinosoma mexicana</i>	1
<i>Halectinosoma tenuis</i>	14
<i>Halectinosoma sp.</i>	2
<i>Halectinosomella texana</i>	1
<i>Ectinosomella brevicauda</i>	1
<i>Ectinosomella sp.</i>	1
<i>Pseudoectinosoma sp.</i>	19
<i>Bradya aff. congenera</i>	48
<i>Bradya longicauda</i>	2
<i>Bradya longispina</i>	1
<i>Bradya aff.macrochaeta</i>	6
<i>Bradya magnus</i>	6
<i>Bradya oligochaeta</i>	4
<i>Bradya aff.proxima</i>	9
<i>Bradya aff.scotti</i>	3
<i>Bradya aff.dilatata</i>	9
<i>Bradya aff.pymaea</i>	1
<i>Bradya aff. simulans</i>	3
<i>Bradya aff.typica</i>	1
<i>Bradya aff.furcata</i>	6
<i>Bradya curvatus</i>	3
<i>Pseudobradya sp.</i>	1
<i>Pseudobradya aff. acuta</i>	3
<i>Pseudobradya aff.ambigua</i>	1

S	N
<i>Pseudobradya aff.parvula</i>	2
<i>Pseudobradya aff.maxima</i>	1
<i>Pseudobradya aff.pygmaea</i>	2
<i>Pseudobradya aff. pelogones</i>	7
<i>Pseudobradya aff.robusta</i>	10
<i>Sigmatidium sp.1</i>	5
<i>Sigmatidium sp.2</i>	4
<i>Sigmatidium aff.difficile</i>	3
<i>Sigmatidium texana</i>	2
<i>Halophytophilus sp.</i>	1
<i>Halophytophilus aff.fusiformis</i>	4
<b>Neobradyidae</b>	
<i>Neobradya sp.</i>	1
<i>Marsteinia sp.1</i>	12
<i>Marsteinia sp.2</i>	1
<i>Marsteinia aff.similis</i>	22
<i>Marsteinia texana</i>	2
<i>Marsteinia aff typica</i>	4
<i>Marsteinia oligosegmenta</i>	1
<i>Marsteinia oligoseta</i>	1
<i>Marsteina longicauda</i>	2
<i>Marsteinia mexicana</i>	1
<i>Marsteinia texana</i>	2
<i>Antarcticobradya sp.</i>	3
<i>Paraneobradya sp.</i>	2
<i>Texasneobradya typica</i>	1
<i>Mexiconeobradya triangulata</i>	3
<b>Euterpinidae</b>	
<i>Euterpina aff.acutifrons</i>	1
<b>Darcythompsonidae</b>	
<i>Paradarcythompsonia texana</i>	1
<i>Kristensenia texana</i>	1
<i>Kristensenia triangulata</i>	1
<i>Leptocaris aff.minutus</i>	1

S	N
<b>Tisbidae</b>	
<i>Tisbe aff. compacta</i>	1
<i>Tisbe aff. graciloides</i>	1
<i>Tisbe aff. finmarchica</i>	2
<i>Tisbe</i> sp.	1
<i>Tisbintra elongata</i>	1
<i>Zosime abberanta</i>	1
<i>Zosime depressa</i>	1
<i>Zosime aff. atlantica</i>	10
<i>Zosime aff. bathyalis</i>	8
<i>Zosime aff. bathybia</i>	39
<i>Zosime aff. bergensis</i>	27
<i>Zosime aff. erythraea</i>	10
<i>Zosime aff. gisleni</i>	35
<i>Zosime aff. mediterranea</i>	64
<i>Zosime not. mediterranea</i>	3
<i>Zosime aff. major</i>	24
<i>Zosime aff. major</i> (large form)	2
<i>Zosime aff. paramajor</i>	20
<i>Zosime aff. typica</i>	27
<i>Zosime aff. incrassata</i>	57
<i>Zosime not. incrassata</i>	3
<i>Zosime aff. incrassta II</i>	2
<i>Zosime longicauda</i>	4
<i>Zosime aff. valida</i>	1
<i>Zosime mexicana</i>	13
<i>Zosime texana</i>	1
<i>Pseudozosime</i> sp.1	5
<i>Pseudozosime</i> sp.2	2
<i>Pseudozosime</i> sp.3	2
<i>Pseudozosime texana</i>	1
<i>Pseudozosime trisetosa</i>	7
<i>Tachidiella aff. minuta</i>	9
<i>Tachidiella aff. kimi</i>	2
<i>Tachidiella aff. parva</i>	1
<i>Tachidiella oligoseta</i>	2
<i>Tachidiella texana</i>	1
<i>Plesiotachidiella quatra</i>	2



S	N
<i>Idyanthe</i> sp.1	6
<i>Idyanthe</i> sp.2	1
<i>Idyanthe</i> aff. dilatata	1
<i>Idyanthe</i> aff.pusilla	2
<i>Idyanthe</i> aff.tenella	4
<i>Idyella</i> sp.	4
<i>Idyella</i> aff. major	4
<i>Idyella</i> aff.pallidula	5
<i>Idyella</i> aff.exigua	2
<i>Idyellopsis</i> sp.	13
<i>Idyellopsis</i> trisetosa	2
<i>Idyellopsis</i> minuta	2
<i>Idyellopsis</i> aff.typica	11
<i>Idyellopsis</i> aberrans	1
<i>Idyellopsis</i> texana	51
<i>Neozosime</i> bisetosa	95
<i>Neozosime</i> bisegmenta	2
<i>Neozosime</i> longicauda	18
<i>Neozosime</i> trisetosa	56
<i>Neozosime</i> sp.	13
<i>Peresime</i> brevifurca	15
<i>Peresime</i> aff.reducta	19
<i>Peresime</i> aff.abyssalis	1
<i>Peresime</i> trisetosa	3
<i>Parazosime</i> longicauda	8
<i>Parazosime</i> sp.	5
<i>Tachidiopsis</i> aff.typica	5
<i>Tachidiopsis</i> aff. bozici	51
<i>Tachidiopsis</i> not.bozici	1
<i>Tachidiopsis</i> aff.cyclopoides	14
<i>Tachidiopsis</i> aff.laubieri	23
<i>Tachidiopsis</i> aff.parasimilis	13
<i>Tachidiopsis</i> aff.similis	4
<i>Tachidiopsis</i> reducta	1
<i>Tachidiopsis</i> texanus	1
<b>Danielsseniidae</b>	
<i>Daniellsenia</i> mexicana	7

S	N
<i>Daniellsenia</i> aff. <i>minuta</i>	1
<i>Daniellsenia</i> aff. <i>reducta</i>	8
<i>Daniellsenia</i> aff. <i>quadriseta</i>	21
<i>Daniellsenia</i> aff. <i>spinipes</i>	1
<i>Daniellsenia</i> aff. <i>typica</i>	1
<i>Jonesiella</i> sp.	5
<i>Jonesiella</i> aff. <i>fusiformis</i>	2
<i>Pseudodanielssenia</i> <i>noendopoda</i>	1
<i>Paradanielssenia</i> aff. <i>biclavata</i>	2
<i>Paradanielssenia</i> aff. <i>kathleenae</i>	8
<i>Paradanielssenia</i> aff. <i>kunzi</i>	2
<i>Telopsammis</i> <i>texana</i>	2
<i>Telopsammis</i> sp.	5
<i>Cylindromexicana</i> <i>texana</i>	1
<i>Psammis</i> aff. <i>longipes</i>	2
<i>Micropsammis</i> <i>texanus</i>	1
<i>Mucrosenia</i> <i>texana</i>	3
<i>Texasdanielssenia</i> <i>typica</i>	2
<i>Neoparanannopus</i> <i>longicauda</i>	1
<b>Thalestridae</b>	
<i>Dactylopodopsis</i> aff. <i>dilatata</i>	1
<i>Dactylopodella</i> aff. <i>clypeata</i>	1
<i>Dactylopodella</i> aff. <i>vervoorti</i>	1
<i>Dactylopodella</i> sp.	1
<i>Pseudotachidius</i> sp.1	3
<i>Pseudotachidius</i> sp.2	1
<i>Pseudotachidius</i> sp.3	1
<i>Pseudotachidius</i> aff. <i>abysallis</i>	14
<i>Pseudotachidius</i> aff. <i>bipartitus</i>	1
<i>Pseudotachidius</i> aff. <i>similis</i>	13
<i>Pseudotachidius</i> aff. <i>coronatus</i>	6
<i>Pseudotachidius</i> aff. <i>vikigus</i>	3
<i>Pseudotachidius</i> <i>bisegmentus</i>	1
<i>Pseudotachidius</i> <i>texana</i>	1
<i>Dactylopodia</i> aff. <i>signata</i>	1
<i>Idomene</i> aff. <i>forficata</i>	1

S	N
<b>Diosaccidae</b>	
<i>Amonardia aff.normani</i>	1
<i>Robertsonia aff. tenuis</i>	1
<i>Amphiascus aff.congenera</i>	1
<i>Amphiascus aff.gracilis</i>	1
<i>Amphiascus aff.hirtus</i>	1
<i>Amphiascus aff.minutus</i>	1
<i>Amphiascus aff.varians</i>	1
<i>Amphiascus aff.propinquus</i>	1
<i>Amphiascus aff.tenuiremis</i>	1
<i>Amphiascus sp.</i>	1
<i>Amphiascoides aff.atopus</i>	17
<i>Amphiascoides aff.breviarticulatus</i>	1
<i>Amphiascoides aff. subdebilis</i>	42
<i>Amphiascoides aff.proxima</i>	4
<i>Amphiascoides aff.lancisetiger</i>	2
<i>Amphiascoides aff.nanoides</i>	5
<i>Amphiascoides aff. neglecta</i>	1
<i>Amphiascoides aff. petkovskii</i>	4
<i>Paramphiascella sp.</i>	3
<i>Paramphiascella aff.robinsoni</i>	7
<i>Paramphiascella aff.vararensis</i>	3
<i>Paramphiascella aff.intermedia</i>	1
<i>Paramphiascella aff.hispida</i>	3
<i>Paramphiascella aff.pacifica</i>	4
<i>Pseudoparamesochra texana</i>	1
<i>Robertsonia sp.</i>	2
<i>Pseudodiosaccus sp.</i>	1
<i>Stenhelia sp.1</i>	4
<i>Stenhelia sp.2</i>	3
<i>Stenhelia sp.3</i>	2
<i>Stenhelia sp.</i>	1
<i>Stenhelia unisegmenta</i>	2
<i>Stenhelia aff.aemula</i>	3
<i>Stenhelia aff.arenicola</i>	4
<i>Stenhelia aff.bisetosa</i>	1
<i>Stenhelia aff. confluens</i>	11
<i>Stenhelia aff.gibba</i>	1

S	N
<i>Stenhelia aff.peniculata</i>	5
<i>Delavalia aff.incerta</i>	1
<i>Delavalia aff. reflexa</i>	7
<i>Delavalia not.reflexa</i>	2
<i>Delavalia aff. hanstromi</i>	13
<i>Delavalia aff.latifes</i>	2
<i>Delavalia aff longicaudata</i>	6
<i>Delavalia aff.longifurca</i>	12
<i>Delavalia aff.incerta</i>	1
<i>Delavalia aff.indica</i>	1
<i>Delavalia aff.latisetosa</i>	1
<i>Delavalia bisegmenta</i>	2
<i>Neodelavalia texana</i>	1
<i>Neostenhelia texana</i>	1
<i>Texastenhelia sp.</i>	2
<i>Haloschizopera aff.abysyi</i>	9
<i>Haloschizopera aff.aegyptica</i>	1
<i>Haloschizopera aff. latisetifera</i>	1
<i>Haloschizopera aff.lima</i>	5
<i>Haloschizopera aff. mathoi</i>	19
<i>Haloschizopera aff. junodi</i>	11
<i>Haloschizopera aff.phyllura</i>	6
<i>Haloschizopera aff. pygmaea</i>	1
<i>Haloschizopera aff. marmarae</i>	6
<i>Haloschizopera aff. tenuipes</i>	4
<i>Haloschizopera aff.ruthorum</i>	3
<i>Schizopera aff.akatovae</i>	2
<i>Schizopera aff.haitiana</i>	1
<i>Schizopera aff.inopinata</i>	1
<i>Schizopera aff.jugurtha</i>	1
<i>Schizopera aff.negelecta</i>	3
<i>Schizopera aff.spinulosa</i>	3
<i>Schizopera aff.triacantha</i>	2
<i>Schizopera sp.</i>	1
<i>Pseudodiosaccus sp.1</i>	1
<i>Pseudodiosaccopsis aff.brunneus</i>	3
<i>Robertgurneya aff.brevipes</i>	8
<i>Robertgurneya aff.ecaudata</i>	2

S	N
<i>Robertgurneya aff. falklandiensis</i>	3
<i>Robertgurneya aff. Ilievecensis</i>	2
<i>Robertgurneya aff.rostrata</i>	7
<i>Robertgurneya aff.similes similis</i>	2
<i>Robertgurneta aff.simulans</i>	6
<i>Robertgurneya aff.spinulosa</i>	18
<i>Robertgurneya sp.</i>	2
<i>Bulbamphiascus aff. imus</i>	31
<i>Bulbamphiascus aff. minutus</i>	7
<i>Bulbamphiascus aff. inermis</i>	5
<i>Paramphiascopsis aff.gieshrechtii</i>	9
<i>Paramphiascopsis aff.longirostris</i>	7
<i>Paramphiascopsis aff. pallidus</i>	6
<i>Paramphiascopsis aff.soyeri</i>	1
<i>Paramphiascopsis aff.triaticulatus</i>	3
<i>Paramphiascopsis aff wihonu</i>	1
<i>Typhlamphiascus brevicaudatus</i>	1
<i>Typhlamphiascus aff.confusus</i>	3
<i>Typhlamphiascus aff.gracilis</i>	1
<i>Typhlamphiascus aff.gracilicaudatus</i>	1
<i>Typhlamphiascus aff. lamellifer</i>	6
<i>Rhyncholagena sp.</i>	1
 <b>Ameiriidae</b>	
<i>Interleptomesochra sp.</i>	1
<i>Leptomesochra sp.</i>	2
<i>Leptomesochra oligoseta</i>	1
<i>Leptomesochra pygmaea</i>	5
<i>Leptomesochra aff. tenuicornis</i>	1
<i>Parapseudoleptomesochra</i>	2
 <i>aff.botosaneanni</i>	
<i>Nitoca aff. affinis</i>	2
<i>Nitocra aff. bdelluræ</i>	2
<i>Nitocra aff. hibernica</i>	2
<i>Nitocra aff. mediterranea</i>	1
<i>Nitocra aff pusilla</i>	3
<i>Nitocra aff.reducta</i>	1

S	N
<i>Nitocra aff.typica</i>	3
<i>Nitocrella sp1(A sp3)</i>	2
<i>Nitocrella aff.chappuisi</i>	6
<i>Nitocrella aff.delayi</i>	1
<i>Nitocrella aff. incerta</i>	7
<i>Nitocrella aff. intermedia</i>	3
<i>Nitocrella aff.negreai</i>	1
<i>Nitocrella aff.omega</i>	1
<i>Nitocrella aff.reducta</i>	1
<i>Nitocrella aff. subterranea</i>	2
<i>Nitocrella not.subterranea</i>	1
<i>Nitocrella aff. tonsa</i>	1
<i>Nitocrella sp.</i>	1
<i>Ameira aff.longipes</i>	6
<i>Ameira aff. parvula</i>	52
<i>Ameira aff.scotti</i>	1
<i>Ameira aff. speciosa</i>	22
<i>Ameira aff.tenella</i>	8
<i>Ameira aff.tenuicornis</i>	5
<i>Pseudameira sp.1</i>	2
<i>Pseudameira sp.2</i>	3
<i>Pseudameira sp.3</i>	1
<i>Pseudameira aff. gracilis</i>	3
<i>Pseudameira aff. crassicornis</i>	17
<i>Pseudameira aff. furcata</i>	16
<i>Pseudameira aff.minutissima</i>	9
<i>Pseudameira longispina</i>	1
<i>Proameira aff. arenicola</i>	5
<i>Proameira aff. dubia</i>	3
<i>Proameira aff. phaedra</i>	2
<i>Proameira aff.simplex</i>	5
<i>Proameira longicauda</i>	1
<i>Parameiopsis longicauda</i>	8
<i>Parameiopsis longirostris</i>	1
<i>Parameiopsis sp.</i>	5
<i>Parameiopsis aff.magnus</i>	1
<i>Parameiopsis aff.peruanus</i>	7
<i>Parameiopsis texana</i>	1

S	N
<i>Ameiropsis aff. abbreviata</i>	20
<i>Ameiropsis aff. brevicornis</i>	3
<i>Ameiropsis aff. longicornis</i>	1
<i>Ameiropsis aff. minor</i>	12
<i>Ameiropsis aff. nobilis</i>	1
<i>Ameiropsis aff. robinsoni</i>	4
<i>Ameiropsis sp.</i>	1
<i>Sarsameira sp.1</i>	2
<i>Sarsameira sp.2</i>	1
<i>Sarsameira sp.3</i>	2
<i>Sarsameira aff. elongata</i>	1
<i>Sarsameira aff. longiremis</i>	2
<i>Sarsameira aff. major</i>	14
<i>Sarsameira aff. giraulti</i>	4
<i>Sarsameira aff. parva</i>	9
<i>Sarsameira aff. propinqua</i>	6
<i>Sarsameira aff. sarsi</i>	3
<i>Sicameira sp.</i>	1
<i>Stenocopia aff. antarctica</i>	1
<i>Anoplasoma multisegmenta</i>	1
<i>Anoplasoma longicauda</i>	1
<i>Malacopsyllus sp.</i>	4
<i>Malacopsyllus multispinatus</i>	1
<i>Malacopsyllus elongatus</i>	1
<b>Paramesochriidae</b>	
<i>Paramesochra aff. acutata</i>	6
<i>Paramesochra aff. brevifurca</i>	3
<i>Paramesochra aff. coelebs</i>	6
<i>Paramesochra aff. constricta</i>	1
<i>Paramesochra aff. holsatica</i>	2
<i>Paramesochra aff. similis</i>	2
<i>Paramesochra aff. unaspina</i>	6
<i>Paramesochra aff. dubia</i>	2
<i>Paramesochra sp.1</i>	1
<i>Paramesochra sp.2</i>	2
<i>Paramesochra sp.3</i>	1
<i>Paramesochra aff. helgolandica</i>	10

S	N
<i>Paramesochra aff. pterocaudata</i>	2
<i>Leptopsyllus aff. typicus</i>	8
<i>Leptopsyllus aff. abyssalis</i>	1
<i>Leptopsyllus aff. dubatyi</i>	1
<i>Leptopsyllus aff. harveyi</i>	3
<i>Leptopsyllus aff. platyspinosus</i>	2
<i>Leptopsyllus aff. reductus</i>	1
<i>Leptopsyllus sp.</i>	1
<i>Leptopsyllus texana</i>	1
<i>Paraleptopsyllus sp.</i>	44
<i>Scotopsyllus aff. herdmani</i>	3
<i>Kliopsyllus sp. 1</i>	3
<i>Kliopsyllus sp. 2 (P.sp1)</i>	7
<i>Kliopsyllus aff. californicus</i>	12
<i>Kliopsyllus aff. laurenticus</i>	1
<i>Kliopsyllus sp. longicauda</i>	2
<i>Kliopsyllus aff. longisetosus</i>	1
<i>Kliopsyllus aff. spiniger</i>	4
<i>Kliopsyllus aff. minutus</i>	1
<i>Rosopsyllus texanus</i>	1
<i>Remanea texana</i>	1
<i>Texaspsyllus typicus</i>	1
<b>Canthocamptidae</b>	
<i>Cletocamptus sp.</i>	4
<i>Mesochra sp.</i>	2
<i>Mesochra aff. lilljeborgi</i>	3
<i>Mesochra aff. nana</i>	1
<i>Mesochra aff. pallaresi</i>	1
<i>Mesochra aff. pygmaea</i>	2
<i>Bathycamptus aff. eckmani</i>	17
<i>Bathycamptus texanus</i>	9
<i>Bathycamptus aff. minutus</i>	2
<i>Bathycamptus sp.</i>	10
<i>Neobathycamptus texana</i>	1
<i>Oligobathycamptus texana</i>	1
<i>Parabathycamptus sp.</i>	2
<i>Cylindromesochra texana 1</i>	4



S	N
<i>Cylindromesochra texana</i> 2	1
<i>Texascamptus taxanus</i>	6
<i>Boreolimella brevifurca</i>	3
<i>Boreolimella longispina</i>	2
<i>Boreolimella oligochaeta</i>	2
<i>Boreolimella rostrata</i>	1
<i>Boreolimella texana</i>	25
<i>Boreolimella aff.trisetosa</i>	1
<i>Leimia aff. vaga</i>	2
<i>Leimia texana</i>	7
<i>Leimia longicauda</i>	4
<i>Leimia mexicana</i>	2
<i>Bathycamptonia longifurca</i>	1
<i>Mesopsyllus</i> sp.	2
<i>Mesopsyllus aff.atargatis</i>	3
<i>Mesopsyllus areolatus</i>	2
<i>Mesopsyllus neos</i>	1
<i>Mesopsyllus gracilis</i>	3
<i>Mesopsyllus longicauda</i>	4
<i>Mesopsyllus longifurca</i>	1
<i>Mesopsyllus texanus</i>	6
<i>Heteropsyllus aff. confluens</i>	3
<i>Heteropsyllus aff.cuticaudatus</i>	5
<i>Heteropsyllus aff. exigus</i>	15
<i>Heteropsyllus aff.nannus</i>	2
<i>Heteropsyllus aff.nunni</i>	1
<i>Heteropsyllus aff.rostratus</i>	29
<i>Heteropsyllus aff.major</i>	14
<i>Heteropsyllus aff. meridionalis</i>	38
<i>Heteropsyllus longisegmenta</i>	1
<i>Heteropsyllus oligosetus</i>	2
<i>Heteropsyllus texanus</i>	1
<i>Heteropsyllus</i> sp.	2
<i>Bushia texana</i>	1
<i>Parepactophanes</i> sp.	1
<i>Pusillargillus aff.nixe</i>	1
<i>Stenocaris</i> sp.	1
<i>Stenocaropsis</i> sp.	1

S	N
<i>Cylindropsyllus areolatus</i>	4
<i>Cylindrotexanella mexicana</i>	1
<i>Arenopontia texana</i>	1
<b>Cletodidae</b>	
<i>Acrenhydrosoma hamus</i>	2
<i>Cletodes</i> sp.	7
<i>Cletodes</i> aff. <i>contiginiensis</i>	3
<i>Cletodes</i> aff. <i>dorae</i>	1
<i>Cletodes</i> aff. <i>latirostris</i>	3
<i>Cletodes</i> aff. <i>longifurca</i>	17
<i>Cletodes</i> aff. <i>longicaudatus</i>	2
<i>Cletodes</i> aff. <i>longifurcatus</i>	21
<i>Cletodes</i> aff. <i>limicola</i>	1
<i>Cletodes</i> aff. <i>macrura</i>	7
<i>Cletodes</i> aff. <i>pusillus</i>	15
<i>Cletodes</i> aff. <i>reyssi</i>	23
<i>Cletodes</i> aff. <i>yotabis</i>	2
<i>Cletodes</i> <i>bifidas</i>	1
<i>Cletodes</i> <i>texana</i>	1
<i>Poria</i> sp.	3
<i>Echinocletodes</i> aff. <i>armatus</i>	2
<i>Echinocletodes</i> <i>longicauda</i>	1
<i>Odiliacletodes</i> <i>texanus</i>	2
<i>Stylicletodes</i> aff. <i>longicaudatus</i>	16
<i>Stylicletodes</i> aff. <i>oligochaeta</i>	4
<i>Stylicletodes</i> aff. <i>reductus</i>	2
<i>Enhydrosoma</i> aff. <i>buchholtzi</i>	1
<i>Enhydrosoma</i> aff. <i>lacunae</i>	1
<i>Schizacran</i> <i>texana</i>	2
<b>Huntemannidae</b>	
<i>Nannopus</i> sp.	3
<i>Pseudonannopus</i> <i>texanus</i>	1
<i>Pseudonannopus</i> <i>secundus</i>	1
<i>Pseudonannopus</i> <i>similis</i>	0
<i>Metahuntemannia</i> sp.	4
<i>Metahuntemannia</i> aff. <i>crassa</i>	1

S	N
<i>Metahuntemannia aff.iberica</i>	8
<i>Metahuntemannia aff. magniceps</i>	4
<i>Metahuntemannia noendopoda</i>	3
<i>Metahuntemannia aff.pseudomagniceps</i>	2
<i>Metahuntemannia aff.spinifes</i>	2
<i>Metahuntemannia texana</i>	1
<i>Metahuntemannia mexicana</i>	1
<i>Talpina aff. bifida</i>	1
<i>Talpina aff. fodens</i>	1
<i>Talpina aff.talpa</i>	1
<i>Pseudocletodes sp.</i>	1
<i>Pseudocletodes longicauda</i>	1
 <b>Paranannopidae</b>	
<i>Pseudomesochra aff.abberans</i>	4
<i>Pseudomesochra aff.abbyssalis</i>	6
<i>Pseudomesochra aff.beckeri</i>	7
<i>Pseudomesochra aff. brucei</i>	17
<i>Pseudomesochra aff brucei II</i>	2
<i>Pseudomesochra aff.crispata</i>	21
<i>Pseudomesochra aff.divaricata</i>	2
<i>Pseudomesochra aff.latifurca</i>	9
<i>Pseudomesochra aff.longifurcata</i>	6
<i>Pseudomesochra aff. media</i>	5
<i>Pseudomesochra aff.meridionensis</i>	6
<i>Pseudomesochra aff.minor</i>	6
<i>Pseudomesochra aff.scheibeli</i>	6
<i>Pseudomesochra aff. similis</i>	30
<i>Pseudomesochra aff. tatiana</i>	8
<i>Pseudomesochra aff. tamara</i>	1
<i>Pseudomesochra exopodata</i>	1
<i>Pseudomesochra texana</i>	2
<i>Pseudomesochra sp.1</i>	3
<i>Pseudomesochra sp.2</i>	2
<i>Pseudomesochra sp.3</i>	1
<i>Pseudomesochra sp.4</i>	1
<i>Pseudomesochra sp.5</i>	1
<i>Pseudomesocra sp.</i>	1

S	N
<i>Paranannopus</i> sp.	1
<i>Paranannopus</i> aff.sarsi	3
<i>Paranannopus</i> oligosetus	1
<i>Paranannopus</i> aff.longithorax	4
<i>Paranannopus</i> aff. minutus	1
<i>Paranannopus</i> aff. reductus	1
<i>Paranannopus</i> aff.singulosestosus	1
<i>Paranannopus</i> aff.trisetosus	1
<i>Paranannopus</i> texanus	3
<i>Paranannopus</i> aff.triarticulatus	2
<i>Paranannopus</i> aff.truncatus	1
<i>Paranannopus</i> aff. denticulatus	1
<i>Archisenia</i> sp.	1
<i>Cylindronannopus</i> aff.elongatus	8
<i>Cylindronannopus</i> aff. primus	1
<i>Cylindronannopus</i> texanus	12
<i>Cylindronannopus</i> bisetosus	1
<i>Cylindronannopus</i> sp.	1
<i>Micropsammis</i> sp.	2
<i>Mucrosenia</i> aff. kendalli	1
<b>Argestidae</b>	
<i>Fultonia</i> sp.1	14
<i>Fultonia</i> sp.2	1
<i>Fultonia</i> aff.bouisi carollicola	4
<i>Fultonia</i> aff.gascognensis	6
<i>Fultonia</i> aff.hirsuta	11
<i>Fultonia</i> aff.sarsi	15
<i>Fultonia</i> elongata	1
<i>Fultonia</i> texana	1
<i>Fultonia</i> trisetosa	3
<i>Argestes</i> sp.	1
<i>Argestes</i> aff.mollis	11
<i>Argestes</i> aff.reducta	1
<i>Argestes</i> oligoseta	1
<i>Argestes</i> texana	2
<i>Parargestes</i> brevifurca	1
<i>Parargestes</i> unisetosa	1

S	N
<i>Paragestes aff tenuis</i>	13
<i>Argestigens aff.abyssalis</i>	1
<i>Argestigens aff.uniremis</i>	7
<i>Argestigens aff.glacialis</i>	7
<i>Argestigens reducta</i>	3
<i>Argestinella texana</i>	1
<i>Argestigens sp.</i>	1
<i>Argestia pseudocervinia</i>	1
<i>Rostrina texana</i>	2
<i>Limnocletodes sp.</i>	2
<i>Limnocletodes aff.behningi</i>	1
<i>Limnocletodes aff. mucratus</i>	1
<i>Mesocletodes sp.</i>	3
<i>Mesocletodes aff.abyssicola</i>	2
<i>Mesocletodes aff. ameliae</i>	1
<i>Mesocletodes aff.brevifurca</i>	1
<i>Mesocletodes aff. farauni</i>	1
<i>Mesocletodes aff.fladensis</i>	4
<i>Mesocletodes aff.foroerensis</i>	3
<i>Mesocletodes aff. inermis</i>	2
<i>Mesocletodes aff irrasus</i>	17
<i>Mesocletodes not.irrasus</i>	2
<i>Mesocletodes aff. commixtus</i>	1
<i>Mesocletodes aff.katharinae</i>	1
<i>Mesocletodes aff.kunzi</i>	4
<i>Mesocletodes aff.makarovi</i>	1
<i>Mesocletodes aff.parirrasus</i>	1
<i>Mesocletodes texana</i>	1
<i>Mesocletodes aff.thielli</i>	2
<i>Eurycletodes aff.aculeatus</i>	1
<i>Eurycletodes aff.echinatus</i>	1
<i>Eurycletodes aff.monardi</i>	1
<i>Eurycletodes aff. serratus</i>	2
<i>Eurycletodes aff.rectangulatus</i>	6
<i>Eurycletodes aff.verisimilis</i>	3
<i>Eurycletodes aff. goburnovi</i>	2
<i>Eurycletodes sp.1</i>	2
<i>Eurycletodes sp.2</i>	1

S	N
<i>Eurycletodes (O.) aff. major</i>	3
<i>Eurycletodes (O.) aff. similes</i>	1
<i>Leptocletodes</i> sp.1	1
<i>Leptocletodes</i> sp.2	2
<i>Leptocletodes brevicaudatus</i>	5
<i>Leptocletodes aff.debilis</i>	4
<i>Leptocletodes gigantes</i>	1
<i>Leptocletodes longicauda</i>	3
<i>Hemimesochra</i> sp.1	6
<i>Hemimesochra</i> sp.2	1
<i>Hemimesochra</i> sp.3	1
<i>Hemimesochra aff.clavularis</i>	5
<i>Hemimesochra gracilis</i>	2
<i>Hemimesochra micronica</i>	3
<i>Hemimesochra longicauda</i>	5
<i>Hemimesochra longisegmenta</i>	1
<i>Neohemimesochra texana</i>	1
<i>Nannopodella texana</i>	4
<i>Monocletodes</i> sp.	1
<i>Oligocletodes areolatus</i>	1
<i>Bathycletopsyllus longicauda</i>	1
 <b>Laophontidae</b>	
<i>Troglophonte texana</i>	4
<i>Troglophonte longicada</i>	1
<i>Texaslaophonte</i> sp.	1
<i>Platychelipus</i> sp.	1
<i>Pontopolites</i> sp.	1
<i>Paleolaophontodes</i> sp.	1
 <b>Normanellidae</b>	
<i>Sagamiella levisa</i>	16
<i>Sagamiella longipedesta</i>	19
<i>Sagamiella brevicauda</i>	3
<i>Sagamiella</i> sp.	1
<i>Texanella brevicauda</i>	4
<i>Texanella longisegmenta</i>	1
<i>Texanella oligoseta</i>	5

S	N
<i>Normanella aff.reducta</i>	1
<i>Normanella</i> sp.	1
<b>Ancorabolidae</b>	
<i>Ancorabolus aff.mirabilis</i>	1
<i>Ancorabolus mexicana</i>	2
<i>Ancorabolus texanus</i>	2
<i>Ancorabolus lateralspinus</i>	1
<i>Neoancorabolus texana</i>	1
<i>Echinopsyllus</i> sp.	6
<i>Echinopsyllus gladius</i>	5
<i>Arthropsoyllus</i> sp.1	3
<i>Arthropsoyllus</i> sp.2	1
<i>Arthropsoyllus serratus</i>	1
<i>Laophontodes aff.wilsoni</i>	1
<i>Ceratonotus</i> sp.	2
<b>Unid. family</b>	
<i>Taekwoenvia mexicana</i>	27
<i>Aesthetascia longicauda</i>	1
<i>Noendopoda texana</i>	6
<i>Noendopoda texana2</i>	1
<i>Cylindrotexanella texana</i>	1
<i>Neohemimesochra antenata</i>	3
<i>Doolia typica</i>	1
Unidentified family	19
Unidentified Ancorabolidae	3
Unidentified Ameiriidae	42
Unidentified Argestidae	7
Unidentified Canthocamptidae	8
Unidentified Cerviniidae	1
Unidentified Cylindropsyllinae	2
Unidentified Danielsseniidae	4
Unidentified Diosaccidae	26
Unidentified Ectinosomatidae	26
Unidentified Laophontidae	1
Unidentified Neobryidae	1

S	N
Unidentified Paramesochridae	6
Unidentified Tisbidae	7
Unidentified harpacticoid(damaged)	1159
Canuellidae copepodites	5
Ameiriidae copepodites	29
Cerviniidae copepodites	26
Cylindropsyllidae copepodites	1
Paranannopidae cepepodites	37
Paramesochridae copepodites	2
Canthocamptidae copepodites	16
Danielssenidae copepodites	7
Diosaccidae copepodites	77
Huntemannidae copepodites	6
Argestidae copepodites	54
Ectinosomatidae copepodites	66
Tisbidae copepodites	85
Cletodidae copepodites	10
Thalestridae copepodites	15
Normanellidae copepodites	5
Neobradyyidae copepodites	6
Ancorbolidae copepodites	3
Unidentified copepodites	7217
<b>Total harpacticoida</b>	<b>12480</b>



## REFERENCES

- Abele LG, Walters K (1979) Marine benthic diversity - critique and alternative explanation. *Journal of Biogeography* 6: 115-126
- Aller JY (1997) Benthic community response to temporal and spatial gradients in physical disturbance within a deep-sea western boundary region. *Deep Sea Research* 44: 39-69
- Alongi DM (1990) Bacterial growth rates, production and estimates of detrital carbon utilization in deep-sea sediments of the Solomon and Coral Seas. *Deep-Sea Research* 37: 731-746
- Alongi DM, Pichon M (1988) Bathyal meiobenthos of the Western Coral Sea - distribution and abundance in relation to microbial standing stocks and environmental-factors. *Deep-Sea Research* 35: 491-503
- Anderson RF, Rowe GT, Kemp PF, Trumbore S, Biscaye PE (1994) Carbon budget for the mid-slope depocenter of the middle Atlantic Bight. *Deep-Sea Research* 41: 669-703
- Ansari ZA, Parulekar AH, Jagtap TG (1980) Distribution of sup-litoral meiobenthos of the Goa coast, India. *Hydrobiologia* 74: 209-214
- Armstrong RA, McGehee R (1980) Competitive exclusion. *American Naturalist* 115:151-170
- Baguley JG, Hyde LJ, Montagna PA (2004) A semi-automated digital microphotographic approach to measure meiofaunal biomass. *Limnology and Oceanography: Methods* 2: 181-190
- Belabbassi L, Nowlin WD Jr., Jochens AE, Biggs DC, and Chapman P. (2004) Summertime nutrient supply to near-surface waters of the northeastern Gulf of Mexico: 1998, 1999, and 2000. submitted to *Continental Shelf Research*, in revision.
- Bell SS (1980) Meiofauna-macrofauna interactions in a high salt-marsh habitat. *Ecological Monographs* 50: 487-505
- Berger WH, Fischer K, Lai C, Wu G (1988) Ocean carbon flux: maps of primary production and export production. In: Agegian CR (ed) . *Biogeochemical*

Cycling and Fluxes between the deep euphotic zone and other oceanic realms. NOAA, Washington D.C. pp. 131-176.

- Bernhard JM, Sen Gupta BK, and Baguley JG (submitted manuscript) Benthic foraminifera living in Gulf of Mexico slope and abyssal sediments: biomass, density, taxonomic composition, and comparison to metazoan meiofaunal biomass and density. *Deep-Sea Research*
- Betzer PR, Showers WJ, Laws EA, Winn CD, DiTullio GR, Kroopnick PM (1984) Primary productivity and particle fluxes on a transect of the equator at 153°W in the Pacific Ocean. *Deep-Sea Research* 31: 1-11
- Biggs DC, Müller-Karger FE (1994) Ship and satellite observations of chlorophyll stocks in interacting cyclone-anticyclone eddy pairs in the western Gulf of Mexico. *Journal of Geophysical Research* 99: 7371-7384
- Blanchard GF (1991) Measurement of meiofauna grazing rates on microphytobenthos: is primary production a limiting factor? *Journal of Experimental Marine Biology and Ecology* 147: 37-46
- Boland GS, Rowe GT (1991) Deep-sea benthic sampling with the GOMEX box corer. *Limnology and Oceanography* 36: 1015-1020
- Brendel PJ, and Luther III GW. (1995) Development of a gold amalgam voltammetric microelectrode for the determination of dissolved Fe, Mn, O<sub>2</sub>, and S(-II) in porewaters of marine and freshwater sediments. *Environmental Science and Technology* 29: 751-761
- Brown CJ (1998) Effects of a phytodetrital input on nematode communities of the abyssal, equatorial Pacific. Ph.D dissertation. University of Southampton, UK
- Buffan-Dubau E, Carman KR (2000) Diel feeding behavior of meiofauna and their relationships with microalgal resources. *Limnology and Oceanography* 45: 381-395
- Burgess R (2001) An improved protocol for separating meiofauna from sediment using colloidal silica sols. *Marine Ecology Progress Series* 214: 161-165
- Carman KR (1990) Radioactive labeling of a natural assemblage of marine sedimentary bacteria and microalgae for trophic studies: An autoradiographic study. *Marine Ecology* 19: 279-290

- Carman KR, Fleeger JW, Pomarico SM (1997) Response of a benthic food web to hydrocarbon contamination. *Limnology and Oceanography* 42: 561-571
- Carman KR, Fry B (2002) Small-sample methods for delta C-13 and delta N-15 analysis of the diets of marsh meiofaunal species using natural-abundance and tracer-addition isotope techniques. *Marine Ecology Progress Series* 240: 85-92
- Carman KR, Thistle D (1985) Microbial food partitioning by three species of benthic copepods. *Marine Biology* 88: 143-148
- Caswell H (1978) Predator-mediated coexistence: A nonequilibrium model. *American Naturalist* 112: 127-153
- Caswell H, Cohen JE (1991) Disturbance, Interspecific Interaction and Diversity in Metapopulations. *Biological Journal of the Linnean Society* 42: 193-218
- Caswell H, Etter R (1999) Cellular automaton models for competition in patchy environments: Facilitation, inhibition, and tolerance. *Bulletin of Mathematical Biology* 61: 625-649
- Childress JJ, Cowles DL, Favuzzi JA, Mickel TJ (1990) Metabolic rates of benthic deep-sea decapod crustaceans decline with increasing depth primarily due to the decline in temperature. *Deep-Sea Research* 6: 929-949
- Clarke KR, Warwick RM (1999) The taxonomic distinctness measure of biodiversity: weighting of step lengths between hierarchical levels. *Marine Ecology Progress Series* 184: 21-29
- Clarke KR, Warwick RM (2001) Change in marine communities: An approach to statistical analysis and interpretation. Primer-E Ltd., Plymouth, UK
- Connell JH (1978) Diversity in tropical rain forests and coral reefs. *Science* 199: 1302-1310
- Couch CA (1989) Carbon and nitrogen stable isotopes of meiobenthos and their food resources. *Estuarine Coastal and Shelf Science* 28: 433-441
- Coull BC (1972) Species diversity and faunal affinities of meiobenthic Copepoda in the deep sea. *Marine Biology* 14: 48-51
- Coull BC, Bell SS (1979) Perspectives of marine meiofauna ecology. In: Livingston RJ

(ed) Ecological Processes in Coastal and Marine Systems. Plenum Publishing Corp, New York

Coull BC, Ellison RL, Fleeger JW, Higgins RP, Hope WD, Hummon WD, Rieger RM, Sterrer WE, Thiel H, Tietjen JH (1977) Quantitative estimates of meiofauna from the deep-sea off North Carolina, USA. *Marine Biology* 39: 233-240

Coull BC, Palmer MA (1984) Field experimentation in meiofaunal ecology. *Hydrobiologia* 118: 1-19

Coull BC, Zo Z, Tietjen JH, Williams BS (1982) Meiofauna of the southeastern United States. *Continental Shelf Bulletin of Marine Science* 32: 139-150

Dahms HU, Qian PY (2004) Life histories of the Harpacticoida (Copepoda, Crustacea): a comparison with meiofauna and macrofauna. *Journal of Natural History* 38: 1725-1734

Danovaro R, Fabiano M, Albertelli G, Dellacroce N (1995) Vertical-distribution of meiobenthos in bathyal sediments of the eastern Mediterranean Sea - relationship with labile organic matter and bacterial biomasses. *Marine Ecology-Pubblicazioni Della Stazione Zoologica di Napoli I* 16: 103-116

Daro MH (1978) A simplified <sup>14</sup>C method for grazing measurements on natural planktonic populations. *Helgoländer Meeresuntersuchungen* 31: 241-248

de Skowronski RSP, Corbisier TN (2002) Meiofauna distribution in Martel Inlet, King George Island (Antarctica): sediment features versus food availability. *Polar Biology* 25: 126-134

Decho AW (1988) How do harpacticoid grazing rates differ over a tidal cycle? Field verification using chlorophyll-pigment analyses. *Marine Ecology Progress Series* 45: 263-270

Decho AW, Fleeger JW (1988) Microscale dispersion of meiobenthic copepods in response to food-resource patchiness. *Journal of Experimental Marine Biology and Ecology* 118: 229-243

deJonge VN, Bouwman LA (1977) A simple density separation technique for quantitative isolation of meiobenthos using the colloidal silica Ludox-TM. *Marine Biology* 42: 143-148

- Deming J (1997) Unusual or extreme high-pressure marine environments. In: Hurst CJ, Knudsen GR, McInerney MJ, Stetzenbach LD, Walter MV (eds.) *Manual of Environmental Microbiology*. ASM Press, Washington DC
- Deming J (2001) Unusual or extreme high-pressure marine environments. In: Hurst CJ, Knudsen GR, McInerney MJ, Stetzenbach LD, Walter MV (eds.) *Manual of Environmental Microbiology*. ASM Press, Washington DC
- Deming JW, Reysenbach AL, Macko SA, and Smith CR (1997) Evidence for the microbial basis of a chemosynthetic invertebrate community at a whale fall on the deep seafloor: Bone-colonizing bacteria and invertebrate endosymbionts. *Journal of Microscopic Research and Technology* 37: 162-170
- Denoux G, Gardinali P, and Wade TL (1998) Quantitative Determination of Polynuclear Aromatic Hydrocarbons by Gas Chromatography/Mass Spectrometry - Selected Ion Monitoring (SIM) Mode. In: *Sampling and Analytical Methods of the National Status and Trends Program, Mussel Watch Project: 1993-1996 Update*. NOAA Technical Memorandum NOS ORCA 130, pp.129-139.
- Dinet A, Vivier MH (1977) Le meiobenthos abyssal du Golfe de Gascogne. *Cahiers de Biologie Marine* 18: 85-97
- Drazen JC, Baldwin RJ, Smith KL (1998) Sediment community response to a temporally varying food supply at an abyssal station in the NE Pacific. *Deep-Sea Research* 45: 893-913
- Dujardin F (1851) Sur up petit animal marin, l'Echinodere, formant un type intermediaire entre les Crustaces et les Vers. *Ann Sci Nat Zool Ser* (3) 15: 158-160
- Eckelbarger KL (1994) Diversity of metazoan ovaries and vitallogenic mechanisms: implications for life history theory. *Proceedings of the Biological Society of Washington* 170: 193-218
- Eckman JE, Thistle D (1988) Small-scale spatial pattern in meiobenthos in the San Diego Trough. *Deep Sea Research* 35: 1565-1578
- Emmerson MC, Raffaelli DG (2000) Detecting the effects of diversity on measures of ecosystem function: experimental design, null models and empirical observations. *Oikos* 91: 195-203
- Escobar E, Lopez M, Soto LA, Signoret M (1997) Density and biomass of the meiofauna

- of the upper continental slope in two regions of the Gulf of Mexico. *Ciencias Marinas* 23: 463-489
- Etter RJ, Grassle JF (1992) Patterns of species-diversity in the deep-sea as a function of sediment particle-size diversity. *Nature* 360: 576-578
- Etter RJ, Mullineaux LS (2001) Deep-sea communities. In: Bertness MD, Gaines SD, Hay ME (eds) *Marine Community Ecology*. Sinauer Associates, Inc., Sunderland
- Fabiano M, Danovaro R (1999) Meiofauna distribution and mesoscale variability in two sites of the Ross Sea (Antarctica) with contrasting food supply. *Polar Biology* 22: 115-123
- Feller RJ, Warwick RM (1988) Energetics. In: Higgins RP, Thiel H (eds) *Introduction to the study of meiofauna*. Smithsonian Institution Press. Washington DC
- Folk RA (1974) *Petrology of sedimentary rocks*. Hemphill Publishing Company. Austin
- Gage JD (1977) Structure of the abyssal macrobenthic community in the Rockall Trough. In: Keegan BF, Ceidigh PO, Boaden PJS (eds.) *Biology of Benthic Organisms*. Pergamon, Oxford
- Gage JD, Lamont PA, Tyler PA (1995) Deep-sea macrobenthic communities at contrasting sites off Portugal, preliminary results 1: Introduction and diversity comparisons. *Internationale Revue der Gesamten Hydrobiologie* 80: 235-250
- Gage JD, Tyler PA (1991) *Deep-sea biology*. Cambridge University Press, Cambridge
- Gerlach DA (1977) Attraction to decaying organisms as a possible cause for patchy distribution of nematodes in a Bermuda beach. *Ophelia* 16: 151-165
- Giere O (1993) *Meiobenthology: The microscopic fauna in aquatic sediments*. Springer-Verlag, Berlin
- Gooday AJ (2002) Biological responses to seasonally varying fluxes of organic matter to the ocean floor: A review. *Journal of Oceanography* 58: 305-332
- Gooday AJ, Levin LA, Linke P, Heeger T (1992) The role of benthic Foraminifera in deep-sea food webs and carbon cycling. In: Rowe GT, Pariente V (eds.) *Deep-sea food chains and the global carbon cycle*. Kluwer Academic Publishers, Boston.

- Gooday AJ, Pfannkuche O, Lambshead PJD (1996) An apparent lack of response by metazoan meiofauna to phytodetritus deposition in the bathyal north-eastern Atlantic. *Journal of the Marine Biological Association of the United Kingdom* 76: 297-310
- Graf G (1992) Benthic-pelagic coupling: a benthic review. *Oceanography and Marine Biology Annual Review* 30: 149-190
- Grassle JF (1989) Species-diversity in deep-sea communities. *Trends in Ecology & Evolution* 4: 12-15
- Grassle JF, Sanders HL (1973) Life histories and the role of disturbance. *Deep-Sea Research* 20: 643-659
- Grassle JF, Maciolek NJ (1992) Deep-sea species richness - regional and local diversity estimates from quantitative bottom samples. *American Naturalist* 139: 313-341
- Grassle JF, Morse-Porteous LS (1987) Macrofaunal colonization of disturbed deep-sea environments and the structure of deep-sea benthic communities. *Deep-Sea Research* 34: 1911-1950
- Gray JS (1968) An experimental approach to the ecology of the harpacticoid *Leptastacus constrictus* Lang. *Journal of Experimental Marine Biology and Ecology* 2: 278-292
- Gray JS (1974) Animal-sediment relationship. *Oceanography and Marine Biology Annual Review* 12: 223-261
- Gray JS (1981) *The ecology of marine sediments*. Cambridge University Press, Cambridge
- Gray JS, Clarke KR, Warwick RM, Hobbs G (1990) Detection of initial effects of pollution on marine benthos - An example from the Ekofisk and Eldfisk oilfields, North-Sea. *Marine Ecology Progress Series* 66: 285-299
- Gray JS, Poore GCB, Uglund KI, Wilson RS, Olsgard F, Johannessen O (1997) Coastal and deep-sea benthic diversities compared. *Marine Ecology Progress Series* 159: 97-103
- Herman PMJ, Middelburg JJ, Widdows J, Lucas CH, Heip CHR (2000) Stable isotopes as trophic tracers: combining field sampling and manipulative labelling of food

- resources for macrobenthos. *Marine Ecology Progress Series* 204: 79-92
- Hessler RR, Jumars PA (1974) Abyssal community analysis from replicate box cores in the central North Pacific. *Deep-Sea Research* 21: 185-209
- Hessler RR, Sanders HL (1967) Faunal diversity in the deep-sea. *Deep-Sea Research* 14: 65-78
- Hicks GRF (1988) Harpacticoid copepods from biogenic substrata in offshore waters of New Zealand 1. New species of Paradactylopodia, Stenhelia, and Laophonte. *Journal of the Royal Society of New Zealand* 18: 437-452
- Hicks GRF, Coull BC (1983) The ecology of marine meiobenthic harpacticoid copepods. *Oceanography and Marine Biology Annual Review* 21: 67-175
- Higgins RP, Thiel H (1988) Introduction to the study of meiofauna. Smithsonian Institution Press, Washington D.C.
- Hu C, Müller-Karger FE, Biggs DC, Carder KL, Nababan B, Nadeau D, and Vanderbloemen J (2003) Comparison of ship and satellite bio-optical measurements on the continental margin of the NE Gulf of Mexico. *International Journal of Remote Sensing* 24: 2597-2612
- Hulings NC, Gray JS (1971) A manual for the study of meiofauna. *Smithsonian Contributions to Zoology* 78: 1-84
- Hurlbert SH (1971) The nonconcept of species diversity: a critique and alternative parameters. *Ecology* 52: 577-586
- Hurtt GC, Pacala SW (1995) The consequences of recruitment limitation: Reconciling chance, history, and competitive differences between plants. *Journal of Theoretical Biology* 176: 1-16
- Huys R and Boxshall GA (1991) *Copepod Evolution*. The Ray Society, London, pp. 468.
- Huys R, Gee JM, Moore CG, Hamond R, and Geddes DC (1996) Marine and brackish water harpacticoid copepods, part 1. In: Barnes RSK and Crothers JH (eds.) *Synopses of the British Fauna (New Series) No. 51*. Field Studies Council, Shrewsbury, U.K.
- Jahnke RA (1996) The global ocean flux of particulate organic carbon: Areal



- distribution and magnitude. *Global Biogeochemical Cycles* 10: 71-88
- Janzen DH (1970) Herbivores and the number of trees species in tropical forests. *American Naturalist* 104: 501-528
- Jensen P (1987) Feeding Ecology of Free-Living Aquatic Nematodes. *Marine Ecology Progress Series* 35: 187-196
- Jumars PA (1975) Environmental grain and polychaete species' diversity in a bathyal benthic community. *Marine Biology* 30: 253-266
- Jumars PA (1976) Deep-sea species diversity - Does it have a characteristic scale. *Journal of Marine Research* 34: 217-246
- Lambshead P (1993) Recent developments in marine benthic biodiversity research. *Oceanis* 19: 5-24
- Lambshead PJD (*in press*) Marine nematode biodiversity. In: Chen ZX, Chen SY, Dickson DW (eds.) *Nematology, advances and perspectives*. ACSE-TUP Book Series
- Lambshead PJD, Boucher G (2003) Marine nematode deep-sea biodiversity - hyperdiverse or hype? *Journal of Biogeography* 30: 475-485
- Lambshead PJD, Brown CJ, Ferrero TJ, Hawkins LE, Smith CR, Mitchell NJ (2003) Biodiversity of nematode assemblages from the region of the Clarion-Clipperton Fracture Zone, an area of commercial mining. *BMC Ecology* 3:1-12
- Lambshead PJD, Brown CJ, Ferrero TJ, Mitchell NJ, Smith CR, Hawkins LE, Tietjen J (2002) Latitudinal diversity patterns of deep-sea marine nematodes and organic fluxes: a test from the central equatorial Pacific. *Marine Ecology Progress Series* 236: 129-135
- Lambshead PJD, Tietjen J, Ferrero T, Jensen P (2000) Latitudinal diversity gradients in the deep sea with special reference to North Atlantic nematodes. *Marine Ecology Progress Series* 194: 159-167
- Levin LA, Gage JD (1998) Relationships between oxygen, organic matter and the diversity of bathyal macrofauna. *Deep-Sea Research* 45: 129-163
- Levin LA, Gage JD, Martin C, Lamont PA (2000) Macrobenthic community structure

within and beneath the oxygen minimum zone, NW Arabian Sea. *Deep-Sea Research* 47: 189-226

Levin LA, Leithold EL, Gross TF, Huggett CL, Dibacco C (1994) Contrasting effects of substrate mobility on infaunal assemblages inhabiting 2 high-energy settings on Fieberling Guyot. *Journal of Marine Research* 52: 489-522

Levin LA, Mccann LD, Thomas CL (1991) The ecology of polychaetes on deep seamounts in the eastern Pacific Ocean. *Ophelia* 5: 467-476

Lochte K (1992) Bacterial standing stock and consumption of organic carbon in the benthic boundary layer of the abyssal North Atlantic. In: Rowe GT, Pariente V (eds) *Deep-sea food chains and the global carbon cycle*. Kluwer Academic Publishers, Boston

Loreau M, Naeem S, Inchausti P, Bengtsson J, Grime JP, Hector A, Hooper DU, Huston MA, Raffaelli D, Schmid B, Tilman D, Wardle DA (2001) Ecology - biodiversity and ecosystem functioning: Current knowledge and future challenges. *Science* 294: 804-808

Luther III GW, Brendel PJ, Lewis BL, Sundby B, Lefrancois L, Silverberg N, and Nuzzio DB. (1998) Simultaneous measurement of O<sub>2</sub>, Mn, Fe, I-, and S(-II) in marine pore waters with a solid-state voltammetric microelectrode. *Limnology and Oceanography* 43: 325-333

MacArthur RH (1972) *Geographical ecology*. Harper and Row, New York

Maciolek NJ, Grassle JF, Hecker B, Boehm PD, Brown B, Dade B, Steinhaur WG, Babbiste E, Ruff RE, and Petrecca R. Study of biological processes on the U.S. Mid-Atlantic Slope and Rise. Phase 2. Final Report. 1987. Washington, D.C., U.S. Dept. of Interior, Minerals Management Service.

Maciolek-Blake NJ, Grassle JF, Blake JA, and Neff, JM (1985) Georges Bank infauna monitoring program: Final report for the third year of sampling. Washington D.C., U.S. Dept. of Interior, Minerals Management Service.

Mahaut ML, Sibuet M, Shirayama Y (1995) Weight-dependent respiration rates in deep-sea organisms. *Deep-Sea Research* 42: 1575-1582

Marcotte BM (1977) Ph.D dissertation. Dalhousie University. 212 pp.

- Mare MF (1942) A study of marine benthic community with special reference to the micro-organisms. *Journal of the Marine Biological Association of the United Kingdom* 25: 517-554
- Marinelli RL, Coull BC (1987) Structural complexity and juvenile fish predation on meiobenthos: and experimental approach. *Journal of Experimental Marine Biology and Ecology* 108: 76-81
- May RM (1988) How many species are there on earth? *Science* 241: 1441-1449
- May RM (1992) Bottoms up for the oceans. *Nature* 357: 278-279
- McIntyre AD, Warwick RM (1984) Meiofauna techniques. In: Holme NA, McIntyre AD (eds.) *Methods for the study of marine benthos*. Blackwell, Oxford
- Meybeck M (1993) C, N, P, and S in rivers: from sources to global inputs In: Wollast R, Mackenzie FT, and Chou L (eds.) *Interactions of C, N, P, and S biogeochemical cycles and global change*. Springer-Verlag, Berlin.
- Middelburg JJ, Barranguet C, Boschker HTS, Herman PMJ, Moens T, Heip CHR (2000) The fate of intertidal microphytobenthos carbon: An in situ C-13-labeling study. *Limnology and Oceanography* 45: 1224-1234
- Moens T, Luyten C, Middelburg JJ, Herman PMJ, Vincx M (2002) Tracing organic matter sources of estuarine tidal flat nematodes with stable carbon isotopes. *Marine Ecology Progress Series* 234: 127-137
- Moens T, Verbeeck L, Vincx M (1999) Preservation and incubation time-induced bias in tracer-aided grazing studies on meiofauna. *Marine Biology* 133: 69-77
- Montagna PA (1982) Morphological Adaptation in the deep-sea benthic harpacticoid copepod family Cerviniidae. *Crustaceana* 42: 37-43
- Montagna PA (1984) In situ measurement of meiobenthic grazing rates on sediment bacteria and edaphic diatoms. *Marine Ecology Progress Series* 18: 119-130
- Montagna PA (1993) Radioisotope technique to quantify in situ microbivory by meiofauna in sediments. In: Kemp PF, Sherr BF, Sherr EB, Cole JJ (eds.) *Handbook of methods in aquatic microbial ecology*. Lewis Publishers, Ann Arbor

- Montagna PA (1995) Rates of metazoan meiofauna microbivory: A review. *Vie et Milieu* 45:1-9
- Montagna PA (2002) Field and laboratory methods for meiofaunal research. In: Hurst CJ, Crawford RL, Knudsen GR, McInerney MJ, Stentzenbach LD (eds.) *Manual of environmental microbiology*. ASM Press
- Montagna PA, Bauer JE (1988) Partitioning Radiolabeled Thymidine Uptake by Bacteria and Meiofauna Using Metabolic Blocks and Poisons in Benthic Feeding Studies. *Marine Biology* 98: 101-110
- Montagna PA, Blanchard GF, Dinet A (1995) Effect of production and biomass of intertidal microphytobenthos on meiofaunal grazing rates. *Journal of Experimental Marine Biology and Ecology* 185: 149-165
- Montagna PA, Harper DE (1996) Benthic infaunal long term response to offshore production platforms in the Gulf of Mexico. *Canadian Journal of Fisheries and Aquatic Sciences* 53: 2567-2588
- Montagna PA, Yoon WB (1991) The effect of fresh-water inflow on meiofaunal consumption of sediment bacteria and microphytobenthos in San-Antonio Bay, Texas, USA. *Estuarine Coastal and Shelf Science* 33: 529-547
- Müller-Karger FE, Walsh JJ, Evans RH, and Meyers MB (1991). On the seasonal phytoplankton concentration and sea surface temperature cycles of the Gulf of Mexico as determined by satellites. *Journal of Geophysical Research* 96: 12645-12665.
- Pace MC, Carman KR (1996) Interspecific differences among meiobenthic copepods in the use of microalgal food resources. *Marine Ecology Progress Series* 143: 77-86
- Paine RT, Levin LA (1981) Intertidal landscapes: disturbance and the dynamics of pattern. *Ecological Monographs* 51: 145-178
- Paterson GLJ, Lambshead PJD (1995) Bathymetric patterns of polychaete diversity in the Rockall-Trough, northeast Atlantic. *Deep-Sea Research* 42: 1199-1214
- Pequegnat WE, Gallaway BJ, Pequegnat LH (1990) Aspects of the ecology of the deepwater fauna of the Gulf of Mexico. *American Zoologist* 30: 45-64
- Peterson BJ (1999) Stable isotopes as tracers of organic matter input and transfer in

benthic food webs: A review. *Acta Oecologica-International Journal of Ecology* 20: 479-487

Pfannkuche O (1993) Benthic response to the sedimentation of particulate organic matter at the BIOTRANS station, 47 degrees N, 20 degrees W. *Deep-Sea Research* 40: 135-149

Pfannkuche O (1993) Organic carbon flux through the benthic community in the temperate Northeast Atlantic. In: Rowe GT, Pariente V (eds) *Deep-sea food chains and the global carbon cycle*. Kluwer Academic Publishers, Boston

Pinckney JL, Carman KR, Lumsden SE, Hymel SN (2003) Microalgal-meiofaunal trophic relationships in muddy intertidal estuarine sediments. *Aquatic Microbial Ecology* 31: 99-108

Poore GCB, Wilson GD (1993) Marine species richness. *Nature* 361: 597-598

Qian Y, Jochens AE, Kennicutt MC II, and Biggs DC (2003) Spatial and temporal variability of phytoplankton blooms and community structure over the continental margin of the northeast Gulf of Mexico based on pigment analysis. *Continental Shelf Research* 23: 1-17

Qian Y, Sericano JL, and Wade TL (1998) Extraction and clean-up of sediments for trace organic analysis. In: *Sampling and analytical methods of the national status and trends program, Mussel Watch Project: 1993-1996 Update*. NOAA Technical Memorandum NOS ORCA 130, pp. 94-97.

Raffaelli D, Emmerson MC, Solan M, Biles CL, Paterson DM (2003) Biodiversity and ecosystem processes in shallow coastal waters: an experimental approach. *Journal of Sea Research* 49: 133-141

Reimers CE, Smith KL (1986) Reconciling measured and predicted fluxes of oxygen across the deep-sea sediment-water interface. *Limnology and Oceanography* 31: 305-318

Remane A (1933) Verteilung und organization der benthonischen microfauna der Kieler Bucht. *Wiss.Meeresunters, Abt Kiel, NF* 21: 161-221

Relexans JC, Deming JW, Dinet A, Gaillard JF, and Sibuet M (1996) Sedimentary organic matter and micro-meiofauna with relation to trophic conditions in the

northeast tropical Atlantic. *Deep-Sea Research* 43:1343-1368

- Rex MA (1981) Community structure in the deep-sea benthos. *Annual Review of Ecology and Systematics* 12: 331-353
- Rex MA (1983) Geographic patterns of species diversity in the deep-sea benthos. In: Rowe GT (ed) *The Sea*. Wiley, New York
- Rex MA, Stuart CT, Hessler RR, Allen JA, Sanders HL, Wilson GDF (1993) Global-scale latitudinal patterns of species diversity in the deep-sea benthos. *Nature* 365: 636-639
- Rhoads DC (1974) Organism-sediment relations on the muddy sea floor. In: Ansell RN, Gibson RN, Barnes N (eds) *Oceanography and Marine Biology*. U.C.L. Press, London
- Rieper M (1978) Bacteria as food for marine harpacticoid copepods. *Marine Biology* 45: 337-345
- Riera P, Richard P, Gremare A, Blanchard G (1996) Food source of intertidal nematodes in the Bay of Marennes-Oleron (France), as determined by dual stable isotope analysis. *Marine Ecology Progress Series* 142: 303-309
- Rocha-Olivares A, Fleeger JW, Foltz DW (2001) Decoupling of molecular and morphological evolution in deep lineages of a meiobenthic harpacticoid copepod. *Molecular Biology and Evolution* 18: 1088-1102
- Rothman DH (2001) Global biodiversity and the ancient carbon cycle. *Proceedings of the National Academy of Sciences of the United States of America* 98: 4305-4310
- Rowe GT (1996) The cycling of organic matter in food-limited environments. In: Uiblein F, Ott J, Stachowitsch M (eds.) *Deep-sea and extreme shallow water habitats: affinities and applications*.
- Rowe GT, Boland GS, Phoel WC, Anderson RF, Biscaye PE (1994) Deep-sea floor respiration as an indication of lateral input of biogenic detritus from continental margins. *Deep-Sea Research* 41: 657-668
- Rowe GT *et al.* (In prep) Deepwater program: Northern Gulf of Mexico continental slope habitats and benthic ecology. Final report. Minerals Management Service,

US Department of the Interior.

- Rowe GT, Sibuet M, Deming J, Khripounoff A, Tietjen J, Macko S, Theroux R (1991) 'Total' sediment biomass and preliminary estimates of organic carbon residence time in deep-sea benthos. *Marine Ecology Progress Series* 79: 99-114
- Sanders HL (1958) Benthic studies in Buzzards Bay I: Animal-sediment relationships. *Limnology and Oceanography* 3: 245-258
- Sanders HL, Hessler RR (1969) Ecology of the deep-sea benthos. *Science* 163: 1419-1423
- SAS Institute Inc. (1991) SAS/STAT guide for personal computers. SAS Institute Inc. Cary, North Carolina
- Schaff T, Levin L, Blair N, Demaster D, Pope R, Boehme S (1992) Spatial heterogeneity of benthos on the Carolina continental-slope - large (100-Km)-scale variation. *Marine Ecology Progress Series* 88: 143-160
- Schizas NV, Street GT, Coull BC, Chandler GT, and Quattro JM (1999) Molecular population structure of the marine benthic copepod (*Microarthridion littorale*) along the southeastern and Gulf coasts of the United States. *Marine Biology* 135: 399-405.
- Schmidt JL, Deming JW, Jumars PA, and Keil RG (1998) Constancy of bacterial abundance in surficial marine sediments. *Limnology and Oceanography* 43: 976-982
- Schmitz WJ Jr. (2004) On the circulation in and around the Gulf of Mexico: Volume I - A Review of the Deep Water Circulation. Online publication, Texas A&M Corpus Christi <http://www.cbi.tamucc.edu/gomcirculation/default.htm>
- Schwinghamer P (1981) Characteristic size distributions of integral benthic communities. *Canadian Journal of Fisheries and Aquatic Sciences* 38: 1255-1263
- Shannon CE, Weaver W (1949) The mathematical theory of communication. University of Illinois Press. Urbana, IL.
- Shirayama Y (1984a) The abundance of deep-sea meiobenthos in the western Pacific in relation of environmental factors. *Oceanologica Acta* 7: 113-121

- Shirayama Y (1984b) Vertical distribution of meiobenthos in the sediment profile in bathyal, abyssal and hadal deep sea systems of the Western Pacific. *Oceanologica Acta* 7: 123-129
- Shirayama Y (1992) Respiration rates of bathyal meiobenthos collected using A deep-sea submersible Shinkai 2000. *Deep-Sea Research* 39: 781-788
- Shimanaga M, Shirayama Y (2000) Response of benthic organisms to seasonal change of organic matter deposition in the bathyal Sagami Bay, central Japan. *Oceanologica Acta* 23: 91-107
- Smith KL (1978a) Benthic community respiration in NW Atlantic Ocean - In situ measurements from 40 to 5200 m. *Marine Biology* 47: 337-347
- Smith KL (1978b) Metabolism of the abysso-pelagic rattail *Coryphaenoides armatus* measured *in situ*. *Nature* 274: 362-364
- Smith KL (1983) Respiration of the two dominant epibenthic echinoderms measured at bathyal depths in the Santa Catalina Basin. *Marine Biology* 72: 249-256
- Smith KL (1987) Food-energy supply-and-demand - A discrepancy between particulate organic carbon flux and sediment community oxygen consumption in the deep ocean. *Limnology and Oceanography* 32: 201-220
- Smith KL (1992) Benthic boundary-layer communities and carbon cycling at abyssal depths in the central north Pacific. *Limnology and Oceanography* 37: 1034-1056
- Smith KL, Baldwin RJ, Karl DM, Boetius A (2002) Benthic community responses to pulses in pelagic food supply: North Pacific Subtropical Gyre. *Deep-Sea Research* 49: 971-990
- Smith KL, Baldwin RJ, Williams PM (1992) Reconciling particulate organic carbon flux and sediment community oxygen consumption in the Deep North Pacific. *Nature* 359: 313-316
- Smith KL, Glatts RC, Baldwin RJ, Beaulieu SE, Uhlman AH, Horn RC, Reimers CE (1997) An autonomous, bottom-transecting vehicle for making long time-series measurements of sediment community oxygen consumption to abyssal depths. *Limnology and Oceanography* 42: 1601-1612



- Smith KL, Hessler RR (1974) Respiration of benthopelagic fishes: *in situ* measurements at 1230 m. *Science* 184: 72-73
- Smith KL, Kaufmann RS, Baldwin RJ, Carlucci AF (2001) Pelagic-benthic coupling in the abyssal eastern North Pacific: An 8-year time-series study of food supply and demand. *Limnology and Oceanography* 46: 543-556
- Smith KL, Laver MB (1981) Respiration of the bathypelagic fish *Cyclothone acclinidens*. *Marine Biology* 61: 261-266
- Smith KL, Teal JM (1972) Deep-sea benthic community respiration: an *in situ* study at 1850 meters. *Science* 179: 282-283
- Smith KL, White GA, Laver MB (1979) Oxygen uptake and nutrient exchange of sediments measured *in situ* using a free vehicle grab respirometer. *Deep-Sea Research* 26: 337-346
- Snelgrove PVR, Grassle JF, Petrecca RF (1996) Experimental evidence for aging food patches as a factor contributing to high deep-sea macrofaunal diversity. *Limnology and Oceanography* 41: 605-614
- Soltwedel T (1997) Meiobenthos distribution pattern in the tropical East Atlantic: indication for fractionated sedimentation of organic matter to the sea floor? *Marine Biology* 129: 747-756
- Soltwedel T (2000) Metazoan meiobenthos along continental margins: a review. *Progress in Oceanography* 46: 59-84
- Soltwedel T, Pfannkuche O, Thiel H (1996) The size structure of deep-sea meiobenthos in the north-eastern Atlantic: nematode size spectra in relation to environmental variables. *Journal of the Marine Biological Association of the United Kingdom* 76: 327-344
- Sousa WP (1979) Disturbance in marine intertidal boulder fields: The nonequilibrium maintenance of species diversity. *Ecology* 60: 1225-1239
- Steele JH (1974) *The structure of marine ecosystems*. Harvard University Press, Cambridge
- Street GT, Montagna PA (1996) Loss of genetic diversity in Harpacticoida near offshore platforms. *Marine Biology* 126: 271-282

- Taghon GL, Greene RR (1990) Effects of Sediment-Protein Concentration on Feeding and Growth-Rates of *Abarenicola-Pacifica* Healy-Et-Wells (Polychaeta, Arenicolidae). *Journal of Experimental Marine Biology and Ecology* 136: 197-216
- Taylor BJ and Presley BJ (1998) TERL trace element quantification techniques. In: Sampling and analytical methods of the national status and trends program, Mussel Watch Project: 1993-1996 Update. NOAA Technical Memorandum NOS ORCA 130, pp.32-92.
- Thiel H (1972) Meiofauna und structur der benthischen Lebensgemeinschaft des Ibrischen Tiefseebeckens. *Meteor Forschungsergebnisse, Ser.D* 12: 36-51
- Thiel H (1975) The size structure of deep-sea benthos. *Internationale Revue gestamen der Hydrobiologia* 60: 575-606
- Thiel H (1978) Benthos in upwelling regions. In: Boje R, Tomczak M (eds) *Upwelling Ecosystems*. Springer-Verlag, Berlin
- Thiel H, Pfannkuche O, Theeg R, Schriever G (1987) Benthic metabolism and standing stock in the central and northern deep red sea. *Marine Ecology* 8: 1-20
- Thistle D (1978) Harpacticoid dispersion patterns - Implications for deep-sea diversity maintenance. *Journal of Marine Research* 36: 377-397
- Thistle, D. 1979. Harpacticoid copepods and biogenic structures: implications for deep-sea diversity maintenance. In: R. J. Livingston (ed.) *Ecological processes in coastal and marine systems*. Plenum, New York. pp. 217-231.
- Thistle D (1983) The role of biologically produced habitat heterogeneity in deep-sea diversity maintenance. *Deep-Sea Research* 30: 1235-1245
- Thistle D (1998) Harpacticoid copepod diversity at two physically reworked sites in the deep sea. *Deep-Sea Research* 45: 13-24
- Thistle D (2001) Harpacticoid copepods are successful in the soft-bottom deep sea. *Hydrobiologia* 453: 255-259
- Thistle D (2003) On the utility of metazoan meiofauna for studying the soft-bottom deep sea. *Vie et Milieu-Life and Environment* 53: 97-101

- Thistle D, Eckman JE (1988) Response of harpacticoid copepods to habitat structure at a deep-sea site. *Hydrobiologia* 167: 143-149
- Thistle D, Eckman JE (1990) The effect of a biologically produced structure on the benthic copepods of a deep-sea site. *Deep-Sea Research* 37: 541-554
- Thistle D, Ertman SC, Fauchald K (1991) The fauna of the Hebble Site - patterns in standing stock and sediment-dynamic effects. *Marine Geology* 99: 413-422
- Thistle D, Hilbig B, Eckman JE (1993) Are polychaetes sources of habitat heterogeneity for harpacticoid copepods in the deep-sea. *Deep-Sea Research* 40: 151-157
- Thistle D, Levin LA, Gooday AJ, Pfannkuche O, Lambshead PJD (1999) Physical reworking by near-bottom flow alters the metazoan meiofauna of Fieberling Guyot (northeast Pacific). *Deep-Sea Research* 46: 2041-2052
- Thistle D, Yingst JY, Fauchald K (1985) A deep-sea benthic community exposed to strong near-bottom currents on the Scotian Rise (Western Atlantic). *Marine Geology* 66: 91-112
- Tietjen J (1971) Ecology and distribution of deep-sea meiobenthos off North Carolina. *Deep-Sea Research* 18: 941-957
- Tilman D (1982) Resource competition and community structure. Princeton University Press, Princeton
- Tilman D (1994) Competition and biodiversity in spatially structured habitats. *Ecology* 75: 2-16
- Turley CM, Lochte K, and Lampitt RS (1995) Transformations of biogenic particles during sedimentation in the northeastern Atlantic. *Philosophical Transactions of the Royal Society of London Sseries B-Biological Sciences* 348: 179-189
- Valiela I (1995) *Marine Ecological Processes*, 2nd Edition. Springer-Verlag, New York
- Vanaverbeke J, Steyaert M, Soetaert K, Rousseau V, Van Gansbeke D, Parent J-Y, Vincx M (2004) Changes in structural and functional diversity of nematode communities during a spring phytoplankton bloom in the southern North Sea. *Journal of Sea Research* 52: 281-292
- Vanhove S, Wittoeck J, Desmet G, Vandenberghe B, Herman RL, Bak RPM, Nieuwland

- G, Vosjan JH, Boldrin A, Rabitti S, Vincx M (1995) Deep-sea meiofauna communities in Antarctica - Structural-analysis and relation with the environment. *Marine Ecology Progress Series* 127: 65-76
- Vivier MH (1978) Conséquences d'un déversement de boue rouge d'alumine sur le méiobenthos profond (Canyon de Cassidaigne, Méditerranée). *Tethys* 8: 249-262
- Warwick RM (1984) Species size distributions in marine benthic communities. *Oecologia* (Berlin) 61: 32-40
- Warwick RM, Gee JM (1984) Community structure of estuarine meiobenthos. *Marine Ecology Progress Series* 18: 97-112
- Warwick RM, Price R (1979) Ecological and metabolic studies on free-living nematodes from an estuarine mud-flat. *Estuarine and Coastal Marine Science* 9: 257-271
- Warwick RM, Clarke KR (1991) A comparison of some methods for analyzing changes in benthic community structure. *Journal of the Marine Biological Association of the United Kingdom* 71: 225-244
- Warwick RM, Clarke KR (1995) New 'biodiversity' measures reveal a decrease in taxonomic distinctness with increasing stress. *Marine Ecology Progress Series* 129: 301-305
- Warwick RM, Connor MS, Gee JM, George CL (1986) Species size distributions of benthic and pelagic metazoan – evidence for interaction. *Marine Ecology Progress Series* 34: 63-68
- Weiser W (1960) Benthic studies in Buzzards Bay. II The meiofauna. *Limnology and Oceanography* 5: 121-137
- Wells JBJ (1976) Keys to aid in the identification of marine harpacticoid copepods. Aberdeen University Press Ltd. Aberdeen, U.K.
- Wigley RL, McIntyre AD (1964) Some quantitative comparisons of offshore meiobenthos and macrobenthos south of Martha's Vineyard. *Limnology and Oceanography* 9: 485-493
- Wilson EO (1985) The biological diversity crisis - A challenge to science. *Issues in Science and Technology* 2: 20-29

Wilson EO (1988) The current state of biological diversity. In: Wilson EO, Peter FM (eds) Biodiversity. National Academy, Washington D.C.

Wright DA (1983) Species-energy theory: An extension of species-area theory. *Oikos* 41: 496-506

## VITA

Jeffrey Greer Baguley was born in Medford, Oregon on December 30, 1977, the son of Thomas G. Baguley and Janis M. Baguley. Jeff attended Galena High School in Reno, Nevada, where he graduated with honors in June 1996. He began university study at Linfield College in September 1996, and received his Bachelor of Arts with Honors in Biology in May 2000. Jeff was a four year intercollegiate letterman on the Linfield College baseball team, with all conference recognition in 1999 and 2001; he also played semi-professional baseball for the Reno Diamonds/Reno Astros from 1997 to 2001. In August 2000, he matriculated into the Graduate School of The University of Texas at Austin, Department of Marine Science. While in graduate school, Jeff has participated in numerous national and international conferences, including six oral presentations.

Permanent Address: 123 Granby Crossing, Cayce, SC 29033

This dissertation was typed by the author.